The Dissertation Committee for Yongzhu Fu certifies that this is the approved version of the following dissertation:

Development of New Membranes Based on Aromatic Polymers and Heterocycles for Fuel Cells

Committee:

Arumugam Manthiram, Supervisor

John B. Goodenough

Harovel G. Wheat

Benny D. Freeman

Christopher W. Bielawski

Development of New Membranes Based on Aromatic Polymers and Heterocycles for Fuel Cells

by

Yongzhu Fu, B. S.; M. S.

Dissertation

Presented to the Faculty of the Graduate School of
The University of Texas at Austin
in Partial Fulfillment
of the Requirements
for the Degree of

Doctor of Philosophy

The University of Texas at Austin

May, 2007

Dedication

To my wife and parents

Acknowledgements

I would like to express my deepest appreciation to my dissertation advisor, Dr. Arumugam Manthiram, for his supervision throughout the duration of this work. His guidance and encouragement have fostered independent thinking and individual initiative, yet he has always been available for consultation. I would also like to thank my supervisory committee, Dr. John B. Goodenough, Dr. Harovel G. Wheat, Dr. Benny D. Freeman, and Dr. Christopher W. Bielawski, for serving on my committee and providing helpful advice and support during this study.

I also wish to take this opportunity to thank past and present members of Dr. Manthiram's group for the exchange of ideas and friendship. It has been a pleasure working with and learning from them during this work. In particular, I would like to thank Dr. Bo Yang, a former graduate student in Dr. Manthiram's group, for all his help during the initial work of this project.

Lastly, and most importantly, I wish to thank my wife and parents, for all their support with endless love. It takes many efforts to finish this long course, and it would not have been possible without them.

This work was supported by the Welch Foundation Grant F-1254.

Development of New Membranes Based on Aromatic Polymers and Heterocycles for Fuel Cells

Publication No._____

Yongzhu Fu, Ph. D.
The University of Texas at Austin, 2007

Supervisor: Arumugam Manthiram

Proton exchange membrane fuel cells (PEMFC) and direct methanol fuel cells (DMFC) have drawn much attention as alternative power sources for transportation, stationary, and portable applications. Nafion membrane is currently used in PEMFC and DMFC as electrolyte, but is confronted with a few difficulties: (i) high cost, (ii) limited operating temperature (< 100 ^{o}C), and (iii) high methanol permeability. With an aim to overcome some of the problems encountered with the Nafion membrane, this dissertation focuses on the design and development of new polymeric materials systems for use in PEMFC and/or DMFC.

Sulfonated polysulfone (SPSf) membranes with various degrees of sulfonation were prepared and investigated in DMFC. With a degree of sulfonation of 50 - 70 %, the SPSf membranes exhibit low methanol permeability and electrochemical performance comparable to that of Nafion 115, making it an attractive low-cost alternative to Nafion. However, lower performance at higher current densities due to their low proton conductivities compared to Nafion is a disadvantage. It is found that the low methanol

crossover is due to narrower hydrophilic channels, resulting in water/methanol confinement as in sulfonated poly(ether ether ketone) (SPEEK) membranes.

Replacement of water by imidazole in Nafion helps to keep high proton conductivity at higher temperatures (> 100 ^{o}C) due to Grotthuss-type mechanism, but imidazole poisons the Pt catalyst. Interestingly, doping the Nafion-Imidazole composite membrane with H_3PO_4 partly suppresses the imidazole poisoning of the Pt catalyst. Employment of Pd-Co-Mo catalyst instead of Pt improves the fuel cell performance at 100 ^{o}C further due to a higher tolerance of the non-platinum Pd-Co-Mo catalyst to imidazole.

Encouraged by this, benzimidazole group was then selected to promote proton conduction in the environment of sulfonic acid groups instead of imidazole (pK_a = 7.0) due to its lower pK_a value (5.5). Accordingly, 1,3-1*H*-dibenzimidazole-benzene containing two benzimidazole groups was synthesized and blended with SPSf. The blend exhibits higher proton conductivity under anhydrous conditions than plain SPSf and offers improved fuel cell performance and lower methanol crossover in DMFC.

Polysulfones containing pendant N-heterocycles like benzimidazole, 2-amino-benzimidazole, or 3-amino-1,2,4-1*H*-triazole units were designed and synthesized. Blend membranes containing these polymers and SPEEK exhibit higher proton conductivities under anhydrous conditions as well as higher fuel cell performance due to acid-base interactions involving Grotthuss-type mechanism. They also lower methanol crossover further due to the insertion of the pendant N-heterocycles into the hydrophilic channels of SPEEK, improving the long-term stability in DMFC and reducing the Pt loading at the cathode side.

Table of Contents

List of Tables

List of Schemes

List of Figures

Chapter 1

Introduction

1.1 FUEL CELLS

Development of alternative energy technologies has drawn much attention in recent years due to the limited availability of fossil fuels and the increasing air pollution from combustion [1]. Fossil fuel, presently used as an energy source for internal combustion engines, could last only for a limited period of time in the future. In this regard, use of hydrogen as an energy carrier has been becoming increasingly popular, and how to effectively utilize hydrogen is a diverse topic. Fuel cells are considered as clean energy devices that can effectively use hydrogen as a fuel with low emission and high conversion efficiency [2].

Fuel cells are devices that are capable of converting chemical energy from fuels directly into electrical energy without combustion. They are not constrained by the maximum Carnot cycle efficiency unlike internal combustion engines, because they do not operate with a thermal cycle. Consequently, they can have very high conversion efficiencies. In addition, they have low or zero emission as water is the only product when hydrogen and oxygen are used as reactants.

In principle, fuel cells operate like a battery, and both of them are electrochemical devices. As such, both have a positive electrode (cathode), a negative electrode (anode), and an ion-conducting material as an electrolyte. Unlike a battery, a fuel cell, however, does not require recharging. It will produce electricity and heat as long as the fuel and an

oxidizer are supplied. The fuel passes over the anode and the oxidizer (O_2 or air) passes over the cathode. The chemical reactions involving the oxidation of the fuel at the anode and reduction of the oxidant at the cathode result in ionic flow through the electrolyte and electron flow through the external circuit between the anode and cathode, providing electrical energy.

1.1.1 Types of Fuel Cells

A variety of fuel cells are in different stages of development. The most common classification of fuel cells is on the basis of the type of electrolyte used in the cells and it includes (1) proton exchange membrane fuel cell (PEMFC), (2) direct methanol fuel cell (DMFC), (3) phosphoric acid fuel cell (PAFC), (4) alkaline fuel cell (AFC), (5) molten carbonate fuel cell (MCFC), and (6) solid oxide fuel cell (SOFC). The choice of electrolyte dictates the operating temperature range of the fuel cell. The operating temperature and useful life of a fuel cell dictate the physicochemical and thermomechanical properties of materials used in the cell components like electrode, electrolyte, interconnect etc. The operating temperature also plays an important role in establishing the degree of fuel processing required. In low temperature fuel cells, all the fuel must be converted into hydrogen prior to entering the fuel cell, and the anode catalyst in low temperature fuel cells (Pt) is strongly poisoned by CO. In high temperature fuel cells, hydrocarbon fuels like CH_4 can be internally converted into hydrogen or even directly oxidized electrochemically. Table 1.1 provides an overview of the key characteristics of the main fuel cells types.

Table 1.1 Overview of the key characteristics of the main fuel cells types [3-5].

	PEMFC	DMFC	AFC	PAFC	MCFC	SOFC
Electrolyte	Proton exchange membrane	Proton exchange membrane	Potassium hydroxide in asbestos matrix	Phosphoric acid in SiC	Molten carbonate in $LiAlO_2$	Ceramic oxide ion conductor
Electrode	Carbon	Carbon	Transition metals	Carbon	Nickel and Nickel oxide	Oxide, oxide/metal cermet
Operating temperature	50 – 90 ^oC	50 – 130 ^oC	50 – 250 ^oC	180 – 200 ^oC	650 ^oC	600 – 1000 ^oC
Charge carrier	H^+	H^+	OH^-	H^+	CO_3^{2-}	O^{2-}
Catalyst	Pt	Pt/PtRu	Pt	Pt	Electrode material	Electrode material
Fuel	Pure or reformed H_2	Aqueous CH_3OH solution	H_2	Reformed H_2	Reformed H_2 and CO, CH_4	Reformed H_2 and CO, hydrocarbons
External reformer for hydrocarbon fuels	Yes	No	Yes	Yes	No, for some fuels	No, for some fuels and cell design
Poison	CO > 10 ppm	Adsorbed intermediates	CO, CO_2	CO > 1 % H_2S > 50 ppm	H_2S > 0.5 ppm	H_2S > 1 ppm
Efficiency (% HHV)[a]	> 50 (direct)	~ 40	> 50 (direct)	36 – 45	43 – 55	43 – 55
Major applications	Transportation, Stationary	Portable power supply	Space, Stationary, Transportation	Stationary	Stationary, Transportation	Stationary, Transportation

[a]HHV: higher heating value, i.e., the total heat released including the latent heat of vaporization of the water formed by the oxidation process.

PEMFC and DMFC are being considered as the most promising types of fuel cells for transportation and portable applications because of their high efficiencies, compact size, ease of construction, absence of liquid electrolyte, rapid startup time, low operating temperatures, and easy maintenance.

1.1.2 Proton Exchange Membrane Fuel Cell (PEMFC)

Proton Exchange Membrane Fuel Cell (PEMFC) is promising as a power supply in the vehicular engine due to its high power density, quick shift in power demand, and quick startup. The fuel for the PEMFC is hydrogen, the oxidizer is O_2 or air, and the charge carrier is proton. The key component in PEMFC is the membrane-electrode assembly (MEA), which consists of anode, cathode, and a proton conductive membrane. The membrane is sandwiched between the two electrodes, and the principle of PEMFC is shown in Fig. 1.1.

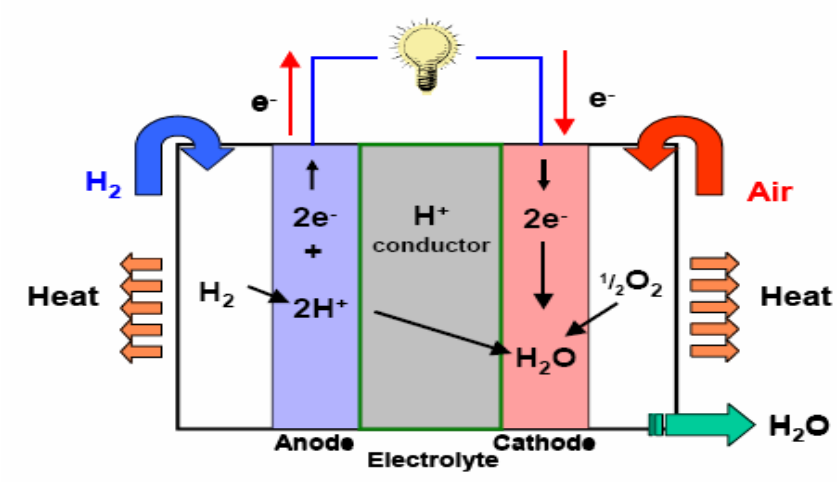

Figure 1.1. Principle of proton exchange membrane fuel cell.

Usually, the electrode consists of three layers. One is a gas diffusion layer (GDL), which is prepared by a deposition of carbon powder onto a carbon paper or carbon cloth. The second layer is a catalyst layer, which is prepared by a deposition of the catalyst (like Pt or Pt alloy) onto the diffusion layer. The third one is a thin Nafion layer, which is used as a binder between electrode and membrane. In the past decade, researchers have reduced the platinum loading in PEMFC from 4 mg/cm^2 to 0.35 mg/cm^2 by depositing platinum (2 ~ 4 nm) on the carbon; in this case, the platinum utilization efficiency is greatly improved [6]. Later, Wilson et al. [7-9] developed a new structure for the Pt/C catalyst layer of the electrode by fabricating the catalyst layers and gas diffusion backings separately. They realized the goal to reduce the platinum use to 0.1 mg/cm^2 and at the same time, maintaining satisfactory fuel cell performance. The efficiency of platinum by this method is about ten times higher than that of the electrodes produced by conventional methods.

In PEMFC, hydrogen gas is fed into the anode compartment and oxidized to protons and electrons. The protons move from the anode to the cathode through the membrane, while the electrons flow through the external circuit. Oxygen at the cathode is then reduced to oxide anions, and the oxide ions and protons combine together to produce water. The reactions at the electrodes are as follows:

Anode reaction: $2H_2 \rightarrow 4H^+ + 4e^-$ [1.1]

Cathode reaction: $O_2 + 4H^+ + 4e^- \rightarrow 2H_2O$ [1.2]

Overall cell reaction: $2H_2 + O_2 \rightarrow 2H_2O$ [1.3]

Compared to other types of fuel cells, PEMFCs generate more power for a given volume or weight of fuel cells. In addition, the solid electrolyte (Nafion membrane, a polymer developed by DuPont Co.) offers some advantages compared to a liquid electrolyte. The sealing of the anode and cathode gases is simpler with a solid electrolyte, and it is less expensive to manufacture. Also, the solid electrolyte has less problems with corrosion compared to many the other electrolytes, leading to a longer cell and stack life.

One of the disadvantages of PEMFC for some applications is that the operating temperature is low. Low operating temperature limits the catalytic activity of Pt and requires high purity hydrogen fuel with very low ppm levels of CO as the poisoning of the Pt catalysts by CO increases with decreasing operating temperature. Also, since the electrolyte is required to be saturated with water to keep high proton conduction as well as high power output, careful control of the moisture of the anode and cathode streams is important, which necessitates complex humidification subsystems. In addition, the production, storage, and transportation of hydrogen pose complex problems.

1.1.3 Direct Methanol Fuel Cell (DMFC)

Direct methanol fuel cell (DMFC) is promising as low-temperature (< 60 ^{o}C) power supply for portable electronic devices due to the use of liquid methanol as a fuel. High-temperature DMFCs (> 100 ^{o}C) utilize methanol vapor as fuel. Compared to PEMFC, it is safer for operation and simplified in system [3]. MEA is also the key component in DMFC, which is much similar to that in PEMFC. It uses a proton exchange membrane as electrolyte. The catalyst used in the anode electrode is usually PtRu alloy

(carbon supported) while the catalyst used in the cathode is Pt, but the loadings (0.6 ~ 5 mg/cm^2) on both sides are much higher than those in PEMFC because the methanol oxidation and oxygen reduction reactions in DMFC are kinetically sluggish [10].

DMFC relies on the oxidation of methanol on catalyst to form carbon dioxide by combining with water. Protons are produced and conducted through the membrane to the cathode, where they react with oxygen to produce water, while the electrons flow through the external circuit. The reactions at the electrodes are as follows:

Anode reaction: $CH_3OH + H_2O \rightarrow CO_2 + 6H^+ + 6e^-$ [1.4]

Cathode reaction: $3/2O_2 + 6H^+ + 6e^- \rightarrow 3H_2O$ [1.5]

Overall reaction: $CH_3OH + 3/2O_2 \rightarrow 2H_2O + CO_2$ [1.6]

Low-temperature DMFCs utilize liquid methanol fuel directly, eliminating the complicated catalytic reforming and the storage and transportation of methanol is much easier than that of hydrogen. The energy density of liquid methanol is orders of magnitude greater than even highly compressed gaseous hydrogen. Unfortunately, efficiency is low due to the high permeation (crossover) of methanol through the membrane and sluggish kinetics of methanol oxidation and oxygen reduction. At the current level of technology, DMFC is limited in the power it can produce. So they are attractive as power supply for consumer goods such as cell phones or laptops. As of 2005, the record for the smallest commercially available fuel cell is held by Toshiba, and their fuel cell device output is 100 mW at 10 hours per mL of fuel.

1.2 PROTON EXCHANGE MEMBRANES

Proton exchange membrane (PEM) is a critical component in PEMFC and DMFC. It strongly determines the fuel cell performance as well as the long-term operation. There are many requirements for PEM. Firstly, it should have high proton conductivity, but should be an electronic insulator to avoid short circuit. Secondly, it should effectively block permeation of fuels and oxidizer through the membrane. In addition, it should be robust, and chemically and thermally stable.

1.2.1 Perfluorinated Proton Exchange Membranes

Currently, polyperfluorosulfonic acids such as the Nafion membranes (Dupont de Nemours and Co., U.S.A.) are almost exclusively used in both PEMFC and DMFC due to their excellent stabilities and relatively high proton conductivity of around 0.08 S/cm in the hydrated state [11,12].

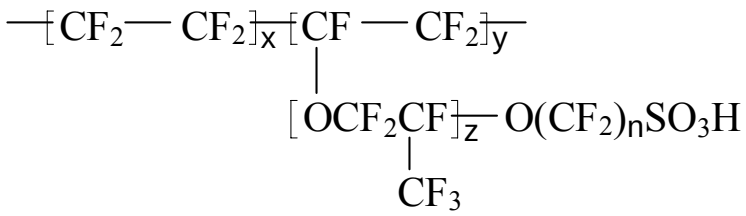

Nafion: x = 6–10, y = 1, z = 1, n = 2
Aciplex: x = 6–8, y = 0–1, z = 1 (0-2), n = 2–5
Flemion: x = 6–10, y = 1, z = 1, n = 2

Figure 1.2. Chemical structure of perfluorinated proton exchange membranes.

In addition, long-term operation (> 60,000 h) in a fuel cell environment has been reported [13]. Besides Nafion membrane, other perfluorinated membranes with similar structures have also been developed, e.g., Aciplex (Asashi Chemical Industry Co.) and Flemion (Asashi Glass Co.). The chemical structure of the perfluorinated PEMs is shown in Fig. 1.2.

Many studies have been made on the structures and properties of Nafion membrane [14-16], but the exact microstructure of Nafion is not fully understood. Reverse cluster network model is generally accepted for Nafion microstructure [17,18], in which the carbon-fluorine backbone forms a crystal hydrophobic region, the sulfonic acid groups and absorbed water form an amorphous hydrophilic region, and the side chains form a medium region. Clusters with around 4.0 nm diameters are arranged periodically among the carbon-fluorine hydrophobic region, the distance between clusters (Bragg distance) is around 5.0 nm, and the clusters are connected by channels (1.0 nm in diameter) as shown in Fig. 1.3. This model satisfies the desire for forming hydronium ions from sulfonic acid groups and avoids strong interactions between water molecules and carbon-fluorine backbone.

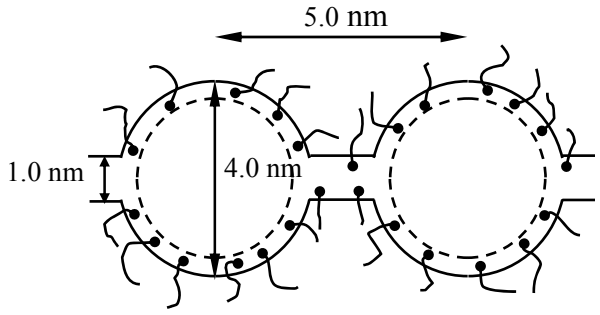

Figure 1.3. Cluster-network model for Nafion membrane.

Cluster structures have been observed in many ionomers. The results from many physical techniques such as small angle X-ray diffraction (SXRD) [19], nuclear magnetic resonance (NMR) spectroscopy [17], infrared (IR) spectroscopy [20], and transmission electron microscopy (TEM) [21] all support the cluster model of perfluorinated PEMs. Fig. 1.4 shows the TEM photographs of two Pb^{2+}-stained fluorinated PEMs. The black dots are hydrophilic regions, which provide channels for conduction of protons. These channels also, however, allow diffusion of methanol, which is a critical issue for DMFC.

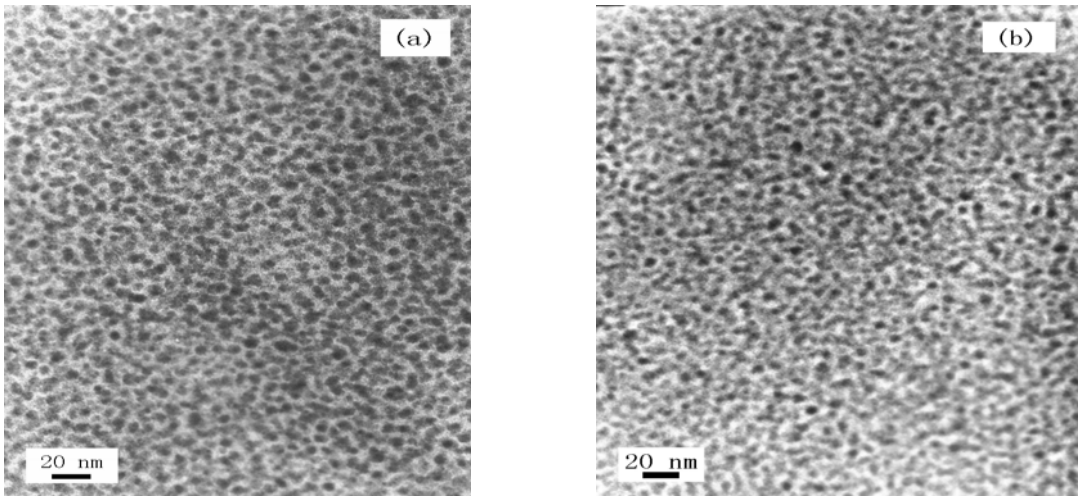

Figure 1.4. TEM images of Pb^{2+}-stained fluorosulfonic acid PEMs: (a) Nafion 115 and (b) Aciplex 1004 [22].

1.2.1.1 Disadvantages of Perfluorinated Proton Exchange Membranes

Despite the obvious advantages of the perfluorinated proton exchange membranes, there are a few disadvantages in using them for PEMFC and DMFC applications,

hampering commercialization of the fuel cell technology: (1) high cost; (2) low operating temperature; and (3) high methanol crossover.

(1) *High cost*: The price of perfluorinated membrane is as high as \$780/m^2 [23], which contributes significantly to the overall cost of PEMFC and DMFC. Perfluorinated structure and complicated processing procedure result in their high cost.

(2) *Low operating temperature*: The hydrophilic regions of the perfluorinated PEMs need to be hydrated to provide high proton conduction, which limits the operating temperature of fuel cells to < 100 ^{o}C at ambient pressure. Based on the measurement of proton conductivity of Nafion membrane, when the average number of water absorbed on each sulfonic acid group exceeds six, proton conductivity increases abruptly [24]; six water molecules are considered to form the first water ball around the sulfonic acid group. For a membrane, the Bragg distance decreases as the extent of hydration decreases. As the diameter of the hydrated clusters decreases, the ion exchange sites expand and rearrange while the number of ion exchange sites in each cluster decreases, lowering proton conduction [19].

    Operating PEMFC at temperatures as high as 150 ^{o}C can provide several advantages. First, it can simplify or eliminate the requirements of complex external humidification systems. Second, it would provide the additional benefit of enhancing the tolerance of Pt catalyst to CO impurities in the fuel [25], offering important cost savings in fuel cleanup, enhancing the commercial viability.

(3) *High methanol crossover*: The DMFC technology is plagued by the high methanol crossover from anode to the cathode, resulting in a severely reduced electrode

potential and overall cell voltage and much poorer fuel cell performance. It also leads to an undesired reaction taking place at the cathode platinum catalyst: the oxidation of methanol permeating through the membrane from the anode to the cathode, requiring a higher loading of Pt catalyst. The methanol can transport along with the protons and water through the membrane. Concentration gradient is another factor for methanol crossover [26,27].

To overcome these disadvantages, there are two strategies. The first one is to modify the present perfluorinated PEMs to offer proton conductivity at high temperature or to lower methanol crossover. The second one is to design and develop other non-fluoropolymer candidate materials. Before discussing these two strategies, it would be necessary to understand the proton conduction mechanisms.

1.2.2 Types of Proton Conduction Mechanisms

Generally, there are two types of mechanisms involved in proton conduction in proton exchange membranes: vehicle-type and Grotthuss-type mechanisms [28,29]. Fig. 1.5 illustrates these two mechanisms.

In the vehicle-type mechanism, the protons migrate through the medium along with a "vehicle" or proton solvent (e.g. as H_3O^+). The overall proton conductivity is strongly dependant on the vehicle diffusion rate Γ_D.

In the Grotthuss-type mechanism, the protons are transferred from one site to the other through hydrogen bonds (proton hopping), so a vehicle or proton solvent is not needed. But reorganization of the proton environment, consisting of reorientation of

individual species or even more extended ensembles, is necessary for the formation of an uninterrupted path for proton migration. The overall proton conductivity is determined by proton transfer rate Γ_{trans} and reorganization rate Γ_{reo} of its environment.

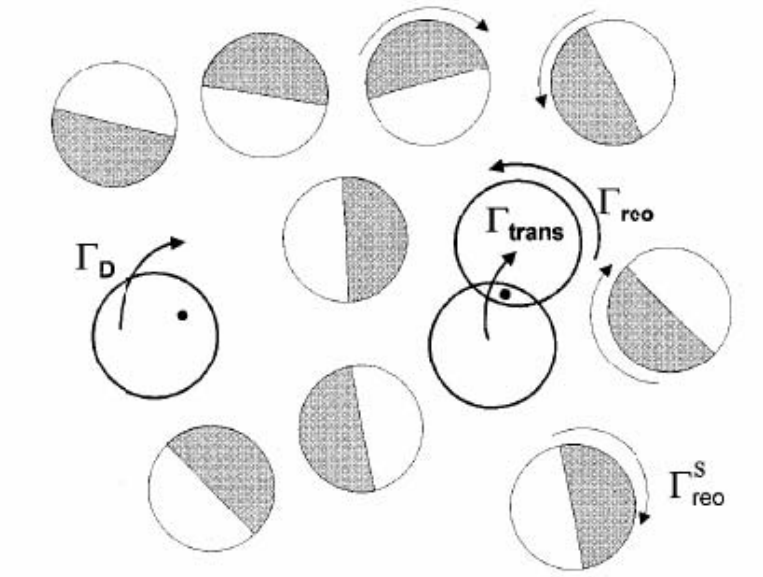

Figure 1.5. Schematic illustration of proton conduction mechanism [29].

These two proton conduction mechanisms are correlated. In all the sulfonated or phosphonated proton exchange membranes, the vehicle-type mechanism is predominant but the Grotthuss-type mechanism is also present. In the poly(benzimidazole)-doping system, the Grotthuss-type mechanism is dominant and vehicle-type mechanism is present as well. Generally, both mechanisms can be present and make contribution to proton conduction.

1.2.3 High Temperature Proton Exchange Membranes

Several approaches have been adopted to develop proton exchange membranes that can be operated at high temperatures (100 ~ 200 ^{o}C). They include (1) modification of present membranes like Nafion by incorporating hygroscopic particles (e.g. SiO_2 [30-34], TiO_2 [35,36], $Ta_2O_5 \cdot H_2O$ [37], and $Zr(HPO_4)_2 \cdot H_2O$ [38-40]) to help retain water at elevated temperatures and (2) exploration of anhydrous polymeric and inorganic proton conductors [41-45], which exhibit high proton conductivity at higher temperatures without involving water.

1.2.3.1 Modification of Nafion with Hygroscopic Particles

Hygroscopic particles such as SiO_2, TiO_2, Ta_2O_5, and $Zr(HPO_4)_2 \cdot H_2O$ can easily adsorb water and the water molecules are bonded strongly to the lattice. These water molecules can be retained to high temperatures (~ 200 ^{o}C). By introducing these particles into Nafion, the operating temperature of Nafion membrane could be increased to > 100 ^{o}C due to the presence of hygroscopic particles leading to improved hydrophilicity of the ionic clusters.

Usually, hygroscopic particles are introduced into Nafion membrane by two main approaches [40]:

- dispersion of hygroscopic particles into a Nafion solution followed by casting [46]. This approach is simple, but the disadvantage is the ease of formation of particle agglomerates inside the polymeric matrix, and thus membranes containing

non-homogeneous dispersions of micro-size particles are usually obtained.

- formation of hygroscopic particles in a preformed Nafion membrane [47-49]. This approach is to introduce a filler precursor into the polymeric matrix by simple impregnation or by ion-exchange reaction followed by converting the precursor into the final inorganic by treating the composite membrane with the necessary reactants. A typical example is the impregnation of Nafion membranes with tetraethoxysilane (TEOS), which is then converted into the final filler, SiO_2. Unfortunately, the stability of the particles in the Nafion membranes is not certain.

A lot of studies have been conducted on the development of Nafion/hygroscopic particle composite membranes, including measurement of water uptake, proton conductivity, and fuel cell test at above 100 ^oC [32,39,50,51]. Although some studies showed better property or performance than plain Nafion membrane, the performance of this kind of composite membrane at higher temperatures (> 100 ^oC) was usually poorer than that of unmodified membrane at 80 ^oC and the power density was low. In addition, the instability is the obvious disadvantage for long-term operation.

1.2.3.2 Exploration of Anhydrous Proton Exchange Membranes

For polysulfonic acid polymers as proton exchange membrane materials, like Nafion or other sulfonated polymers, the proton conduction is strongly dependent on water, in other words, the vehicle-type mechanism is dominant in this kind of membranes. Incorporation of hygroscopic particles is only a ‘temporary’ approach to keep high proton conduction at higher temperatures, since it cannot entirely solve the problem of loosing

water at higher temperatures during long-term operation. So, other approaches need to be explored. The first one is to replace water by other proton solvents, which have higher boiling point but is capable of conducting protons in a similar way as water at higher temperatures, like phosphoric acid. The second approach is to develop polymers, which are capable of conducting protons as an intrinsic property. The third approach is to explore inorganic proton conductors, which have special structures and are capable of conducting protons at higher temperatures without water.

1.2.3.2.1 Acid-doped Membranes

Phosphoric acid is a strong acid and it is capable of ionizing sulfonic acid in the Nafion membrane (super acid) and solvating the proton in the same manner as water. However, ionization and salvation are not lost at higher temperature due to the low vapor pressure of phosphoric acid. Incorporation of phosphoric acid into Nafion membrane has been investigated, and the doped membrane exhibits proton conductivity at above 100 ^{o}C as high as that of hydrated Nafion membrane at 80 ^{o}C [52].

Doping of phosphoric acid into other membranes for operation at higher temperatures has also been widely investigated, e.g. poly(ethyleneoxide) (PEO) [53,54], poly(ethyleneimine) (PEI) [55,56], and poly(acrylamide) (PAAM) [57]. Reasonable proton conductivities have been obtained for these systems at temperatures > 100 ^{o}C. However, long-term stability is the critical issue for these systems.

Poly(benzimidazole) (PBI) is a basic (pK_a = 5.5) aromatic polymer with exceptional thermal, mechanical, and chemical stability [58]. It decomposes at as high as 650 ^{o}C, its

glass transition temperature is around 420 ^{o}C, and it is very stable in strong reducing or oxidizing environment. In 1995, Wainright et al. [59] proposed a blend of PBI and strong acids like sulfuric acid or phosphoric acid as a proton exchange membrane for high temperature PEMFC for the first time. Acid-doped PBI can be prepared by casting PBI and acid into membranes or by immersing the PBI membrane in acid solution for some time. Scheme 1.1 shows the PBI chemical structure. The intrinsic ionic conductivity is around 10^{-12} S/cm, but after doping with acid, the conductivity drastically increases up to 10^{-2} S/cm at 130 ^{o}C under anhydrous condition [60]. Acid-doped PBI has shown good performance and durability in high temperature PEMFC [61].

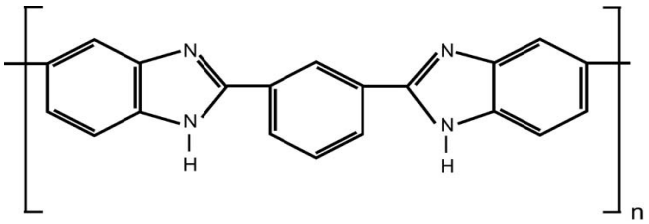

Scheme 1.1. Chemical structure of PBI.

Figure 1.6 shows the proton conduction mechanism in sulfuric acid doped PBI. Usually, Grotthuss-type mechanism is considered to be dominant. The proton transfers from one basic site (nitrogen atom of imide site) to another or from a basic site to one of the doping acid molecules by hopping. The interaction between acid and PBI forms a hydrogen bonding network, which immobilizes the anions, leading to long-term stablity. Continuous operation for thousand hours has been demonstrated in single cell PEMFC at high temperatures [61].

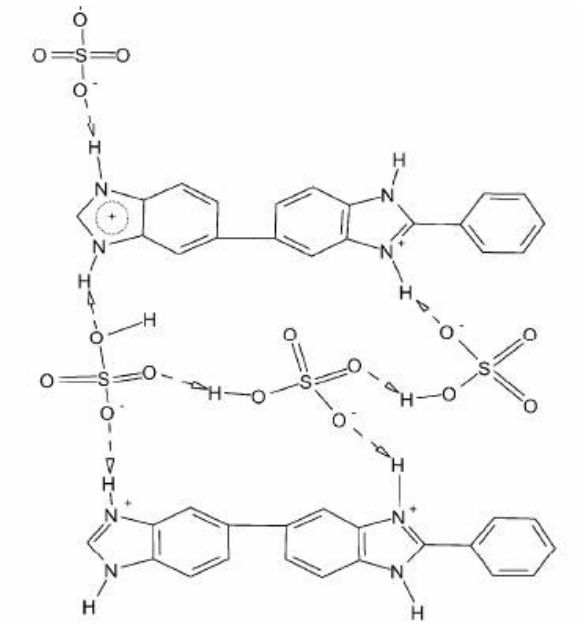

Figure 1.6. Proton conduction mechanism in acid doped PBI [62,63].

The overall proton conductivity is strongly dependent on the temperature and acid-doping level [64,65]. At a doping level of 2.0 mol of H_3PO_4 per repeat unit, the conductivity of the membrane is about 2.5×10^{-2} S/cm at 200 ^oC [66]. At an acid-doping level of 5.7 mol H_3PO_4, the measured conductivity is 4.6×10^{-3} S/cm at room temperature, 4.8×10^{-2} S/cm at 170 ^oC, and 7.9×10^{-2} S/cm at 200 ^oC [66]. The presence of water also facilitates the protonation of the acid and, therefore, increases the overall proton conductivity even though the proton transfer does not depend on water [59].

Although long-term operation of acid-doped PBI has been investigated in fuel cell, the stability of acid in the membrane still needs to be confirmed. Also, the use of phosphoric acid may still have the disadvantage in that H_3PO_4 or its dissociation products are strongly adsorbed on Pt-based catalyst [52].

1.2.3.2.2 Anhydrous Polymeric Proton Conductors

For a fast Grotthuss-type mechanism, the formation of protonic defects and the presence of proton donor and acceptor in an unpolar environment are necessary for the process of proton transfer (hopping). Strong solvent effects would suppress proton transfer reactions [67]. Heterocycles like imidazole and pyrazole are suitable in this respect. First, they are unpolar molecules; second, their nitrogen (basic) sites can act as proton acceptors. The protonated and unprotonated nitrogen sites may act as donors and acceptors due to their isometric characteristics by forming extended local dynamics. In addition, they are unpolar molecules, so they are good proton solvents for higher temperature applications compared to water [68].

Replacement of water in Nafion or sulfonated polymers by N-heterocycles like imidazole is a good strategy to improve the operating temperature of membranes above 100 ^{o}C [68,69]. Unfortunately, imidazole is known to poison the platinum catalyst, making them impossible for application in PEMFC with the conventional Pt-based electrocatalysts. Thus, tethering of N-heterocycles to some polymer network is a promising strategy to obtain high proton conductivity at high temperatures and at reduced humidity, involving structural diffusion without requiring water [70]. Recently, some new strategies have been proposed and several model material systems have been investigated [71-75]. Such heterocycles have been tethered to an appropriate polymer network through a soft side chain. The liquid-like domain (side chain with an ending of heterocycles) provides the proton conductivity while the solid-like part (polymer backbone) gives the material morphological stability. For example, Schuster et al. [74]

tethered imidazole to the end of the chains in a series of oligo(ethylene oxide)s and obtained proton conductivities of up to 8×10^{-5} S/cm at 120 ºC. Pu et al. [76] prepared styrene-maleic imide copolymer with benzimidazole side group and showed proton conductivity values of 3.9×10^{-3} S/cm after doping with H_3PO_4; they also found an increase in proton conductivity with increasing imidazole content and acid doping level.

However, the developments based on tethering N-heterocycles to polymer chains strategy are still in the state of basic research rather than close to the application stage due to the difficulty of tethering the N-heterocycles onto appropriate polymer networks to obtain stable membranes with high proton conductivity at high temperatures. Most model materials developed are based on aliphatic polymer backbones which are unable to be used at higher temperatures. So there is still a big challenge to develop practical materials from concept to a stable, optimized membrane.

1.2.3.2.3 Inorganic Proton Conductors

Some solid acids such as $CsHSO_4$ and CsH_2PO_4 have been widely studied because of their high proton conductivities and phase-transition behaviour. They offer the advantages of anhydrous proton transport and high-temperature stability (up to 250 °C) [43,44,77,78]. For example, $CsHSO_4$ is known to undergo a "superprotonic" phase transition at around 140 ^oC into a superionic phase exhibiting a high proton conductivity of $10^{-3} \sim 10^{-2}$ S/cm [77,78]. Heile et al. [44] showed a cell made of a $CsHSO_4$ electrolyte membrane (about 1.5 mm thick) operating at 150 ~ 160 °C in a H_2/O_2 configuration for the first time. Open circuit voltages of 1.11 V and current densities of 44 mA/cm^2 at short

circuit have been obtained.

However, the issue of solubility in water and difficulty to fabricate thin membranes with these inorganic proton conductors make them unsuitable to be practical used in PEMFC. In addition, the chemical stability of these materials in the fuel cell environment is another issue. Bo et al. [79] investigated the chemical stability of $CsHSO_4$ in hydrogen atmosphere in the presence of platinized carbon (Pt/C) catalysts. The experimental data demonstrated that although $CsHSO_4$ is quite stable at elevated temperatures in H_2 atmosphere, it is prone to rapid degradation evolving H_2S in presence of the Pt/C catalyst. So it is difficult to use $CsHSO_4$ as an electrolyte in PEMFCs with the conventional Pt-based electrocatalysts. It is possible that the decomposition may not occur at higher temperature in presence of other non-platinum electrocatalysts.

1.2.4 Proton Exchange Membranes with Reduced Methanol Permeability

High methanol permeability facing the present perfluorinated proton exchange membranes like Nafion is a serious issue for DMFC. The fuel cell performance could be greatly improved and the platinum catalyst loading at the cathode side could be lowered if membranes with reduced methanol permeability could be developed, enhancing the commercial feasibility of DMFC technology.

So far, two strategies have been employed to develop proton exchange membranes with reduced methanol permeability: (1) modification of the Nafion membrane and (2) exploration of alternative polymer materials.

1.2.4.1 Nafion-based Membranes

The ionic cluster in Nafion membrane is the channel for proton transfer as well as the methanol crossover. So, modification of Nafion membrane with reduced methanol permeability is focused on incorporation or blending with other polymers or hygroscopic particles to change the form and distributions of clusters in Nafion.

Polymers like polypyrrole [80-82], polyaniline [83], and poly(1-methylpyrrole) [84] have been chemically or electrochemically impregnated into the clusters in the Nafion membranes. Monomers like 1-methylpyrrole is incorporated into the clusters by soaking dried Nafion membrane in the solution of monomers, followed by radiation (UV lamp). The presence of polymer in the clusters destroys the distribution of sulfonic acid groups and block methanol crossover to some extent.

Modification of the surface of Nafion membrane by plasma or electron beam has also been investigated [85-89]. A thin methanol barrier at the surface is created. Up to about 50 % increase in peak DMFC power output over plain Nafion membrane was obtained due to reduced methanol crossover.

These modifications on Nafion membranes are potential for blocking the methanol transport. However, proton conductivity and mechanical strength are always sacrificed at the expense of the reduction in methanol crossover.

1.2.4.2 Alternative Non-Nafion Membranes

A variety of polymer materials have been synthesized and functionalized with sulfonic acid or phosphoric acid groups as proton exchange membranes for DMFC.

These materials are usually based on non-fluorinated polymers due to their low cost and ease of preparation [90-102]. Among these materials, sulfonated aromatic polymers show promising features for possible applications in DMFC. For example, sulfonated polyimide (SPI) [95,96], sulfonated polyphenylene (SPPO) [97-99], sulfonated polysulfone (SPSf) [100-102], and sulfonated poly(ether ether ketone) (SPEEK) [103-105] are actively being investigated. The structures of some sulfonated polymer materials are shown in Scheme 1.2.

SPI

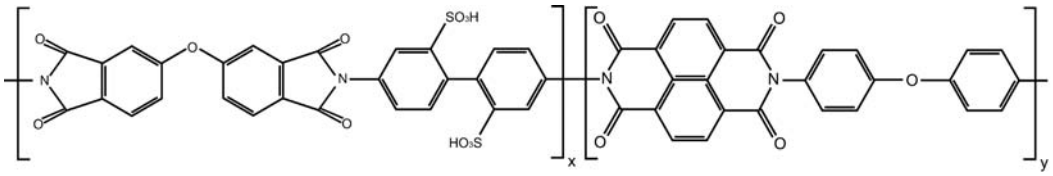

SPSf

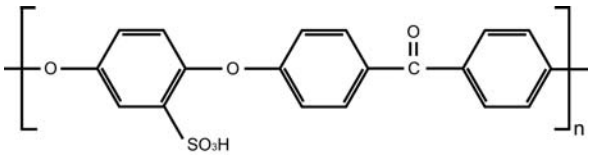

SPEEK

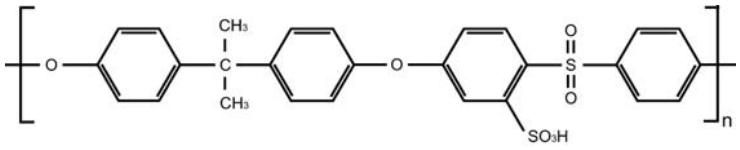

Scheme 1.2. Chemical structures of some sulfonated polymers (SPI: sulfonated polyimide; SPSf: sulfonated polysulfone; SPEEK: sulfonated poly(ether ether ketone)).

Introduction of sulfonic acid groups to these polymers are performed in several ways as follows: (1) direct sulfonation in concentrated sulfuric acid or chlorosulfonic acid [106-111], (2) radiation-grafting of monomers onto the polymer backbone followed by sulfonation [112], (3) synthesis from monomers bearing sulfonic acid groups [96], and (4) lithiation-sulfonaton-oxidation [113].

Table 1.2 summarizes the IEC, DS, and % water uptake at 25 and 80 ^{o}C for SPEEK membranes [104].

Table 1.2 Ion exchange capacity (IEC), degree of sulfonation (DS), proton conductivity (σ), and water uptake of SPEEK membranes obtained with different sulfonation reaction times [104].

IEC (meq./g)	DS (%)	Water uptake (%)[a]	
		25 ºC	80 ºC
0.98	31	-	-
1.23	39	-	-
1.36	44	1.4	8.6
1.42	46	2.4	22.8
1.62	54	5.1	140
1.74	58	5.3	509.5
1.92	65	19.9	dissolved
1.95	67	17.4	dissolved
2.06	71	18.3	dissolved
2.09	72	25.1	dissolved

[a]Membranes could not be prepared for low sulfonation levels due to the limited solubility of the membranes in the *N,N*-dimethylacetamide solvent.

The DS is critical to the proton conductivity, fuel cell performance, and stability of the sulfonated polymers. High DS usually leads to higher proton conductivity, but

sometimes results in high methanol crossover, high liquid (water) swelling, and poor stability. Low DS results in low proton conductivity and poor fuel cell performance, which is not enough for application. Therefore, the DS must be optimized to get the satisfactory proton conductivity as well as mechanical property.

Usually, non-fluorinated membranes like SPEEK show lower methanol crossover than Nafion membrane due to their different structure [104]. Based on the SAXS data and a cubic hydrophilic channel system in a hydrophobic matrix, a model for the microstructure was proposed and compared with Nafion membrane (Fig. 1.7) [91].

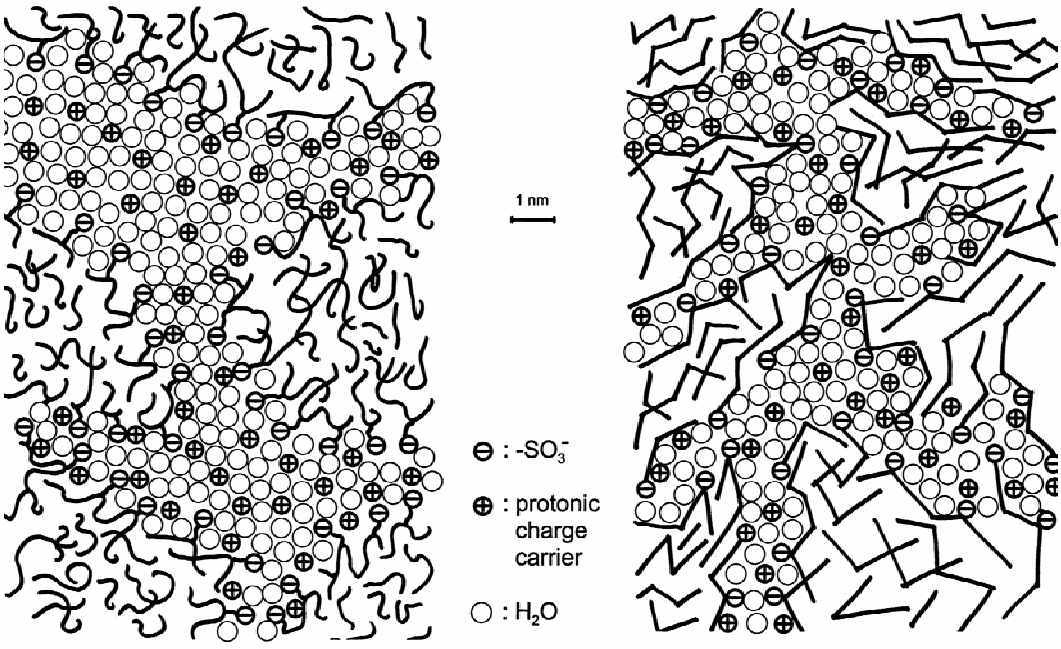

(a) (b)

Figure 1.7. Schematic representation of the microstructures of (a) Nafion and (b) a sulfonated poly(ether ether ketone ketone) (SPEEKK) [91].

The water filled channels in SPEEKK are narrower compared to those in Nafion. They are less separated and they have larger hydrophilic/hydrophobic interface (larger average separation of neighboring sulfonic acid functional groups). The stronger confinement of the water in the narrow channels of the aromatic polymers leads to a significantly lower dielectric constant of the water of hydration, leading to much lower methanol crossover than Nafion membrane [91]. In addition, the pK_a value of sulfonic acid in sulfonated PEEKK is around – 1, which is much higher than that of the Nafion membrane ($pK_a \sim -6$), leading to lower proton conductivity and usually lower fuel cell performance.

Many studies have focused on the physical properties such as swelling, thermal stability, methanol permeability, and proton conductivity. However, little information is available on the performance of DMFC, and the long-term stabilities of these hydrocarbon polymers need to be investigated before they can get practical use in DMFC. In addition, development of composite membranes based on the above-mentioned polymers is also being pursued [114-118]. In the meantime, many efforts are being made to explore suitable membranes for DMFC by blending two or even three of the above-mentioned polymers [119-121]. Covalent cross-linking of the ionomer membranes has also been tried to reduce the strong swelling of membranes with high degree of sulfonation. Unfortunately, the proton conductivity is usually sacrificed at the same time.

1.3 OBJECTIVES OF THIS DISSERTATION

The objective of this dissertation is to design and develop proton exchange membranes that can overcome some of the problems encountered with the conventional Nafion membrane. Several membrane systems are designed and investigated systematically, and their advantages and disadvantages compared to Nafion are presented. The primary membrane characteristics such as proton conductivity, thermal stability, swelling behavior, and proton conduction mechanism are investigated. The membranes are tested in practical fuel cells. The knowledge gained can provide a better understanding of the proton conduction mechanisms and help in designing new membrane materials. With this perspective, this dissertation focuses specifically on the following:

(1) With an aim to develop other polymer material as proton exchange membrane for DMFC with low methanol crossover, commercial aromatic polymer material (polysulfone) is chosen as starting material and sulfonated polysulfone is synthesized and investigated for use in DMFC. Sulfonated polysulfone is expected to have low cost and offer good fuel cell performance. The variations of % liquid uptake at different temperatures and methanol concentrations, proton conductivity, methanol crossover, and polarization data in DMFC with various degree of sulfonation are studied. The optimum conditions under which the membrane will have acceptable proton conductivity and satisfactory fuel cell performance are identified.

(2) With an aim to investigate the role of imidazole as a proton solvent in Nafion

membrane, Nafion-Imidazole composite membrane is prepared and investigated. The variations of proton conductivity and polarization data in high temperature PEMFC are studied. To overcome the poisoning of imidazole on the Pt catalyst, strategy of doping with phosphoric acid is adopted. In addition, non-platinum catalysts such as Pd-Co-Mo alloy to improve the fuel cell performance and lower the poisoning of imidazole is pursued. Based on the study of the Nafion-Imidazole system, molecules and polymers with novel structures (benzimidazole or amino-benzimidazole) and viable synthesis routes are designed.

(3) With an aim to explore molecules containing benzimidazole groups, 1,3-1*H*-dibenzimidazole-benzene is synthesized and investigated. A new synthesis route is adopted and the structure is confirmed. Blend membranes consisting of sulfonated polysulfone and 1,3-1*H*-dibenzimidazole-benzene are investigated by the measurements of proton conductivity, polarization data, and methanol crossover in DMFC. Additionally, a relationship between proton conduction and the ratio of sulfonic acid to benzimidazole is established.

(4) With an aim to develop polymer materials with benzimidazole and good stability, polysulfone containing benzimidazole side groups is designed and developed. An easy synthesis route is developed and the structure is carefully characterized. Blend membranes with sulfonated poly(ether ether ketone) (SPEEK) are investigated by measuring proton conductivity, liquid uptake, ion exchange capacity, and polarization data for high temperature PEMFC. In addition, a proton conduction mechanism is proposed and validated in DMFC by polarization data and methanol

crossover.

(5) With an aim to further improve proton conduction as well as fuel cell performance and lower methanol crossover, polysulfone containing amino-benzimidazole or amino-triazole is designed and developed. Blend membranes fabricated with SPEEK are investigated by proton conductivity, liquid uptake, polarization data and methanol crossover in DMFC.

Chapter 2

Experimental Procedures

In this dissertation, all commercial chemicals were used as received without further purification.

2.1 MATERIAL SYNTHESIS

Most of the material synthesis conditions, preparation procedures, and membrane fabrication processes will be described in the respective Chapters. The general procedures adopted are presented in this Chapter.

2.2 NAFION MEMBRANE PRE-TREATMENT

Usually, the commercial Nafion membranes need to be pre-treated before use. The common membrane cleaning procedure is given below. The membranes were boiled for over 1 h in 5 % hydrogen peroxide (H_2O_2) to remove the organic impurities. Then they were rinsed in de-ionized water several times and boiled in 0.5 M H_2SO_4 for another 1 h to exchange any cations like Na^+ to H^+ in the membrane. Finally, the membranes were rinsed in boiling deionized water for another 1 h. The membranes were then stored in de-ionized water before use.

2.3 MATERIALS CHARACTERIZATION

The general materials characterization methods used in this study will be discussed here briefly and the special details will be presented in the respective chapters.

2.3.1 Differential Scanning Calorimetry (DSC)

A Perkin-Elmer series 7 differential scanning calorimeter (DSC) was used to study the thermal behaviors such as phase transition, decomposition, and melting point. Usually, the experiments were conducted with around 10 mg of sample in N_2 atmosphere at a heating rate of 10 ^{o}C/min.

2.3.2 Thermogravimetric Analysis (TGA)

A Perkin-Elmer series 7 thermogravimetric analyzer (TGA) was used to study the change in mass with temperature of the samples, especially the decomposition. Usually, the experiments were carried out at a heating rate of 5 ^{o}C/min in a flowing air atmosphere.

2.3.3 Liquid Uptake of Polymer Membranes

Liquid uptake of the polymer membranes was calculated by the difference between the dry mass (m_{dry}) and wet mass (m_{wet}) of a membrane sample. The dry weight was measured after the sample was dried at 110 ^{o}C under vacuum for 24 h. To obtain the wet mass, a membrane was equilibrated with de-ionized water or methanol solution at different temperatures for 1 h. The wet membrane was then blotted carefully with a filter

paper to remove surface water droplets before weighing. The percent liquid uptake was determined using the following formula:

$$\text{Percentage Uptake} = (m_{wet} - m_{dry}) \cdot 100 / m_{dry} \qquad [2.1]$$

2.3.4 Proton Conductivity Measurement

The proton conductivities of the membranes were calculated from the impedance data, which were collected with a computer interfaced HP 4192A LF Impedance Analyzer, in the frequency range of 5 Hz ~ 13 MHz with an applied voltage of 10 mV. Measurements were carried out using a two-electrode setup and stainless steel was used as the blocking electrodes. In order to realize a good electrode/electrolyte contact, the electrode/membrane/electrode sandwich was pressed together by three screws. The components of the cell for impedance measurements are shown in Fig. 2.1.

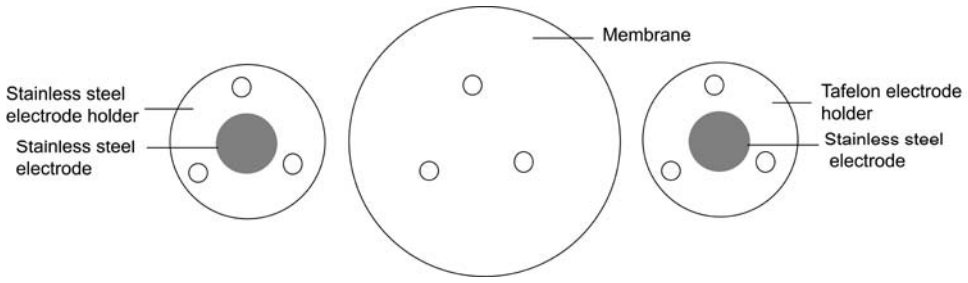

Figure 2.1. Schematic configurations of the cell components employed for impedance measurement.

For those measurements where humidity was needed, the sample fixture was put

into an environmental chamber (Model 9000L, VWR Scientific), where the temperature and humidity could be controlled. The data were collected after equilibrium was obtained and the impedance reached a stable value.

The conductivity of the membrane is calculated using the equation,

$$\sigma = l/RA \qquad [2.2]$$

where σ, l, R and A are, respectively, the ionic conductivity, thickness of the membrane, resistance of the membrane, and area of the electrode.

2.3.5 Fourier Transform Infrared (FT-IR) Spectroscopy

The structure of the synthesized materials was characterized using Fourier Transform Infrared (FT-IR) Spectroscopy with a Nicolet FT-IR instrument in nitrogen atmosphere. The scanned wavenumber range was 4000 to 400 cm^{-1}, and 116 spectra were recorded and averaged to reduce noise.

2.3.6 ^{1}H-NMR Spectroscopy

^{1}H-NMR spectra were recorded on a Varian INOVA-500 spectrometer at room temperature by dissolving the synthesized materials in dimethyl sulfoxide-d_6 (DMSO-d_6). Chemical shifts δ were expressed in parts per million (ppm).

2.4 MEMBRANE-ELECTRODE ASSEMBLY (MEA) PREPARATION

2.4.1 Electrode Preparation

(a) PEMFC electrodes: The anode and cathode consist of three layers: gas diffusion layer, catalyst layer, and Nafion layer. The gas diffusion layer was prepared by spraying a mixture of the Vulcan XC-72R carbon black, solvent (mixture of water and isopropyl alcohol in a volume ratio of 1:3), and 30 wt.% PTFE (Teflon T-30 Dispersion, E. I. Du Pont de Nemours & Co., Inc.) onto a teflonized carbon cloth (Electrochem. Inc.); the carbon black loading was 5 mg/cm^2. The catalyst layer was prepared by spraying a mixture of the required amount of carbon-supported catalyst, solvent (mixture of water and isopropyl alcohol in a volume ratio of 1:3), and 20 wt.% PTFE onto the gas diffusion layer, followed by sintering under vacuum at 280 ^{o}C for 2 h; the catalyst loading was 0.4 mg/cm^2. The Nafion layer was prepared by spraying diluted commercial 5 wt.% Nafion solution (mixture of isopropyl alcohol and Nafion solution in a volume ratio of 2:1) onto the catalyst layer and drying in an oven at 90 ^{o}C for 1 h.

(b) DMFC electrodes: The anode and cathode consist of two layers: gas diffusion layer and catalyst layer. The gas diffusion layer was prepared by spraying a mixture of the Vulcan XC-72R carbon black, solvent (mixture of water and isopropyl alcohol in a volume ratio of 1:3), and 40 wt.% PTFE onto a teflonized carbon cloth (Electrochem. Inc.) followed by sintering under vacuum at 280 ^{o}C for 2 h; the carbon black loading was 5 mg/cm^2. The catalyst layer was prepared by spraying a mixture of the required amount of carbon-supported catalyst, solvent (mixture of water and isopropyl alcohol in a volume ratio of 1:3), and Nafion solution onto the gas diffusion layer; the catalyst loading for

anode was 0.6 mg/cm^2, the catalyst loading for cathode was 1.0 mg/cm^2, and the content of Nafion was 33 wt.%. Finally, they were dried in an oven at 90 ^{o}C for 1 h.

2.4.2 Membrane-Electrode Assembly (MEA) Preparation

To prepare the MEA, a piece of the polymer membrane was sandwiched between an anode and a cathode; then they were hot pressed uniaxially using a Chemplex SpectroPress. For the MEA consisting of Nafion membrane, the hot-pressing temperature was 140 ^{o}C, the pressure was 1000 psi, and the pressing duration was 2 min. For the other MEAs containing non-Nafion membranes, the hot-pressing temperature was 142 ^{o}C, the pressure was 1500 psi, and the pressing duration was 2 min. The reason for higher hot-pressing temperature and higher pressure is due to the structural differences between non-Nafion membrane and Nafion in the electrode. Higher temperatures and higher pressures are beneficial for good contact between the membrane and electrode.

2.5 ELECTROCHEMICAL EVALUATION

The electrochemical performances of the MEAs in PEMFC and DMFC were evaluated with a commercial fuel cell test system (Compucell GT, Electrochem Inc.) using a single cell fixture having an active area of 5 cm^2 (Fig. 2.2). The experimental results were collected under steady-state conditions.

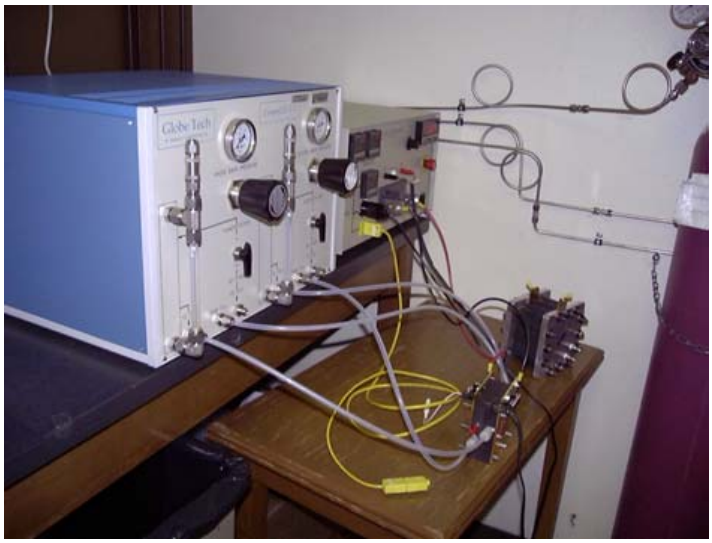

Figure 2.2. Single cell fuel cell test station used in this study.

2.5.1 PEMFC Evaluation

For PEMFC evaluation, high purity hydrogen (H_2) and oxygen (O_2) were fed, respectively, into the anode and cathode. The temperature, pressure, humidity, and gas flow rates could be controlled through the test station. The humidification and temperature of H_2 and O_2 were controlled by bubbling through water contained in stainless steel bottles at a specified temperature.

2.5.2 DMFC Evaluation

Around 1 liter methanol solution was stored in a glass flask which was heated with a heating mantle (Electrothermal Engineering Ltd.), while the temperature in the flask was monitored and controlled. The flask has four ports at the top: one for a temperature probe, one for an outlet supplying methanol solution to the pump/cell, one for an air condenser, and the last one for the inlet return from the cell. Usually, the methanol solution with

certain concentration (1 M or 2 M) was preheated to the same temperature as the cell operating temperature and was fed into the anode at a flow rate of 2.5 mL/min controlled by a peristaltic pump without back pressurization. Oxygen was fed into the cathode side at a flow rate of 200 mL/min with a back pressure of 20 psi, and the humidification temperature was same as cell operating temperature.

2.5.3 Methanol Crossover Evaluation

Methanol crossover was evaluated in the same single DMFC by a qualitative method [122]. Methanol solution was fed into the anode side while the cathode side was kept in an inert humidified N_2 atmosphere with a temperature same as the cell operating temperature. By applying a positive potential at the cathode side from 0 to 1 V, the methanol permeation flux through the membrane could be calculated by measuring the transport-controlled limiting current of the methanol electro-oxidation process at the Pt/membrane interface at the cathode. During the measurement, the fuel cell was kept at open circuit state. The limiting current of the methanol electro-oxidation was collected by using voltammetry (PGZ 402, VoltaLab).

Chapter 3

Synthesis and Characterization of Sulfonated Polysulfone for Direct Methanol Fuel Cells

3.1 INTRODUCTION

As discussed in Section 1.2.4.2, various alternate polymer materials have been developed as proton exchange membranes for DMFC due to the high cost and high methanol permeability of Nafion membrane. Candidates, such as poly (ether ether ketone) (PEEK) [23,71,91,104], polyimidazole [123,124], polyimide (PI) and polysulfone (PSf) [95,125-128] have been widely investigated. They are cheap and easily synthesized, and most importantly they usually show much lower methanol permeability, which could greatly benefit the commercialization prospects of DMFC technology.

Membranes based on sulfonated poly(ether ether ketone) (SPEEK) have been demonstrated to have fuel cell performance comparable to that of Nafion but with much lower methanol crossover [104]. For a given water content, SPEEK has narrower hydrophilic channels and more branched with increased dead-ends compared to that in Nafion, leading to low water/methanol permeation, and alleviating the effects of methanol crossover [71,91,129]. Polysulfone (PSf), another available industrial product, has aromatic backbone similar to that in PEEK and is easy to be sulfonated. Low methanol crossover as SPEEK is expected for sulfonated PSf. In addition, polysulfone is also thermally and mechanically stable, which makes it a promising material as proton exchange membrane for DMFC applications.

Lufrano et al. [100,101] used a mild sulfonation process to prepare sulfonated polysulfone (SPSf) under room temperature. They compared the thermal stabilities of SPSf and PSf, and also the proton conductivities and PEMFC performances of SPSf membranes with those of Nafion membranes. However, previous studies did not explore SPSf membreans as promising candidates for DMFC, and little information is available on the performance of SPSf membrane in DMFCs as well on the methanol crossover through SPSf membranes. In this Chapter, SPSf membranes are systematically investigated in DMFC, and the optimum synthesis condition, membrane processing, and fuel cell operating conditions are discussed.

3.2 EXPERIMENTAL

The SPSf samples were synthesized by a sulfonation process of the commercial polysulfone Udel 1700 at room temperature [95,100,101,128]. 5 g of polysulfone were dissolved in 100 mL of chloroform at room temperature and subsequently treated with trimethylsilyl chlorosulfonate (Aldrich) to produce a silyl sulfonate polysulfone intermediate product. The amount of intermediate product depends on the mole ratio of sulfonating agent and polymer repeated units. A slight excess of sodium methoxide was added to the solution to cleave silyl sulfonate intermediate and to obtain the final sulfonated product. All samples were vigorously washed with methanol, rinsed several times with de-ionized water, and dried in a vacuum oven at 110 ºC for 24 h.

The degree of sulfonation was calculated from the ion exchange capacity (IEC) of SPSf. The IEC was determined by suspending 0.3 g of SPSf in 30 mL of 2 M NaCl

solution for 24 h to liberate the H^+ ions and then titrating with 0.1 M standard NaOH solution using phenolphthalein indicator.

The membranes were obtained by casting onto a glass plate a *N,N*-dimethylacetamide (DMAc) solution of SPSf polymer (~ 5 % w/v) and drying at 115 ºC overnight. The thickness of the membrane was controlled by changing the amount of SPSf in the solution and all the membranes in this study had a thickness of 100 ~ 120 μm.

The thermal stabilities of PSf and SPSf were assessed by TGA. Approximately 20 mg of samples was heated from room temperature to 600 ^oC at a rate of 5 ^oC/min under a flowing air atmosphere.

The percent liquid uptake was determined from the weight gain found on equilibrating the dry membrane (dried at 110 ºC for 24 h) in distilled water or methanol solution for 1 h at different temperatures. Proton conductivity values were obtained from the impedance data after equilibrating the membranes with water vapor at 100 % relative humidity (RH).

The anode catalyst was a commercial 40 % Pt-Ru (1:1)/Vulcan (E-TEK) and the cathode catalyst was a commercial 20 % Pt/C (Alfa Aesar). The membrane-electrode assembly (MEA) was fabricated by uniaxially hot-pressing anode and cathode onto a SPSf membrane. A MEA consisting of Nafion 115 membrane was also prepared for comparison. 1 M or 2 M methanol solutions were pre-treated to the cell operating temperature and pumped through the anode side.

Methanol crossover was evaluated by the method as described in Chapter 2.

3.3 RESULTS AND DISCUSSION

3.3.1 Sulfonation of Polysulfone

The structures of polysulfone and synthesis of sulfonated polysulfone are shown in Fig. 3.1.

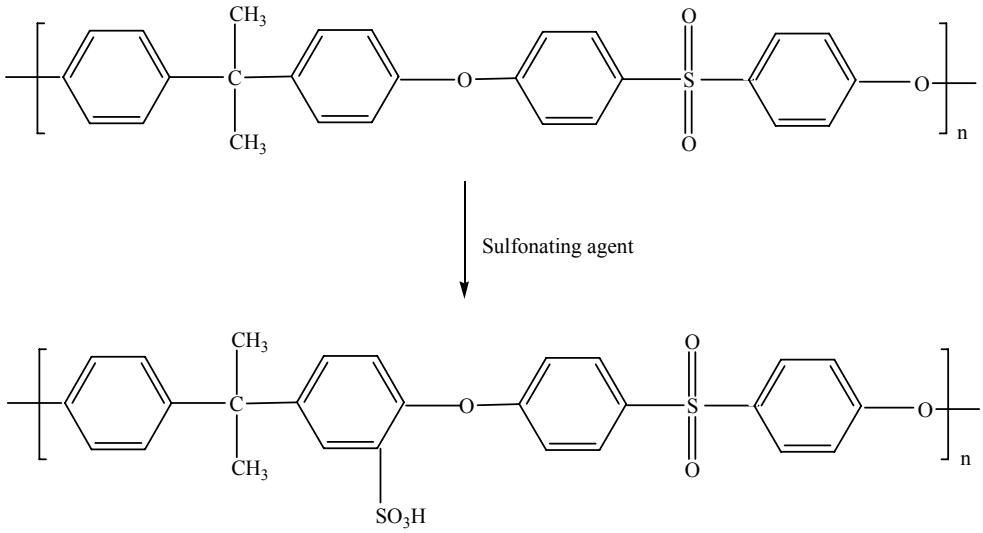

Figure 3.1. Synthesis of sulfonated polysulfone.

Chemical modification of polysulfone by different sulfonation procedures have been reported [100,130-132]. Usually there are two approaches. The first one is to carry out direct polymer sulfonation in heterogeneous media using sulfuric or chlorosulfonic acid as both solvent and sulfonating agent [131,132]. Sometimes, phase separation was found during the synthesis process, leading to uneven degree of sulfonation. The second one is to use the trimethylsilyl chlorosulfonate as sulfonating agent at room temperature, and the reaction medium is homogeneous. In this study, we adopted the second approach. Since

the sulfonation is an electrophilic substitution reaction, the substitution takes place in the position of the phenyl ring as shown in Fig. 3.1.

SPSf is soluble in polar aprotic solvents like DMAc, *N,N*-dimethylformamide (DMF), and dimethylsulfoxide (DMSO).

3.3.2 Determination of the Ion Exchange Capacity (IEC), Degree of Sulfonation (DS), and Liquid Uptake

The unit of IEC is milliequivalent per gram of the dry material (meq./g). It indicates the capacity of dissociated ions in the membrane. Comparison of IEC could give an idea of the capability of proton conduction in different materials. Usually, IEC was determined by the titration method. Certain amount of the dried sample was immersed in standard NaCl solution. The H^+ released from SPSf was titrated against standard NaOH solution. The quantity of sulfonic acid groups in the SPSf sample can be determined using the following equation:

$$N_{\text{-}SO3H} = (M \cdot V)_{NaOH} \qquad [3.1]$$

where M and V are, respectively, the molar concentration and volume of the standard NaOH solution consumed by released H^+. The IEC can then be obtained by the following equation:

$$\text{IEC} = (N_{\text{-}SO3H}/m_{sample}) \cdot 1000 \text{ (meq./g)} \qquad [3.2]$$

where m_{sample} is the mass of the dried SPSf sample.

The DS is calculated by the following equation:

$$DS = N_{\text{-}SO3H}/(N_{\text{-}SO3H} + N_{PSf}) \quad [3.3]$$

where N_{PSf} is the molar quantity of the PSf repeating unit without sulfonic acid groups. It is calculated by the following equation:

$$N_{PSf} = (m_{sample} - N_{\text{-}SO3H} \cdot M_1)/M_2 \quad [3.4]$$

where M_1 = 522 and M_2 = 442 are the molecular weights of the repeating unit of PSf containing sulfonic acid groups and that of PSf without sulfonic acid groups. So the DS can be calculated from equations 3.2, 3.3, and 3.4, as shown in equation 3.5 below:

$$DS = 442 \cdot IEC/(1000 - 80 \cdot IEC) \quad [3.5]$$

Table 3.1 summarizes the DS, IEC, proton conductivity (σ) at 65 and 80 ºC and 100 % RH of the SPSf membranes prepared with various mole ratios of the sulfonating agent to the polymer-repeat unit (x). For a comparison, the data for Nafion 115 membrane are also given in Table 3.1. As the value of x increases, the DS, IEC and σ increase as expected. The conductivity of the SPSf membranes increases on increasing the temperature (from 65 to 80 ºC) similar to that found with Nafion, but the σ values are

lower than that of Nafion 115. For convenience, the SPSf membranes studied are hereafter designated as SPSf-28, SPSf-57, and SPSf-65 where the numbers refer to DS. Data for SPSf with DS > 65 are not presented as they exhibited severe swelling and consequent solubility in water [128].

Table 3.1. Ion exchange capacity (IEC), degree of sulfonation (DS), and proton conductivity (σ) of the SPSf membranes obtained with different mole ratios of the sulfonating agent to polymer-repeat units (x).

x	DS (%)	IEC (meq./g)	σ at 100 % RH (S/cm)	
			65 ºC	80 ºC
2.3	28	0.60	1.3×10^{-4}	1.9×10^{-4}
3.2	57	1.17	4.9×10^{-4}	1.7×10^{-3}
3.7	65	1.32	2.2×10^{-3}	3.1×10^{-3}
Nafion 115	-	0.91	3.2×10^{-2}	3.5×10^{-2}

Table 3.2 compares the percent liquid uptake at different temperatures and methanol concentrations for the SPSf membranes with various DS and for Nafion 115. The liquid uptake increases (i) as the temperature or the methanol concentration increases with a given DS and (ii) as the DS increases at a given temperature and methanol concentration.

Table 3.2. Comparison of the liquid uptake of SPSf and Nafion 115 membranes in methanol solution with various concentrations and at different temperatures.

Membrane	Methanol Concentration (M)	Liquid uptake (wt.%)	
		65 ºC	80 ºC
SPSf-28	0	9.1	13.7
	1	15.2	16.0
	2	16.7	18.3
SPSf-57	0	25.7	31.0
	1	34.2	46.0
	2	47.1	50.3
SPSf-65	0	39.4	53.6
	1	46.4	55.2
	2	50.4	57.1
Nafion115	0	24.0	26.6
	1	29.1	30.2
	2	32.2	33.7

The liquid uptake generally reflects the trend in swelling, which is a critical issue for the MEA stability in fuel cells. At a DS of around 50 %, the liquid uptake, irrespective of water or methanol is being used, reaches the level generally found with the Nafion membrane. As the DS increases above 50 %, the increase in the number of sulfonic acid groups in SPSf leads to a higher absorption of water than that in Nafion 115. Interestingly, as the DS increases further, but below 70 %, the liquid uptake does not increase too much even at 80 ºC, unlike in the case of the SPEEK membranes [104].

3.3.3 TGA Analysis

Fig. 3.2 shows the TGA curves of plain PSf and SPSf with various degree of sulfonation.

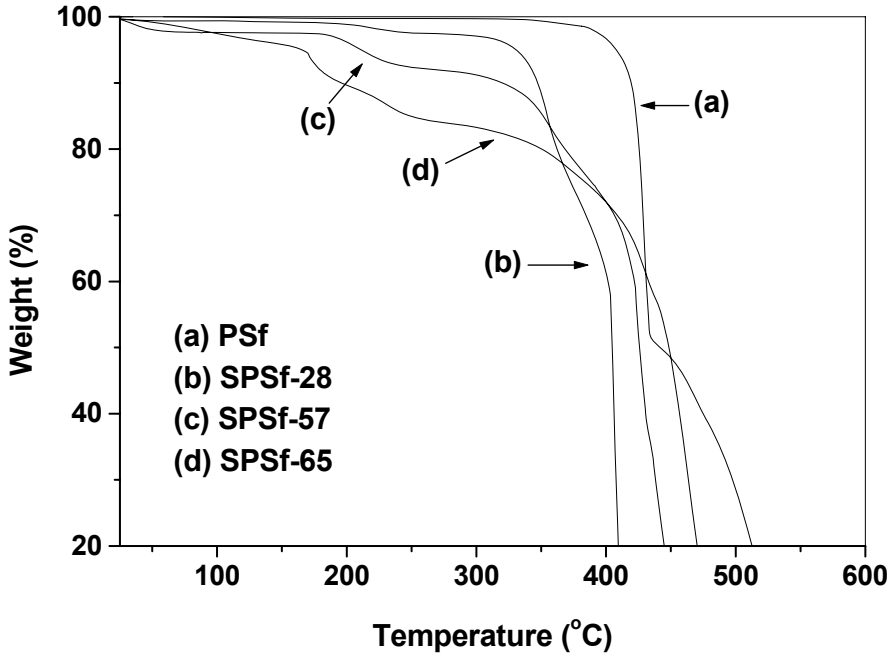

Figure 3.2. Thermogravimetric analysis of PSf and SPSf membranes in flowing air atmosphere at a heating rate of 5 ^{o}C/min.

In Fig. 3.2, the onset of weight loss of plain PSf starts at about 380 ^{o}C, which is due to the main chain decomposition. For the SPSf membranes, the onsets of weight loss start below 100 ^{o}C, which is due to the loss of water adsorbed to the sulfonic acid groups of SPSf. Besides that, there are two other weight loss steps. The first weight loss at around

200 ^{o}C is due to the sulfonic acid decomposition. The second weight loss is due to the main chain decomposition. The lower decomposition temperatures of SPSf compared to PSf is due to the enhancement of the irregularity of the PSf structure because of the introduction of the sulfonic acid groups. As the DS increases, the decomposition temperature decreases for the SPSf membranes. The data reveal that the SPSf-57 membrane shows good enough stability for fuel cell application.

3.3.4 DMFC Evaluation and Methanol Crossover Measurements

Fig. 3.3 compares the electrochemical performance data of the SPSf and Nafion 115 membranes in DMFCs at 65 and 80 ºC that were collected with 1 M methanol solution at the anode side. The SPSf-28 membrane with a DS of 28 % showed poor performance in DMFC due to its low σ arising from a lower DS and so it is not presented in Fig. 3.3. We can see from Fig. 3.3 that both the SPSf-57 and SPSf-65 membranes show better performances with lower polarization losses at 65 or 80 ºC than the Nafion 115 membrane despite lower proton conductivities. Particularly at low current densities, the performances of the SPSf membranes are much better than that of Nafion 115 with higher open circuit voltages (OCV).

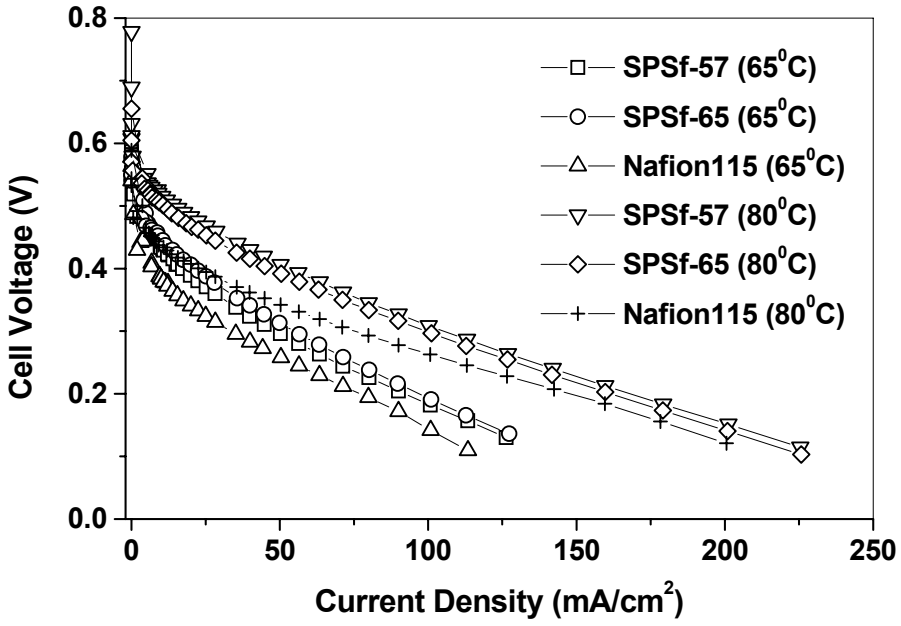

Figure 3.3. Comparison of the polarization curves of the SPSf membranes with that of Nafion 115 in DMFC. The data were collected with a methanol flow rate of 2.5 mL/min at the anode and an O_2 flow rate of 200 mL/min with a pressure of 20 psi at the cathode. The humidifier temperature for O_2 was same as the cell temperature. Anode: 0.6 mg PtRu/cm^2, cathode: 1.0 mg Pt/cm^2, and methanol concentration: 1 M.

The better performance despite lower proton conductivities could be attributed to the lower methanol crossover, as indicated by a lower methanol crossover limiting current density compared to that for the Nafion 115 membrane in Fig. 3.4. Although the thickness of SPSf-57 and SPSf-65 membranes is similar to that of Nafion 115, the methanol crossover limiting current densities are only one third of that found with Nafion 115, indicating much lower methanol permeability [104].

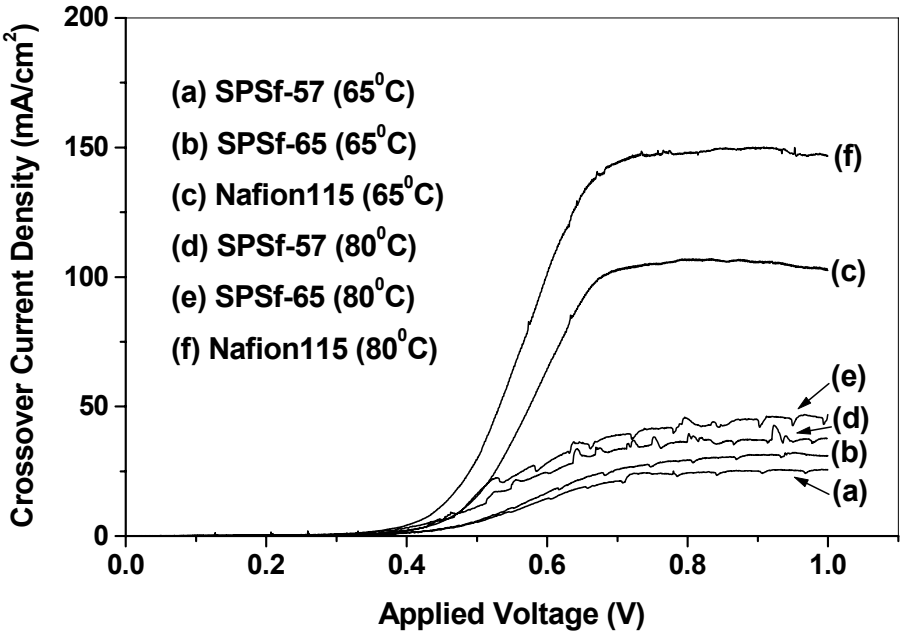

Figure 3.4. Comparison of the variations of the methanol crossover current density for the SPSf and Nafion 115 membranes in DMFC. Methanol concentration: 1 M.

Fig. 3.5 compares the electrochemical performance data of the SPSf-57 and SPSf-65 membranes with that of Nafion 115 at 65 and 80 ºC that were collected with 2 M methanol solution. For both the SPSf and Nafion 115 membranes, the performances are better than those found with 1 M methanol solution in Fig. 3.3 due to higher methanol flux. However, although the SPSf membranes show better performance than the Nafion 115 membrane with higher OCV at lower current densities due to lower methanol crossover as indicated by the data in Fig. 3.6, the performances of the SPSf-57 and SPSf-65 membranes at higher current densities are lower than that of Nafion 115 due to the lower proton conductivities.

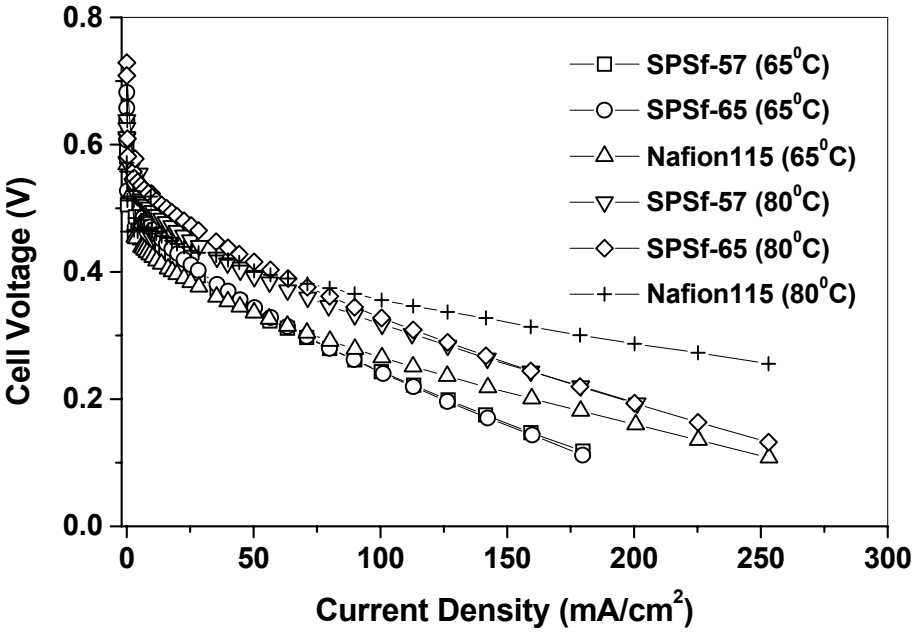

Figure 3.5. Comparison of the polarization curves of the SPSf membrane with that of Nafion 115 in DMFC. The experimental conditions were same as those in Fig. 3.3 excepting the methanol concentration was 2 M.

Both the SPSf-57 and SPSf-65 membranes show similar performances (with both 1 M and 2 M methanol solutions) despite the differences in the DS and higher proton conductivity for the SPSf-65 membrane. This is because of an increase in the methanol crossover as well with increasing DS as indicated by the data in Figs. 3.4 and 3.6. The higher methanol crossover encountered with the SPSf-65 membrane offsets the improvement gained with the higher proton conductivity. In Fig. 3.6, the plot of methanol crossover current of Nafion 115 at 80 ºC is not shown because it exceeded the current limit of our equipment.

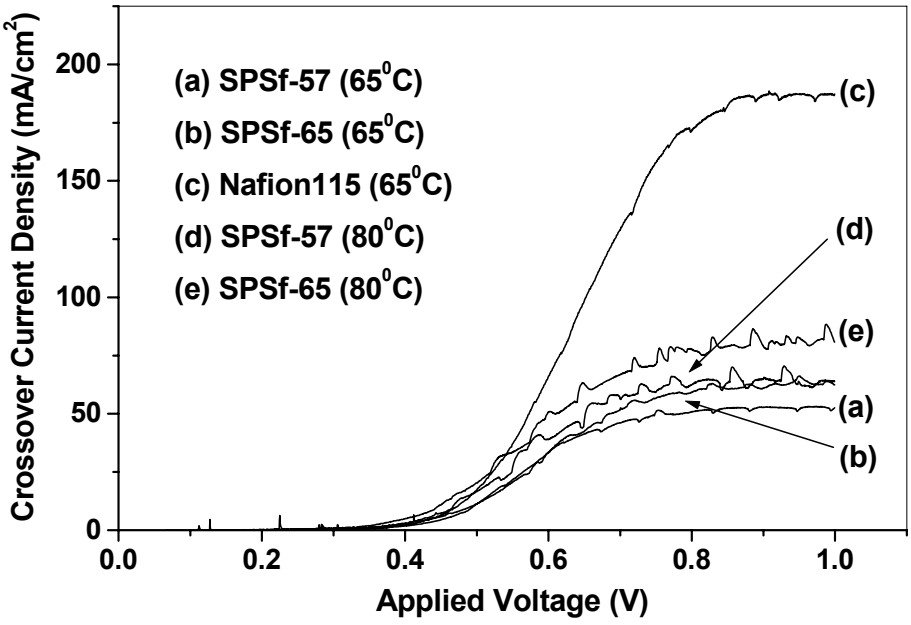

Figure 3.6. Comparison of the variations of the methanol crossover current density for the SPSf and Nafion 115 membranes in DMFC. Methanol concentration: 2 M. Since the current exceeded the limit of our equipment, the data for Nafion 115 at 80 ºC is not given.

The lower methanol crossover observed with the SPSf membranes compared to that with the Nafion 115 membrane could be attributed to the narrower pathways for methanol/water permeation in the former. As discussed in Section 1.2.4.2, the smaller separation between the hydrophobic and hydrophilic groups in SPEEK compared to that in Nafion leads to narrower, less connected hydrophilic channels, resulting in a stronger confinement of water/methanol in the narrow channels and significantly lower water/methanol permeation [71,91,133]. SPSf has an aromatic backbone similar to that in SPEEK, and so SPSf can also be expected to have a smaller separation between the

hydrophobic and hydrophilic groups, resulting in a lower methanol permeation.

Although the SPSf membranes exhibit lower methanol crossover than Nafion 115 membrane in DMFC, separation of the MEAs from the SPSf membranes were observed after 2 days of operation. This finding is similar to that found before for the SPEEK membranes in PEMFC and DMFC [104,134]. The separation of the MEAs is due to the poor adhesion properties of the SPSf membranes [135]. Modifications in the MEA fabrication such as the use of SPSf solution instead of Nafion solution to spray onto the electrodes as bonding resin could help in this regard.

3.4 CONCLUSIONS

The electrochemical performances of SPSf membranes with different degrees of sulfonation have been investigated in DMFC. SPSf membranes with 50 ~ 70 % sulfonation exhibit performances comparable to that of Nafion 115 due to lower methanol crossover, but the performances at high current densities with high concentrations of methanol (2 M) are lower than that of Nafion 115 due to the lower proton conductivity. However, separations of the electrodes from the SPSf membranes were observed after 2 days of operation in DMFC due to the poor adhesion and bonding properties. Further work is needed to overcome this problem and fully assess the long-term stability. Nevertheless, the lower cost and methanol crossover compared to those of Nafion make the SPSf membranes promising alternatives for DMFC.

Chapter 4

Nafion-Imidazole-H_3PO_4 Composite Membranes for Proton Exchange Membrane Fuel Cells

4.1 INTRODUCTION

As discussed in Section 1.2.3.1, there have been many attempts to modify the Nafion membrane so that it can offer adequate proton conductivity at elevated temperatures. One approach is to incorporate hygroscopic inorganic nanoparticles such as $SiO_2 \cdot nH_2O$, $TiO_2 \cdot nH_2O$, $Zr(HPO_4)_2 \cdot nH_2O$ and $Ta_2O_5 \cdot nH_2O$ into Nafion, which can help it retain water at elevated temperatures. Another strategy is to replace water in Nafion by anhydrous proton solvents like imidazole [50]. Kreuer et al. [68] were the first to use imidazole and pyrazole (heterocycles) as proton solvents in sulfonated poly(ether ether ketone) (SPEEK) to promote proton conduction under low humidity conditions. These membranes containing the heterocycles as proton solvents were found to show good proton conduction behavior at elevated temperatures unlike the plain Nafion or SPEEK membranes. Under anhydrous conditions, a Grotthuss-type mechanism is preferred for proton conduction. The proton conducting solvent should enable the formation of protonic defects and provide strongly fluctuating proton donor and acceptor functions. The basic nitrogen sites of the heterocycles such as imidazole and pyrazole can act as strong proton acceptors with respect to the sulfonic acid groups, forming the protonic charge carriers $(C_3H_3N_2H_2)^+$ [68]. Compared to water, these heterocycles are good proton solvents at temperature higher than 100 ^oC.

Accordingly, efforts have been made to replace water in proton exchange membranes by imidazole or pyrazole derivatives [69,72,74,75,124,136-138]. Unfortunately, due to the adsorption of imidazole onto the platinum catalyst (poisoning effect) [50], it has been difficult to obtain fuel cell performance data with Nafion-Imidazole membranes. Yamada et al. [139] were, however, able to test the acid-base hybrid materials obtained by mixing imidazole and the strong phosphoric acid polymer poly(vinylphosphoric acid) (PVPA) and found a low current density of < 100 mA/cm^2 and an open circuit voltage (OCV) of ~ 0.75 V. Recently, study in our group showed that non-platinum catalysts such as Pd-Co-Au and Pd-Co-Mo exhibit performance close to that of commercial Pt catalyst in PEMFC at 60 ºC with conventional Nafion membrane [140,141]. The Pd-Co-Au and Pd-Co-Mo catalysts were also found to show better tolerance to methanol compared to Pt, suggesting that these catalysts may have the possibility of showing better tolerance to imidazole as well. With this perspective, the preparation of Nafion-Imidazole membranes, their doping with H_3PO_4, and a comparison of the performances of the membrane-electrode assemblies in single cell PEMFC with both Pt and the newly developed Pd-Co-Mo catalysts are presented in this Chapter.

4.2 EXPERIMENTAL

Nafion 115 membranes were pre-treated as described in Section 2.2 and dried in a vacuum oven at 100 C overnight to remove almost all the water. The Nafion-Imidazole membranes were prepared by soaking the pre-treated, dried Nafion membranes in

imidazole-methanol solutions of various concentrations at 55 ^{o}C for 2 h, followed by drying in a vacuum oven at 90 ^{o}C for 5 h. The imidazole content in the Nafion-Imidazole membranes were calculated from the weight gains of the dried membranes before and after soaking in the imidazole-methanol solutions. The ratio n = [Imidazole]/[-SO_3H] in the composite membranes could be obtained from the imidazole content and the equivalent weight (EW = 1100) of the Nafion 115 membrane, which is calculated using the following equation as

$$n = [\text{Imidazole}]/[\text{-}SO_3H] = EW \cdot \Delta m / M_3 \cdot m_{Nafion} \quad [4.1]$$

where Δm is weight gain of the dried membranes before and after soaking in the imidazole-methanol solutions, M_3 = 68.08 is the molecular weight of imidazole, m_{Nafion} is the mass of dried Nafion membrane.

Nafion-Imidazole-H_3PO_4 membranes were prepared by soaking the dry Nafion-Imidazole membranes in 85 wt.% H_3PO_4 solution at 60 ^{o}C for 4 h, followed by removing the surface H_3PO_4 by rinsing with de-ionized water and drying in a vacuum oven at 90 ºC for 5 h. Carbon-supported Pd-Co-Mo (70:20:10 atom %) catalyst with a metal(s) loading of 20 wt.% was prepared with a reverse microemulsion method as described elsewhere [140,141].

The proton conductivities of the membranes were obtained from impedance data and measured under anhydrous conditions. Cyclic voltammetry measurements were carried out with a typical three electrode cell containing an acetonitrile solution of 0.1 mol/dm^3

$N(C_4H_9)_4PF_6$ and 5×10^{-3} mol/dm^3 imidazole or imidazole-H_3PO_4 (1:1 mole ratio) and a potential sweep rate of 50 mV/s using a glassy carbon electrode, a platinum auxiliary electrode, and an Ag/AgCl reference electrode.

The MEA of Nafion-Imidazole composite membrane was fabricated by hot-pressing. A thin plain cast Nafion membrane (~ 15 μm) was inserted between the composite membranes and the electrodes on both the sides were then hot-pressed. A commercial 20 wt.% Pt on Vulcan XC-72R (E-TEK) catalyst was used as anode and cathode and Pd-Co-Mo/C was used only as a cathode. The electrodes were prepared by a spray technique as described in Section 2.4.1, and the catalyst metal loadings (Pt or Pd-Co-Mo) were 0.4 mg/cm^2.

4.3 RESULTS AND DISCUSSION

4.3.1 Determination of the Content of Imidazole in Nafion-Imidazole Composite Membranes

Table 4.1 gives the imidazole to sulfonic acid ratio n in the Nafion-Imidazole composite membranes prepared with various imidazole concentrations in methanol. The imidazole content in the Nafion-Imidazole membrane increases initially with increasing imidazole concentration in methanol and reaches a maximum of $n \approx 1.6$ around an imidazole concentration of 250 g/L. Further increase in imidazole concentration could not increase the imidazole content in the membrane and crystallized imidazole could be found on the surface of the composite membranes, implying a saturation of the membrane by imidazole. For $n < 1$, the number of imidazole molecules in the Nafion-Imidazole

membrane is less than the number of $–SO_3H$ groups, and so the imidazole molecules may be completely involved in forming protonic charge carriers $(C_3H_3N_2H_2)^+$ by combining with the H^+ ions [68]. For n > 1, some free imidazole molecules may be present in the membranes.

Table 4.1. Effect of imidazole concentration in methanol on the imidazole content in the Nafion-Imidazole composite membranes.

Imidazole concentration in methanol solution (g/L)	50	150	200	250
Imidazole content in the membrane, n = [Imidazole]/[$-SO_3H$]	0.46	1.29	1.57	1.62

4.3.2 Proton Conductivity of Nafion-Imidazole Composite Membranes

The proton conductivities of the Nafion-Imidazole membranes measured under anhydrous conditions are compared with that of plain Nafion membrane in Fig. 4.1. At room temperature, the Nafion-Imidazole membranes exhibit lower proton conductivity than plain Nafion due to the decreased amount of water as a proton conducting solvent. However, the proton conductivity of the plain Nafion membrane decreases with increasing temperature due to the decreasing water content in the membrane, while those of the Nafion-Imidazole membranes increase with increasing temperature due to the presence of imidazole as the proton solvent instead of water. In the water environment, proton conduction occurs by a vehicle-type mechanism. But in the imidazole environment, a fast Grotthuss-type mechanism plays a primary role because the rather isometric molecules ($(C_3H_3N_2H_2)^+$) are advantageous for extended local dynamics with

their protonated and unpronated nitrogen functions acting as donors and acceptors in proton transfer reactions [68].

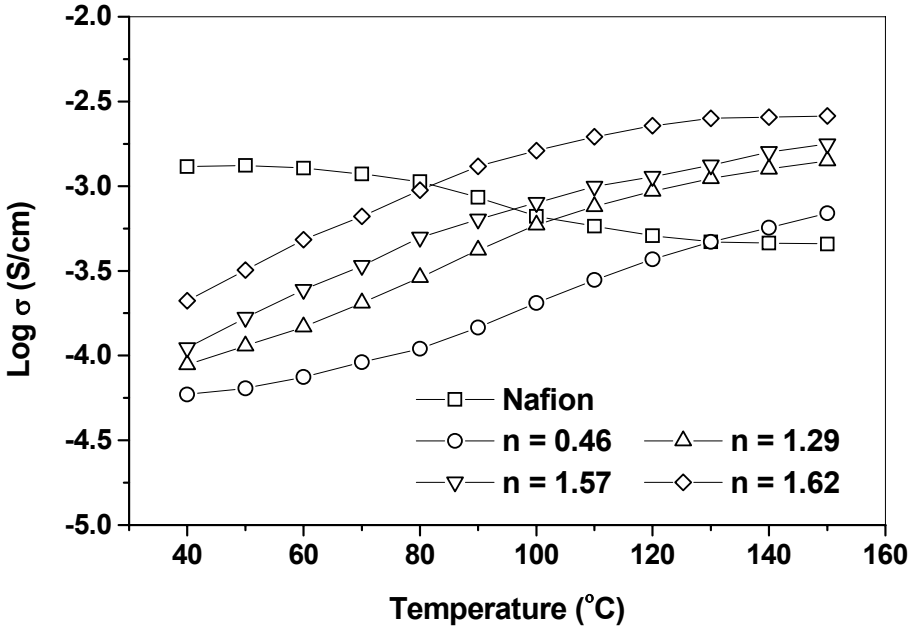

Figure 4.1. Proton conductivity of Nafion and Nafion-Imidazole composite membranes under anhydrous conditions.

The increasing temperature not only helps the proton transfer from donors to acceptors but also enhances the reorientation of the imidazole chain, which has been found to be rate-determining [73], resulting in an increase in proton conductivity with temperature. Also, the proton conductivity increases with the imidazole content in the Nafion-Imidazole membrane. This is because the spatial hindrance of proton transfer is reduced due to the availability of more neighbors around each imidazole molecule.

However, the proton conductivity reaches a maximum at n = 1.62. Efforts to increase the proton conductivity further by employing higher concentration solutions of imidazole in methanol were unsuccessful since homogeneous composite membrane could not be obtained as pointed out earlier. This could be related to the limited size of the clusters in the Nafion membrane (~ 5 nm) [142].

4.3.3 TGA Analysis

Fig. 4.2 compares the TGA plots of the Nafion-Imidazole membranes with that of plain Nafion membrane. The membranes lose weight in two steps. While the first step at T < 200 ^{o}C corresponds to the loss of the proton solvent (water or imidazole), the second step at T > 200 ^{o}C corresponds to the degradation of the $–SO_3H$ groups [143]. The first weight loss step occurs at temperatures as low as 40 ^{o}C in plain Nafion while it begins to occur around 100 ^{o}C in the Nafion-Imidazole membranes. This suggests a much stronger interaction between imidazole and $–SO_3H$ group compared to that between water and $–SO_3H$. Above 100 ^{o}C, the imidazole molecules that are free in the membrane begin to diffuse out from the membrane. This is consistent with the increase in the first weight loss step with increasing n. Moreover, the second weight loss step corresponding to the degradation of the $–SO_3H$ groups also shift to higher temperatures (> 300 ^{o}C) in the Nafion-Imidazole membranes compared to that in the plain Nafion membrane (~ 200 ^{o}C). Thus the replacement of water by imidazole improves the thermal stability of Nafion.

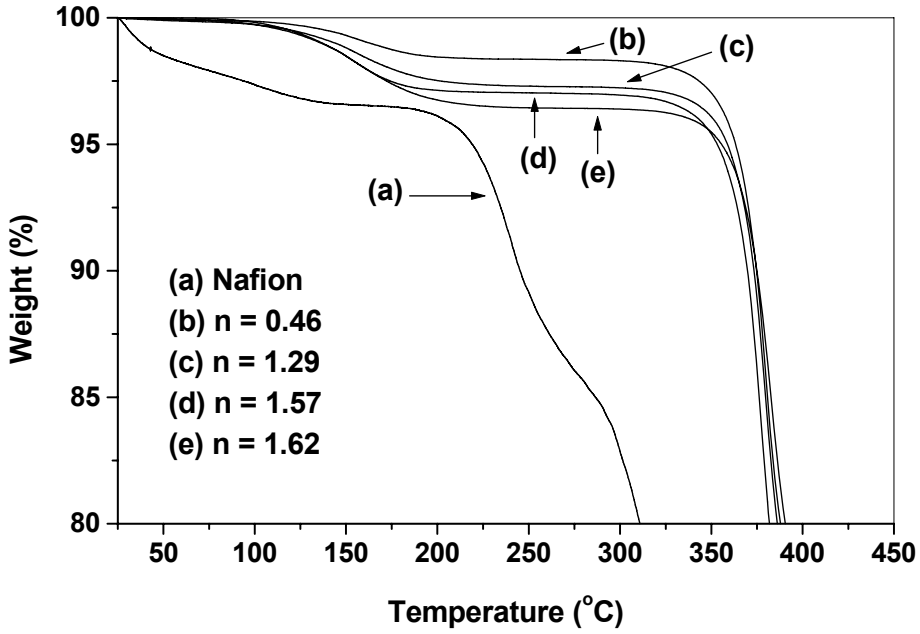

Figure 4.2. Thermogravimetric analysis plots of Nafion and Nafion-Imidazole membranes in flowing air atmosphere at a heating rate of 5 ^{o}C/min. The n values refer to the imidazole/-SO_3H ratio in the membrane.

4.3.4 Proton Conductivity of Nafion-Imidazole-H_3PO_4 Composite Membranes

The idea of doping the Nafion-Imidazole membranes stems from the doping of poly(benzimidazole) (PBI) with H_3PO_4, which is known to give good performance in fuel cell at higher temperatures [61]. No poisoning of Pt by phosphoric acid doped PBI occurs even though PBI has a structure similar to imidazole excepting the bonding of imidazole to phenyl rings. Recognizing this, we adopted a strategy in which imidazole is doped with

phosphoric acid to form the imidazolium salt as shown in Fig. 4.3.

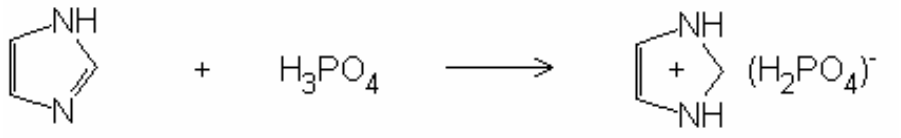

Figure 4.3. Illustration of the 'imidazolium salt formation' upon doping imidazole in the Nafion-Imidazole composite membrane with H_3PO_4.

Fig. 4.4 compares the proton conductivity of the Nafion-Imidazole-H_3PO_4 membrane with those of plain Nafion and Nafion-Imidazole membranes under anhydrous condition. Unlike the Nafion-Imidazole membrane, the proton conductivity of the doped Nafion-Imidazole-H_3PO_4 membrane decreases with increasing temperature as in the case of plain Nafion membrane. This is due to the transformation of the imidazole molecules into salts (as shown in Fig. 4.3), which are not very hydrophilic and could not play an effective role in the dissociation of protons from the sulfonic acid groups attached to the Nafion backbones [69], and the difficulty of reorientation of the imidazole molecules after forming salts, which is the most important factor for proton mobility in imidazole environment [73]. However, the Nafion-Imidazole-H_3PO_4 membrane shows higher conductivity than the plain Nafion membrane, but lower conductivity than the Nafion-Imidazole membrane under anhydrous conditions.

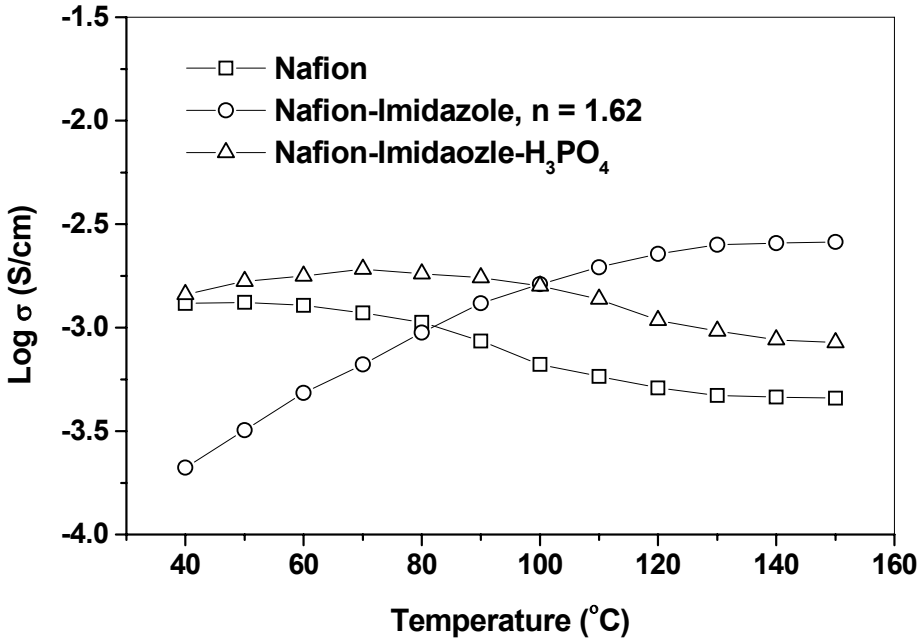

Figure 4.4. Comparison of the proton conductivities of Nafion, Nafion-Imidazole, and Nafion-Imidazole-H_3PO_4 membranes in the temperature range of 40 ~ 150 ^oC under anhydrous conditions.

4.3.5 Electrochemical Characterization of Nafion-Imidazole Based Composite Membranes

For n > 1, the free imidazole molecules present can form salt with H_3PO_4 and thereby suppress the poisoning effect on Pt catalyst. Fig. 4.5 compares the polarization curves of the Nafion-Imidazole and Nafion-Imidazole-H_3PO_4 membranes at low temperatures (60 and 80 ^oC).

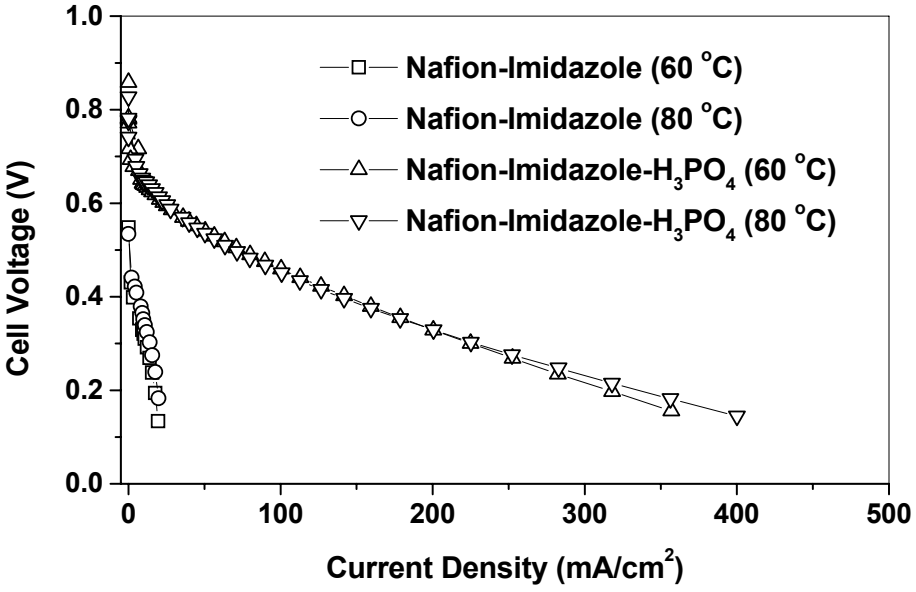

Figure 4.5. Comparison of the fuel cell performances (polarization curves) of the Nafion-Imidazole and Nafion-Imidazole-H_3PO_4 composite membranes with the Pt/C catalyst.

The Nafion-Imidazole-H_3PO_4 membrane shows much better performance compared to the Nafion-Imidazole membrane due to a suppression of the imidazole poisoning effect on Pt. Although one would expect an increase in the catalytic activity of Pt on going from 60 to 80 ^oC, the performance in Fig. 4.5 does not change much due to the possible dissociation of some imidazolium salts at higher temperatures and a consequent increase in the imidazole poisoning effect, which is also supported by the decrease in the OCV value as seen in Table 4.2. A comparison of the OCV values in Table 4.2 before and after doping with H_3PO_4 clearly demonstrates a suppression of the imidazole poisoning effect

on doping with H_3PO_4 as indicated by higher OCV values.

Table 4.2 Open-circuit voltages (OCV) of the Nafion-Imidazole composite membranes before and after doping with H_3PO_4.

Temperature (^oC)	60	80
OCV of undoped Nafion-Imidazole membrane (V)	0.548	0.534
OCV of doped Nafion-Imidazole-H_3PO_4 membrane (V)	0.858	0.827

To confirm this observation further, we compare in Fig. 4.6a and b the cyclic voltammograms of imidazole and imidazole-H_3PO_4 in $N(n\text{-}C_4H_9)_4PF_6$-CH_3CN solution in the presence of Pt catalyst. Clearly, a large irreversible oxidation peak is seen in the voltammogram of imidazole similar to that observed by Zhou et al. [144]. In contrast, no obvious redox peaks are observed in the case of imidazole-H_3PO_4 in the potential range of 0 to +1.8 V, indicating that the imidazolium dihydrogen phoshpate salt exhibits better electrochemical stability than imidazole under the fuel cell operating conditions. While the oxidation products formed in the case of bare imidazole can block the active sites of the Pt catalyst and degrade the electrochemical performance, such poisoning could be suppressed by doping imidazole with H_3PO_4.

Although H_3PO_4 doping suppresses the imidazole poisoning of the Pt catalyst to some extent, the fuel cell performance of the Nafion-Imidazole-H_3PO_4 membrane with Pt catalyst is still not close to being acceptable for application. This is because not all of the

imidazole molecules in the composite membrane could be transformed into the salt after doping, and any residual, free imidazole present can still poison the Pt catalyst. To overcome this difficulty, we then turned into new non-platinum catalysts.

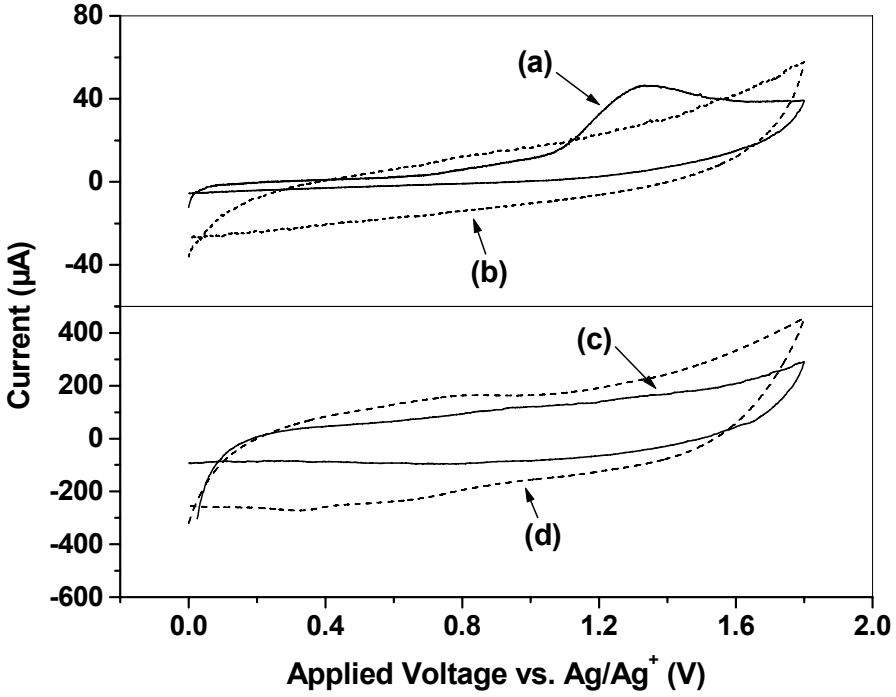

Figure 4.6. Typical cyclic voltammograms (first cycle) of Pt/C and Pd-Co-Mo/C catalysts in imidazole and imidazole-H_3PO_4 solution at 25 ºC: (a) Pt/C catalyst with imidazole, (b) Pt/C catalyst with imidazole-H_3PO_4, (c) Pd-Co-Mo/C catalyst with imidazole, and (d) Pd-Co-Mo/C catalyst with imidazole-H_3PO_4. The experiments were carried out with an acetonitrile (CH_3CN) solution consisting of 5×10^{-3} mol/dm^3 imidazole or imidazole-H_3PO_4 and 0.1 mol/dm^3 tetra-n-butylammonium hexafluorophosphate ($N(n\text{-}C_4H_9)_4PF_6$).

Figures 4.6c and d compare the cyclic voltammograms of imidazole and imidazole-H_3PO_4 in $N(n\text{-}C_4H_9)_4PF_6$-CH_3CN solution in the presence of the new Pd-Co-Mo catalyst. Only a minor irreversible oxidation peak is found in the voltammogram of imidazole in the presence of Pd-Co-Mo catalyst (Fig. 6c) compared to that found with the Pt catalyst in Fig. 6a, indicating that Pd-Co-Mo exhibits better electrochemical stability than Pt in the presence of imidazole. Moreover, no obvious redox peaks are observed in the voltammogram of imidazole-H_3PO_4 in the presence of Pd-Co-Mo.

Fig. 4.7 compares the performances in fuel cell (polarization curves) at 90 ºC of the Nafion, Nafion-Imidazole, and Nafion-Imidazole-H_3PO_4 membranes combined with the Pt and Pd-Co-Mo catalysts. Plain Nafion with the Pt catalyst shows the best performance, while Nafion-Imidazole with the Pt catalyst shows the worst performance with a huge polarization loss due to a strong poisoning of the Pt catalyst by imidazole. However, doping with H_3PO_4 decreases the polarization loss slightly in the presence of the Pt catalyst. In contrast, the Nafion-Imidazole-H_3PO_4 membrane with the Pd-Co-Mo catalyst shows much better performance with significantly low polarization loss compared to that with the Pt catalyst, even though the Pd-Co-Mo catalyst exhibits lower catalytic activity than Pt with plain Nafion membrane at this temperature (90 ^oC); Pd-Co-Mo shows catalytic activity similar to that of Pt at 60 ^oC with plain Nafion membrane [140,141]. The data indicate that the Pd-Co-Mo catalyst is more tolerant to imidazole poisoning than the Pt catalyst, which is consistent with the cyclic voltammogram results in Fig. 4.6.

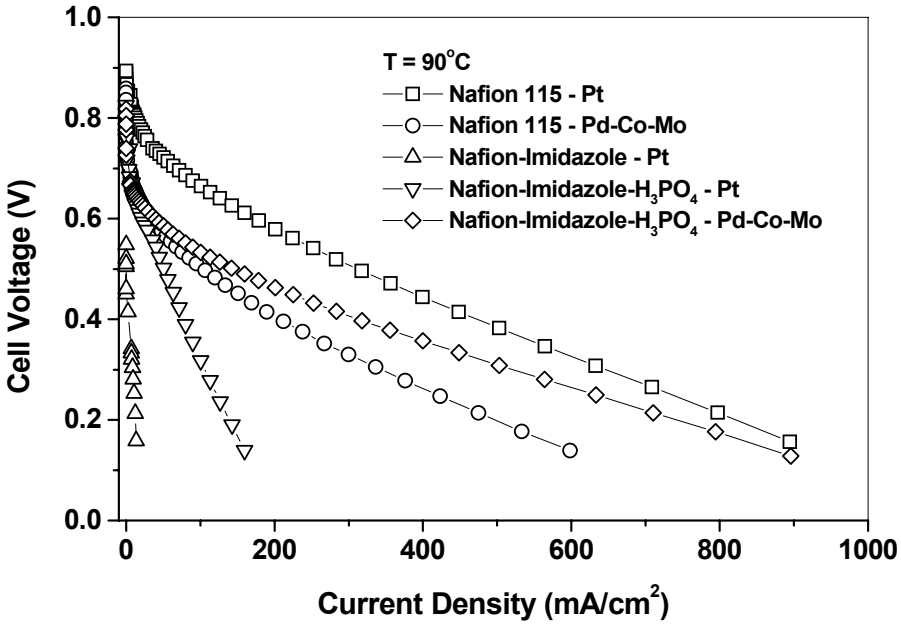

Figure 4.7. Comparison of the fuel cell performances (polarization curves) at 90 ^{o}C of the Nafion, Nafion-Imidazole, and Nafion-Imidazole-H_3PO_4 composite membranes with the Pt/C and Pd-Co-Mo/C catalysts.

Fig. 4.8 compares the fuel cell performances (polarization curves) at 100 ºC of the Nafion, Nafion-Imidazole, and Nafion-Imidazole-H_3PO_4 composite membranes combined with the Pt and Pd-Co-Mo catalysts. Plain Nafion with the Pt catalyst exhibits a larger polarization loss than that at 90 ^{o}C (Fig. 4.7) due to the lower proton conductivity resulting from a dryness of the membrane at 100 ^{o}C. In contrast, Nafion-Imidazole-H_3PO_4 with the Pd-Co-Mo catalyst shows much better performance than Nafion with the Pt catalyst due to the maintenance of still high enough proton conductivity through the hopping mechanism involving the imidazolium ions. The data

demonstrate that Nafion-Imidazole-H_3PO_4 membranes can perform better than Nafion at elevated temperatures (≥ 100 ^oC). Although the catalytic activity of Pd-Co-Mo catalyst at elevated temperatures is lower than that of Pt catalyst, the Nafion-Imidazole-H_3PO_4 membranes offer much better fuel cell performance with the Pd-Co-Mo catalyst than with the Pt catalyst due to a greater tolerance of Pd-Co-Mo to imidazole poisoning.

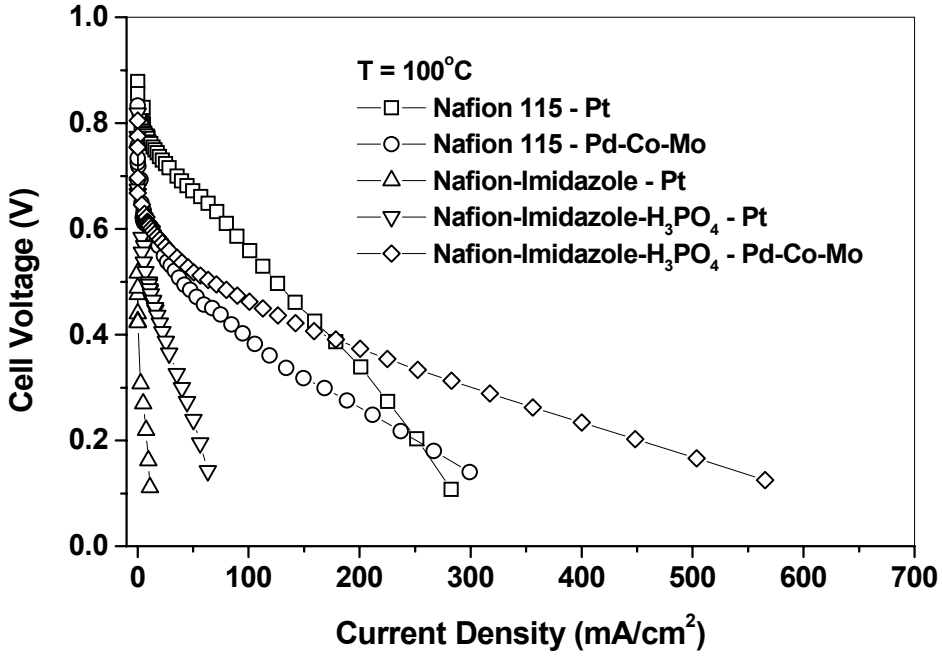

Figure 4.8. Comparison of the fuel cell performances (polarization curves) at 100 ^oC of the Nafion, Nafion-Imidazole, and Nafion-Imidazole-H_3PO_4 composite membranes with the Pt/C and Pd-Co-Mo/C catalysts.

4.4 CONCLUSIONS

Replacement of water by imidazole in Nafion offers higher operating temperatures for fuel cells, but imidazole poisons the Pt catalyst. Although the imidazole poisoning could be partly suppressed by doping the Nafion-Imidazole membranes with H_3PO_4, the performance of the Nafion-Imidazole-H_3PO_4 membranes with the conventional Pt catalyst is still much inferior to that of Nafion with the Pt catalyst. This difficulty could be overcome by employing a recently discovered Pd-Co-Mo catalyst with the Nafion-Imidazole-H_3PO_4 membranes. The Nafion-Imidazole-H_3PO_4 membranes with the Pd-Co-Mo catalyst offer electrochemical performance in PEMFC at 100 ^oC superior to that of Nafion membrane with the Pt or Pd-Co-Mo catalyst, demonstrating a tolerance of the Pd-Co-Mo catalyst to imidazole poisoning. The study demonstrates that water-free membranes based on Nafion and heterocycles that could successfully operate at elevated temperatures ($\geq$ 100 ^oC) could be developed with non-platinum catalysts such as Pd-Co-Mo. However, the long-term stability of the heterocycle groups within the membrane needs to be fully assessed in future studies.

Chapter 5

Synthesis and Characterization of Membranes Based on 1,3-1*H*-dibenzimidazole-benzene for Fuel Cells

5.1 INTRODUCTION

In Chapter 4, Nafion-Imidazole system was investigated as a membrane for fuel cell application. The poisoning of Pt catalyst by imidazole is a serious drawback for its application in fuel cell even though imidazole can promote proton conduction under anhydrous conditions. Also, diffusion of imidazole from the Nafion-Imidazole composite membrane is another issue. Therefore, other larger molecules or polymers containing N-heterocycles need to be designed and developed for practical application in fuel cells. In addition, it is difficult to achieve good proton conductivity after tethering imidazole to a polymer since it is hard for the imidazole molecule to reorient and the reorientation step has been found to be rate-determining for proton conduction through imidazole [73].

Complexes of polybenzimidazole (PBI) and phosphoric acid are known to be good candidates for high temperature PEMFC. The main repeating unit in PBI is benzimidazole, which play the primary role in proton transfer. Also, no poisoning of the Pt catalyst by PBI-doped membranes was found in fuel cells. In other words, benzimidazole is less poisonous than imidazole. In addition, the benzimidazole unit in PBI is known to support good proton conductivity after doping with H_3PO_4 without involving reorientation due to its lower pK_a value of 5.5 compared to 7.0 for imidazole, enhancing the possibility of achieving higher proton conductivity in the presence of

sulfonic or phosphoric acid environment. In this Chapter, the investigation of 1,3-1*H*-dibenzimidazole-benzene which consists of two benzimidazole groups, as a medium for proton transfer, was presented (Scheme 5.1).

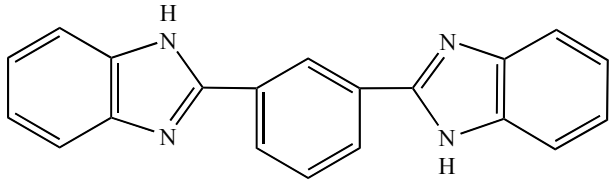

Scheme 5.1. Chemical Structure of 1,3-1*H*-dibenzimidazole-benzene.

The followings are the reasons for selecting 1,3-1*H*-dibenzimidazole-benzene. Firstly, it contains two benzimidazole groups, which could enhance the probability of proton transfer due to the more number of proton transfer sites. Secondly, synthesis of 1,3-1*H*-dibenzimidazole-benzene gives an opportunity to study the formation of benzimidazole, which would benefit the investigation of other material systems. Thirdly, the main parts of 1,3-1*H*-dibenzimidazole-benzene are phenyl rings, which are compatible with other aromatic polymers. Fourthly, although 1,3-di(substituted)-benzene has been found to have many applications such as an antitumour [145], there is no report on its use for fuel cell applications. In this Chapter, the synthesis of 1,3-1*H*-dibenzimidazole-benzene by a new method and its characterization are presented. To study its effectiveness to promote proton conduction, it is blended with sulfonated polysulfone and investigated for use in DMFC.

5.2 EXPERIMENTAL

1,3-1*H*-dibenzimidazole-benzene was synthesized by using phosphorus pentoxide-methanesulfonic acid (PPMA) as a dehydration agent. 3 g of phosphorus pentoxide was dissolved in 20 mL of methanesulfonic acid at room temperature while purging with dry nitrogen in a three-necked flask to prepare PPMA. 1.661 g (0.01 mol) of isophthalic acid and 2.163 g of 1,2-diaminobenzene (0.02 mol) were then added to PPMA and the mixture was stirred at 120 ^{o}C for 24 h. After the reaction was complete, the mixture was poured into de-ionized water to precipitate 1,3-1*H*-dibenzimidazole-benzene from the PPMA solution. The precipitate was then filtered and the solid was neutralized with 500 mL of 10 % NaOH solution overnight, followed by filtering and washing with de-ionized water before drying the product in a vacuum oven at 110 °C for 24 h. The details of the synthesis of SPSf are available in Chapter 3.

The structure of the synthesized 1,3-1*H*-dibenzimidazole-benzene was analyzed by FT-IR and ^{1}H-NMR. The thermal properties of 1,3-1*H*-dibenzimidazole-benzene were assessed by differential scanning calorimetry (DSC) with a heating rate of 10 ^{o}C/min under a flowing nitrogen atmosphere from room temperature to 200 ^{o}C and thermogravimetric analysis (TGA) at a heating rate of 5 ^{o}C/min under flowing air from room temperature to 600 ^{o}C.

The plain SPSf membrane as well as the blend membranes consisting of SPSf and various amounts of 1,3-1*H*-dibenzimidazole-benzene were obtained by casting onto a glass plate a *N,N*-dimethylacetamide (DMAc) solution (~ 5 % w/v) and drying at 95 ºC overnight, followed by boiling in de-ionized water for 1 h. The thickness of the

membrane was controlled via the amount of SPSf and 1,3-1*H*-dibenzimidazole-benzene in the solution, and all the membranes in this study had a thickness of ~ 50 μm.

The ion exchange capacity was determined by suspending ~ 0.3 g of SPSf or blend membranes in 20 mL of a saturated aqueous solution of sodium chloride for 4 days to liberate the H^+ ions and then titrating with 0.1 M NaOH solution using phenolphthalein as an indicator. Proton conductivity values of the membranes were obtained from the impedance data as described in Chapter 2. The anode and cathode were prepared as described in Chapter 2 and 1 M methanol solution was used. Methanol crossover was evaluated by a voltammetric method as described in Chapter 2.

5.3 RESULTS AND DISCUSSION

5.3.1 Synthesis of 1,3-1*H*-dibenzimidazole-benzene

1,3-1*H*-dibenzimidazole-benzene has been synthesized in the literature by using isopthalaldehyde and benzyl derivatives with ammonium acetate or 1,2-phenylenediamine derivatives with $NaHSO_3$ in glacial acetic acid or alcohol (Fig. 5.1) [146-148].

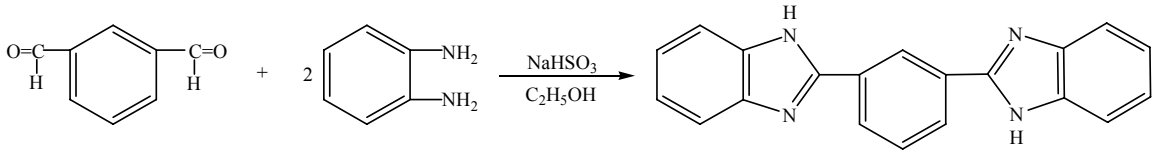

Figure 5.1. Synthesis of 1,3-1*H*-dibenzimidazole-benzene by $NaHSO_3$.

In this study, PPMA was used as a solvent and dehydration agent to form the benzimidazole groups by a condensation reaction between the carboxylic acid groups of isopthalic acid and 1,2-diaminobenzene as shown in Fig. 5.2. PPMA is a colorless liquid with low viscosity that can be poured and stirred without difficulty and organic compounds dissolve readily in it. It has been used successfully previously to synthesize PBI or poly(2,5-benzimidazole) (ABPBI) [149-152].

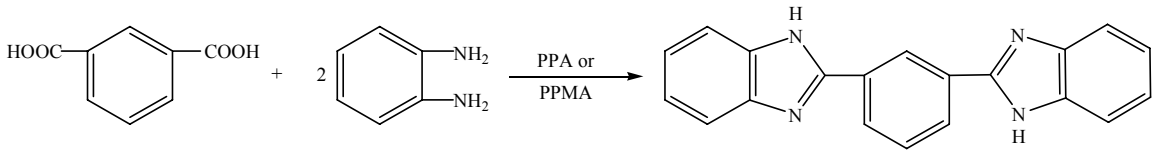

Figure 5.2. Synthesis of 1,3-1*H*-dibenzimidazole-benzene by PPMA.

5.3.2 Structural Characterization of 1,3-1*H*-dibenzimidazole-benzene

The structure of the synthesized 1,3-1*H*-dibenzimidazole-benzene was confirmed by FT-IR and ^{1}H-NMR. Fig. 5.3 shows the spectra of the synthesized 1,3-1*H*-dibenzimidazole-benzene and reactants. The bands around 3400 cm^{-1} in 1,3-1*H*-dibenzimidazole-benzene are attributed to the isolated N-H stretching. The strong absorption at 1740 cm^{-1} due to the C=O asymmetric stretching in isophthalic acid almost disappeared in 1,3-1*H*-dibenzimidazole-benzene, confirming the conversion of the carboxylic acid groups into benzimidazole groups. In addition, the peak at 1630 cm^{-1} corresponds to the stretching of C=C and C=N.

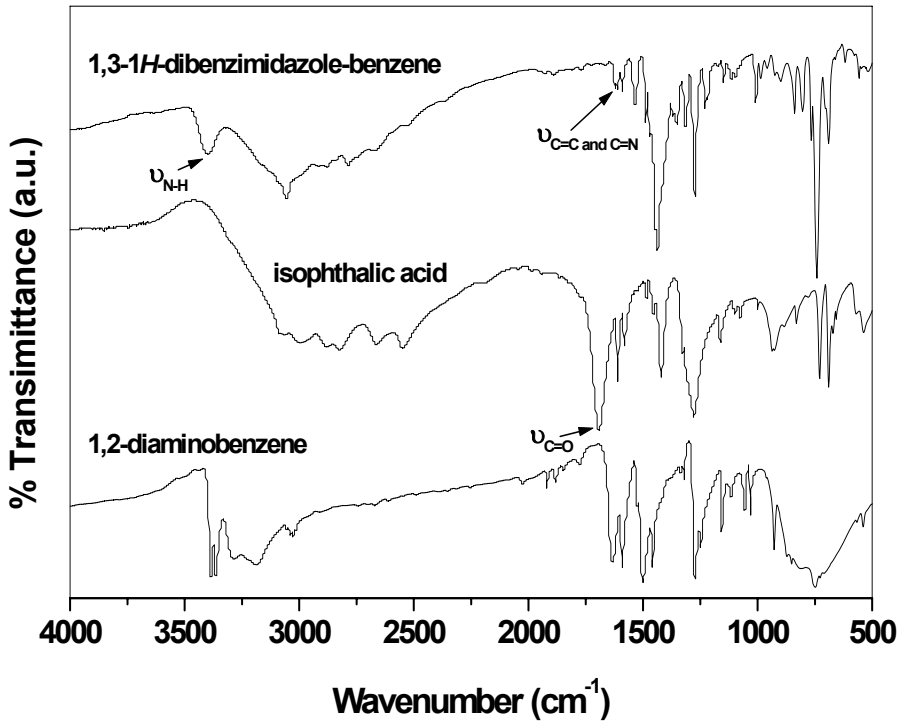

Figure 5.3. FT-IR spectra of the 1,3-1*H*-dibenzimidazole-benzene and the reactants.

Fig. 5.4 shows the ^{1}H-NMR spectra of the synthesized 1,3-1*H*-dibenzimidazole-benzene. The NMR [^{1}H-NMR (DMSO-d_6) data with δ = 7.19-7.27 (4H), 7.53-7.59 (2H), and 7.67-7.75 (3H)] further confirm the formation of 1,3-1*H*-dibenzimidazole-benzene, and the results of the structural analysis are consistent with the literature data [148]. The yield for the condensation reaction was 96 %.

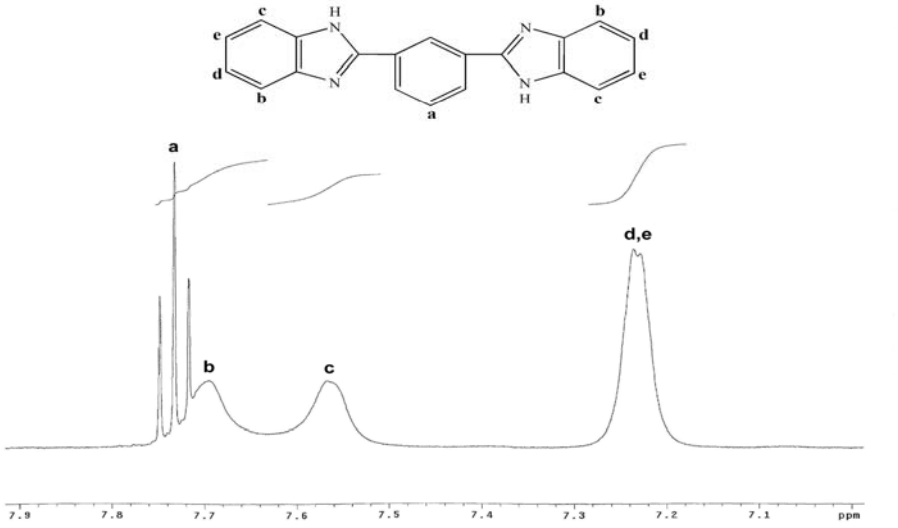

Figure 5.4. ^{1}H-NMR spectra of the synthesized 1,3-1*H*-dibenzimidazole-benzene.

5.3.3 TGA and DSC Analysis

Fig. 5.5 shows the TGA and DSC plots of the synthesized 1,3-1*H*-dibenzimidazole-benzene. The sample loses weight in two steps. While the first step at T < 120 ^{o}C corresponds to the loss of the water, the second step at T > 300 ^{o}C corresponds to the degradation of main bonds. The data suggest that 1,3-1*H*-dibenzimidazole-benzene is stable enough for fuel cell application. The DSC plot shown in Fig. 5.5 confirms the melting point of 1,3-1*H*-dibenzimidazole-benzene to be 146 ~ 148 ^{o}C, which is similar to the value reported in the literature (148 ^{o}C) [148].

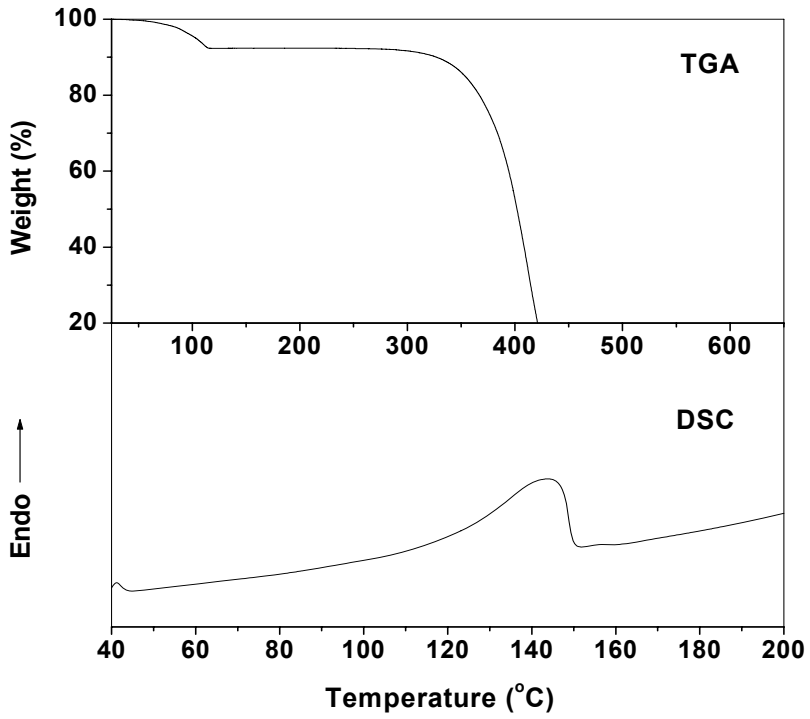

Figure 5.5. TGA and DSC plots of the synthesized 1,3-1*H*-dibenzimidazole-benzene.

5.3.4 Proton Conductivity of SPSf/1,3-1*H*-dibenzimidazole-benzene Blend Membranes

In order to study the effectiveness of 1,3-1*H*-dibenzimidazole-benzene as a proton transfer medium, blend membranes consisting of SPSf and various amounts of 1,3-1*H*-dibenzimidazole-benzene were prepared. The blend membranes are hereafter referred to as SPSf/DBImBenzene for convenience. Fig. 5.6 compares the proton conductivities of the SPSf/DBImBenzene blend membranes and the plain SPSf membrane under anhydrous conditions.

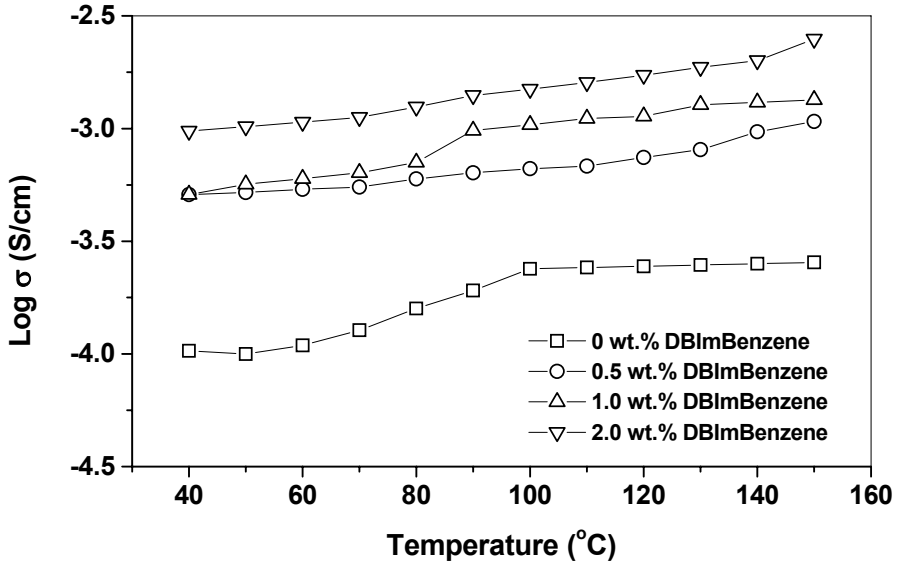

Figure 5.6. Proton conductivities of the plain SPSf and SPSf/DBImBenzene blend membranes under anhydrous conditions.

Proton conduction under anhydrous conditions would reflect the hopping of proton between sulfonic acid groups of SPSf and the benzimidazole groups of DBImBenzene, which is commonly referred to as Grotthuss-type mechanism. It can be seen that the proton conductivity increases with increasing DBImBenzene content in the blend membrane, indicating the promotion of proton conduction by the benzimidazole groups of DBImBenzene through the Grotthuss-type mechanism. However, the amount of DBImBenzene in the SPSf/DBImBenzene blend membrane is low (0.5 – 2.0 wt.%), and therefore, one could anticipate proton conduction by both vehicle-type and Grotthuss-type mechanisms, especially under humidified conditions. While the vehicle-type mechanism could occur in the hydrophilic channels formed by the clustering

of the sulfonic acid groups, the Grotthuss-type mechanism could occur in the regions where the DBImBenzene molecules may insert into the hydrophilic channels formed by the sulfonic acid groups, as illustrated in Fig. 5.7. With a pK_a value of 5.5, the DBImBenzene groups may be expected to facilitate the transfer of protons between sulfonic acid groups readily.

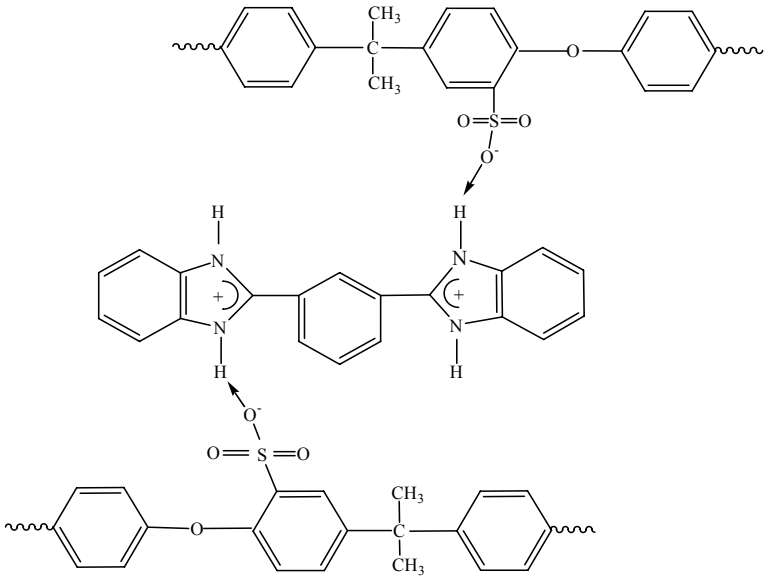

Figure 5.7. Proton conduction mechanism between sulfonic acid in SPSf and 1,3-1*H*-dibenzimidazole-benzene.

5.3.5 Determination of Ion Exchange Capacity (IEC) and Proton Conductivity Under Humidified Conditions

Under humidified conditions, both types of proton conduction mechanisms may occur as evident from the data of ion exchange capacity (IEC) and proton conductivity.

Table 5.1 compares the values of ion exchange capacity and proton conductivity measured under 100 % RH humidity at 65 ^{o}C for various ratios of sulfonic acid groups in SPSf to benzimidazole groups in DBImBenzene (*i.e.* [-SO_3H]/[BIm] ratios) in the blend membranes. The ratio of sulfonic acid to benzimidazole [-SO_3H]/[BIm] was calculated by the following equation:

$$[\text{-}SO_3H]/[BIm] = m_{SPSf} \cdot IEC_{SPSf} \cdot M_{DBImBenzene} / (m_{DBImBenzene} \cdot 1000 \cdot 2) \qquad [5.1]$$

where m_{SPSf} is the mass of the SPSf in the blend membrane, IEC_{SPSf} is the IEC value of SPSf, $m_{DBImBenzene}$ is the mass of DBImBenzene in blend membrane, and $M_{DBImBenzene}$ = 310 is the molecular weight of DBImBenzene.

It can be seen in Table 5.1 that the IEC values of the blend membranes are lower than that of plain SPSf, indicating the occurrence of acid-base interactions in the blend membranes and the consequent reduction in the amount of H^+ ions dissociating from sulfonic acid groups. Moreover, the IEC value decreases as the DBImBenzene content increases due to an increase in the degree of acid-base interaction. Regarding the proton conductivity, the blend membranes with 0.5 and 1.0 wt.% DBImBenzene show higher values than plain SPSf at a given temperature due to the enhancement of proton conduction in the presence of the benzimidazole groups of DBImBenzene through acid-base interactions. However, as the DBImBenzne content increases to 2.0 wt.%, the proton conductivity becomes lower than that of plain SPSf, suggesting that the proton conductivity is maximized at an optimum DBImBenzene content.

Table 5.1. Ion exchange capacity (IEC) and proton conductivity (σ) of SPSf/DBImBenzene blend membranes with various [-SO_3H]/[BIm] molar ratios

Wt. % DBImBenzene in SPSf/ DBImBenzene	[-SO_3H]/[BIm] Raio	IEC (meq./g)	σ at 100 % RH (S/cm)
			65 ºC
0	-	0.86	2.4×10^{-4}
0.5	26.5	0.81	3.4×10^{-4}
1	13.2	0.75	2.9×10^{-4}
2	6.5	0.68	1.8×10^{-4}
Nafion 115	-	0.91	3.2×10^{-2}

As mentioned earlier, the overall proton conductivity is determined by two proton conduction mechanisms. Under humidified conditions, the vehicle-type mechanism may be predominant due to the availability of more number of sulfonic acid groups compared to the benzimidazole groups in the blend membranes, while the Grotthuss-type mechanism providing an enhancement. Moreover, the insertion of DBImBenzene molecules could expand the width of ionic clusters formed by the sulfonic acid groups, enhancing the proton transfer by the vehicle-type mechanism. However, if the benzimidazole content becomes too high as in the case of 2 wt.% DBImBenzene with a [-SO_3H]/[BIm] ratio of 6.5, then the presence of hydrophobic DBImBenzene molecules within the ionic clusters could perturb the proton conduction by the vehicle-type mechanism, resulting in an overall reduction in proton conductivity. Thus, the content and

microscopic distribution of the heterocycles as well as the morphology will play critical role in maximizing the acid-base interaction and enhancing the proton conductivity in this type of blend membranes. Optimization of the microstructure and a uniform distribution of the sulfonic acid and benzimidazole groups could help to increase the proton conductivity values further.

5.3.6 Evaluation of SPSf/DBImBenzene Blend Membranes and Methanol Crossover in DMFC

Fig. 5.8 compares the polarization curves and power densities of the SPSf/DBImBenzene blend membrane with 0.5 wt.% DBImBenzene with those of both plain SPSf and Nafion 115 membranes. The SPSf/DBImBenzene blend membrane shows better performance than the plain SPSf membrane due to higher proton conductivity as seen in Table 5.1. More importantly, although the plain SPSf membrane shows lower performance than Nafion 115 membrane due to lower proton conductivity, the SPSf/DBImBenzene blend membrane exhibits performance comparable to that of Nafion 115, confirming the assistance of DBImBenzene in increasing the proton conduction.

For practical application in DMFC, methanol crossover is a critical parameter for long-term operation. Fig. 5.9 compares the methanol crossover current density of the PSf/DBImBenzene blend membrane with those of plain SPSf and Nafion 115 membranes. The plain SPSf membrane shows much lower methanol crossover than Nafion 115 due to the narrower hydrophilic channels in SPSf even though it is much thinner (~ 50 μm) than Nafion 115 (125 μm) [102].

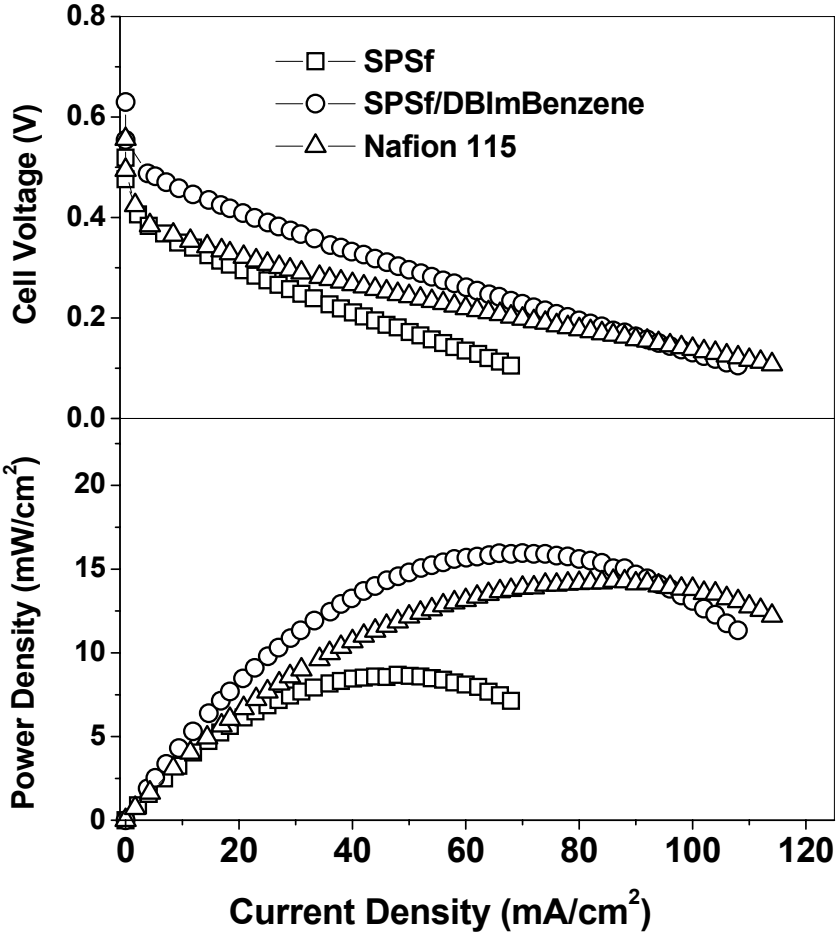

Figure 5.8. Comparison of the polarization curves for the plain SPSf, SPSf/DBImBenzene (0.5 wt.% DBImBenzene) blend membrane, and Nafion 115 in DMFC. The data were collected with a methanol flow rate of 2.5 mL/min at the anode and an O_2 flow rate of 200 mL/min with a pressure of 20 psi at the cathode. The humidifier temperature for O_2 and the cell temperature were 65 ^oC. Anode: 0.6 mg PtRu/cm^2, cathode: 1.0 mg Pt/cm^2, methanol concentration: 1 M.

Interestingly, the SPSf/DBImBenzene blend membrane exhibits even much lower methanol crossover than plain SPSf, indicating the effectiveness of DBImBenzene in blocking methanol crossover by inserting into the hydrophilic channels. The lower methanol crossover in the SPSf/DBImBenzene blend membrane could not only offer better long-term stability in DMFC compared to Nafion 115 and plain SPSf membranes but also help to lower the Pt catalyst loading at the cathode, enhancing the commercialization feasibility of the DMFC technology.

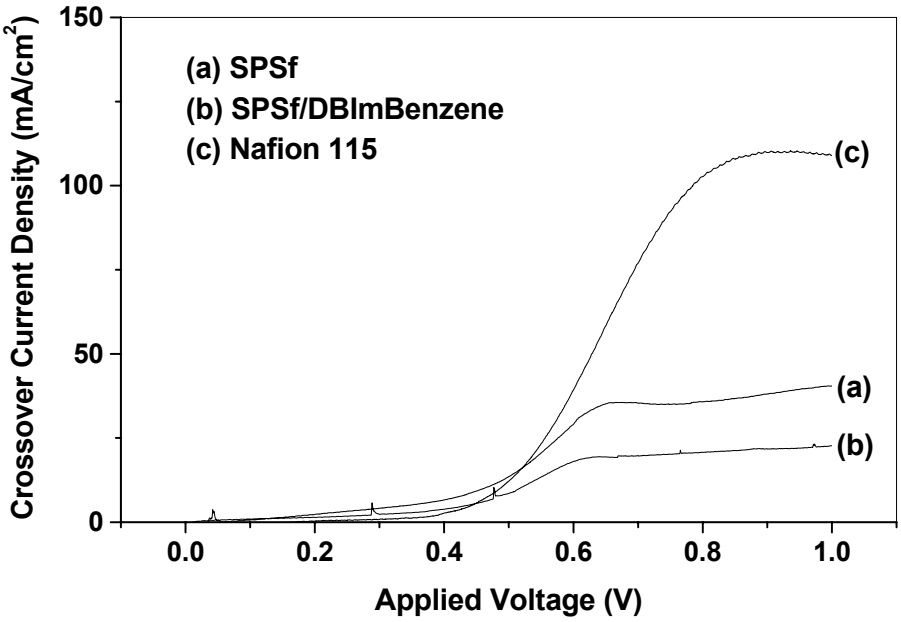

Figure 5.9. Comparison of the variations of the methanol crossover current density for the plain SPSf, SPSf/DBImBenzene (0.5 wt.% DBImBenzene) blend membrane, and Nafion 115 in DMFC. Methanol concentration: 1 M, cell temperature: 65 ^{o}C.

Fig. 5.10 compares the polarization curves and power density of the SPSf/DBImBenzene blend membranes with various DBImBenzene contents. The power density values of the blend membranes are higher than that of plain SPSf membrane up to a DBImBenzene content of 1 wt.%, but lower than that of plain SPSf on going to 2 wt.% DBImBenzene, which is consistent with the proton conductivity values in Table 5.1. Fig. 5.11 compares the methanol crossover current densities of the SPSf/DBImBenzene blend membranes with various DBImBenzene contents. The crossover decreases with increasing DBImBenzene content, indicating the effectiveness of DBImBenzene in blocking the methanol crossover. However, the blend membrane with 1.0 wt.% DBImBenzene shows slightly higher methanol crossover than the blend with 0.5 wt.% DBImBenzene. Although the reason for this is not clear, it could possibly be related to the differences in membrane-electrode assembly preparation.

Finally, the content and microscopic distribution of the DBImBenzene molecules will influence both the proton conductivity and methanol crossover values. As known in the literature, the separation between the hydrophobic and hydrophilic groups in SPSf is already smaller compared to that in Nafion, resulting in a stronger confinement of water/methanol in the narrow channels and significantly lower water/methanol permeation [71,133]. The insertion of the benzimidazole groups into the hydrophilic regions of SPSf can reduce the methanol permeability further, while enhancing proton conduction through acid-base interactions at least at low DBImBenzene contents and offering good compatibility with SPSf at the molecular scale due to the presence of phenyl rings in both SPSf and DBImBenzene. Optimization of the degree of sulfonation

in SPSf, the DBImBenzene content in the SPSf/DBImBenzene blend membrane, and the MEA configuration could help to enhance the fuel cell performance in DMFC further.

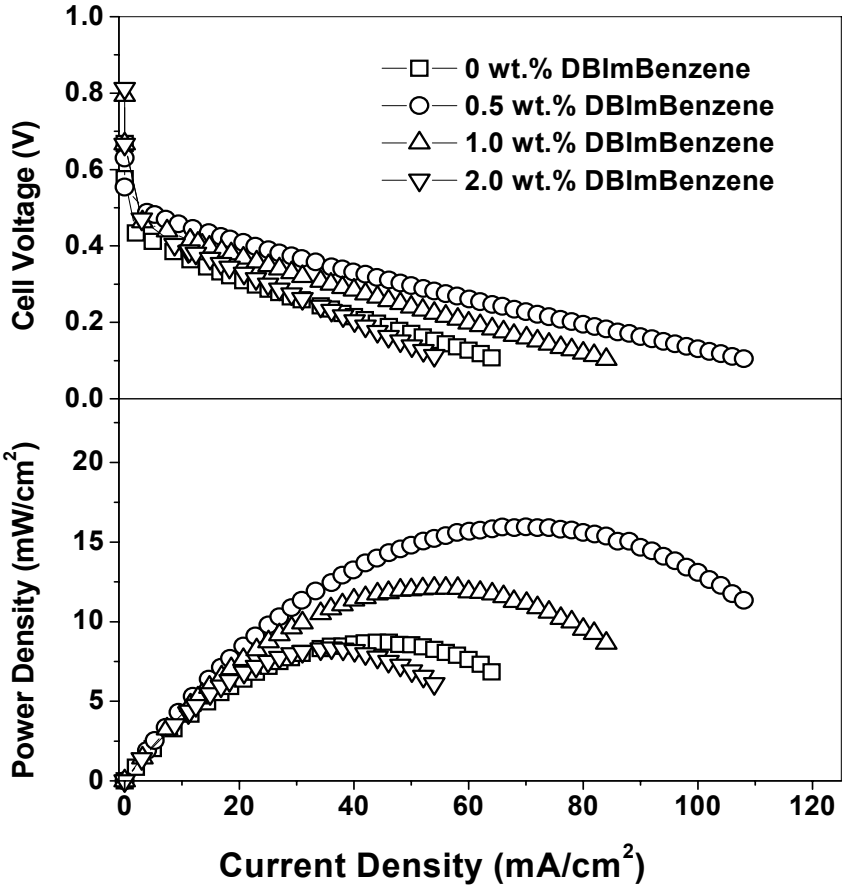

Figure 5.10. Comparison of the polarization curves for the SPSf/DBImBenzene blend membranes and plain SPSf in DMFC. The experimental conditions were same as those in Fig. 5.8.

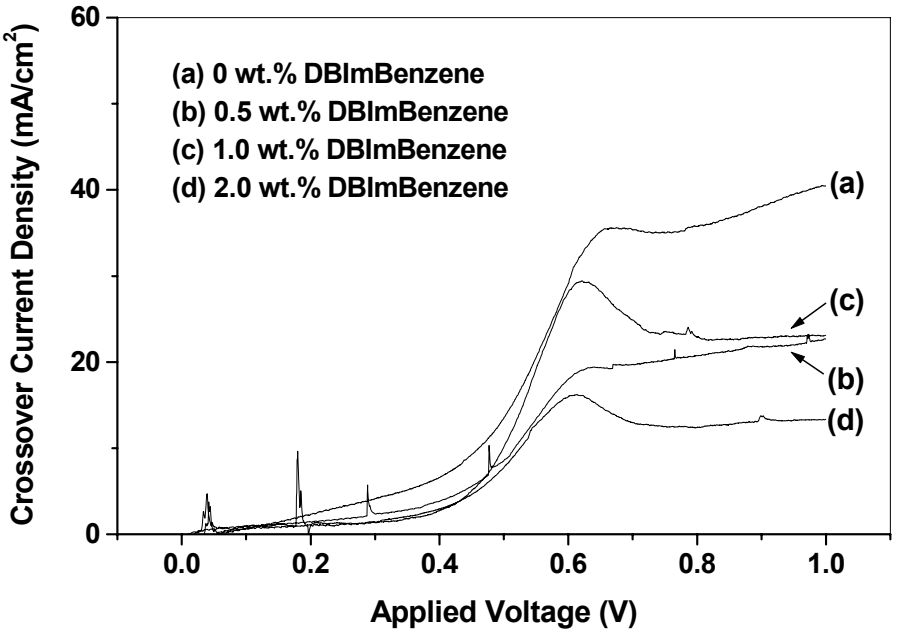

Figure 5.11. Comparison of the variations of the methanol crossover current density for the SPSf/DBImBenzene blend membranes and plain SPSf in DMFC. Methanol concentration: 1 M, cell temperature: 65 ^{o}C.

5.4 CONCLUSIONS

1,3-1*H*-dibenzimidazole-benzene (DBImBenzene) has been synthesized by a new route and explored as an additive in sulfonated polysulfone (SPSf) membrane for use in DMFC for the first time. The ion exchange capacity, proton conductivity, electrochemical performance in DMFC, and methanol crossover data of the SPSf/DBImBenzene blend membranes with various DBImBenzene contents (0 – 2 wt.%) have been compared with those of plain SPSf membrane. The blend membranes with an optimum DBImBenzene content of 0.5 and 1.0 wt.% exhibit better performance in DMFC than plain SPSf

membrane due to an enhancement in proton conductivity through acid-base interactions and a reduction in methanol crossover. Although the performance of the SPSf/DBImBenzene blend membranes in DMFC is comparable to that of Nafion 115 membrane, the former exhibits much lower methanol crossover than the latter, offering the possibility of better long-term performance and lower cathode catalyst loading. The study demonstrates that aromatic polymer membranes based on acid-base interactions could prove to be a viable strategy to overcome the difficulties of the currently used Nafion membrane.

Chapter 6

Polymer Blends Containing Benzimidazole for PEMFC and DMFC

6.1 INTRODUCTION

In Chapter 5, use of benzimidazole to promote proton conduction in the environment of sulfonic acid was demonstrated by the blend membrane containing 1,3-1*H*-dibenzimidazole-benzene and sulfonated polysulfone. However, for practical application in the fuel cells, materials with good membrane-forming and stable properties are required. Aromatic polymer is preferred in this regard. Therefore, tethering of N-heterocycles like benzimidazole to an aromatic polymer network could be a promising strategy to achieve high proton conductivity at high temperatures, involving a Grotthuss-type mechanism without requiring water, while preserving good chemical and mechanical stabilities at higher temperatures. It is also expected to be good for blocking methanol crossover as 1,3-1*H*-dibenzimidazole-benzene does.

Tethering of benzimidazole to an aromatic polymer backbone has not been pursued before in the literature. Moreover, carboxylic acid groups attached to some aromatic polymers like polysulfone [153] can be easily transformed to benzimidazole units through condensation reactions. With this perspective, a novel strategy in which the benzimidazole group is attached to an aromatic polymer like polysulfone, which exhibits good stability and local mobility, is adopted. The aromatic polymer with the tethered benzimidazole groups (basic polymer) is then blended with an acid polymer like

sulfonated poly(ether ether ketone) (SPEEK) to obtain high proton conductivity through acid-base interactions under anhydrous conditions.

Sulfonated poly(ether ether ketone) has been studied as a membrane material for DMFC. This material generally exhibits lower methanol crossover and is less expensive than Nafion [104,154]. With an optimized degree of sulfonation, it shows performance comparable to that of Nafion. However, high degrees of sulfonation to maximize the proton conductivity tend to lead to undesirable swelling of the membrane and mechanical integrity problems. To reduce the swelling, covalently and ionically cross-linked polymer membranes have been investigated by Kerres and co-workers [103,155,156]. Swelling is greatly suppressed by covalent cross-linking, but the polymers usually become brittle on drying out. On the other hand, acid-base blends containing ionic cross-links show good flexibility and thermal stability, but the dimensional stability at $T > 70$ ºC is inadequate with some blends like SPEEK/PBI and SPPO/PBI (PBI and SPPO refer, respectively, to poly(benzimidazole) and sulfonated poly(2,6-dimethyl-1,4-phenylene oxide)). They also exhibit lower methanol crossover in DMFC [156-159]. Unfortunately, microphase-separation is easy to occur in such blends due to different, incompatible acidic (aromatic) and basic (PBI) polymer structures [155].

In this Chapter, the blend membrane concept is based on industrially available, inexpensive polymer precursors (polysulfone and poly(ether ether ketone)) that are compatible with each other due to similar aromatic backbones. In addition to SPEEK being known to exhibit lower methanol crossover compared to Nafion, the benzimidazole side groups tethered to the polysulfone backbone could also help to suppress methanol

crossover further by inserting into the hydrophilic channels. The synthesis, fabrication, characterization, and evaluation of such blend membranes for high temperature PEMFC and DMFC are presented in this Chapter.

6.2 EXPERIMENTAL

The polysulfone bearing benzimidazole side group (PSf-BIm) was synthesized starting from carboxylated polysulfone (CPSf). The details of the synthesis of CPSf having different degrees of carboxylation per repeat unit are available elsewhere [153], and the CPSf precursor samples with a degree of carboxylation of 1.03, 1.58, and 1.90 was supplied by Dr. Michael D. Guiver of the National Research Council, Canada. The PSf-BIm samples prepared are hereafter designated as, respectively, PSf-BIm-103, PSf-BIm-158, and PSf-BIm-190. For PSf-BIm-103, 0.5 g of CPSf and 0.1296 g of 1,2-diaminobenzene were dissolved in 20 mL of *N,N*-dimethylformamide (DMF) or *N,N*-dimethylacetamide (DMAc) in a three-necked flask, followed by an addition of 2.86 mL of triphenylphosphite (TPP) into the flask. The solution was stirred at 100 ºC for 3 h and then at 150 ºC for 10, 24, or 36 h under nitrogen atmosphere and poured into 500 mL of methanol to precipitate the polymer. The precipitate was collected by filtration and dried in a vacuum oven at 110 ºC overnight. The SPEEK was prepared by using concentrated sulfuric acid as solvent and sulfonation agent, and the details are available elsewhere [104]. SPEEK with an ion exchange capacity (IEC) of 1.63 and a degree of sulfonation (DS) of 54 % was used in PEMFC study, and the SPEEK with an ion exchange capacity (IEC) of 1.52 and a degree of sulfonation (DS) of 51 % was used in

DMFC study. The blend membranes with various PSf-BIm compositions were obtained by casting onto a glass plate a *N,N*-dimethylacetamide (DMAc) solution of the SPEEK and PSf-BIm polymers (~ 5 % w/w) and drying at 95 ºC overnight, followed by boiling in de-ionized water for 2 h. The thicknesses of all the membranes were kept at around 50 μm.

The structure of the synthesized PSf-BIm was characterized with FT-IR and ^{1}H-NMR. Proton conductivity values of the membranes were obtained from the impedance data as described in Chapter 2. The percent liquid uptake was obtained from the weight change before and after equilibrating the dry membrane in de-ionized water or methanol solution at 65 and 80 ºC for 30 min.

The ion exchange capacity was determined by suspending ~ 0.3 g of SPEEK or SPEEK/PSf-BIm blend membranes in 20 mL of a saturated aqueous solution of sodium chloride for 4 days to liberate the H^{+} ions and then titrating with 0.1 M NaOH solution using phenolphthalein as an indicator. The mole ratio of [-SO_3H]/[BIm] in the SPEEK/PSf-BIm blend membranes was determined based on the weight fraction of PSf-BIm and SPEEK.

The SPEEK/PSf-BIm blend membranes were evaluated in PEMFC using PEMFC electrodes and in DMFC using DMFC electrodes, which were prepared as described in Chapter 2. Methanol crossover was evaluated by a voltammetric method as described in Chapter 2.

6.3 RESULTS AND DISSCUSION

6.3.1 Synthesis and Characterization of Polysulfone-benzimidazole (PSf-BIm)

Carboxylated polysulfone (CPSf) was first synthesized as reported elsewhere by Guiver et al. [153]. The degree of carboxylation (DC) per repeat unit could be varied from 0.2 to 1.9, which provides the flexibility to convert the carboxylic acid groups to benzimidazole side groups over a wide range. Fig. 6.1 shows the synthesis of polysulfone bearing benzimidazole side group by a reaction between carboxylated polysulfone and 1,2-diaminobenzene.

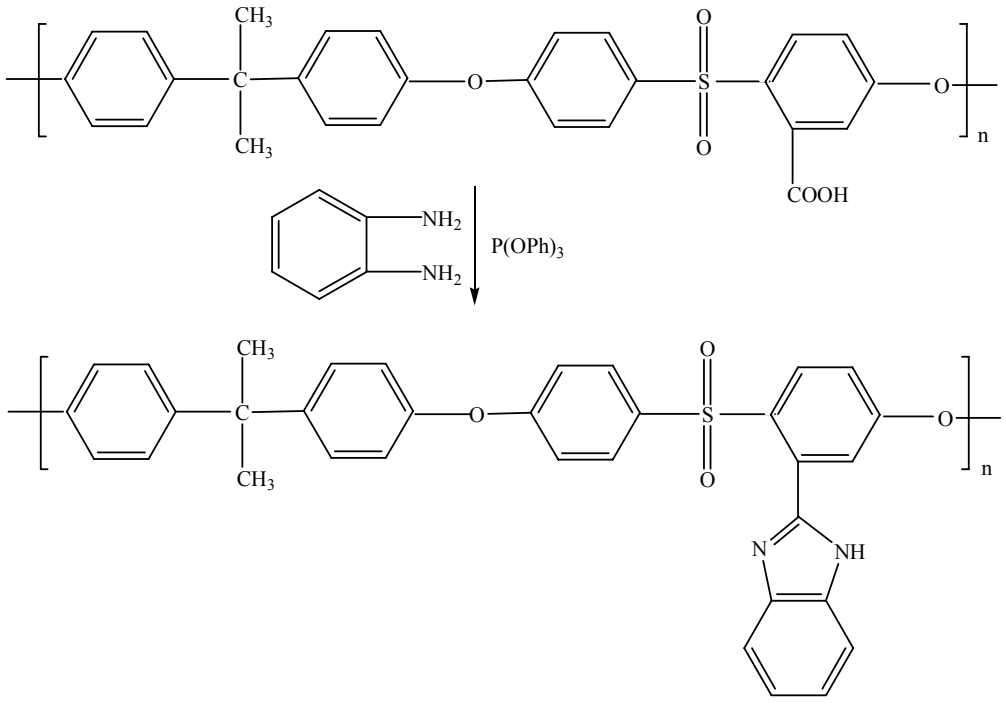

Figure 6.1. Synthesis of polysulfone bearing benzimidazole side group.

Due to the insolubility of CPSf in polyphosphoric acid (PPA) or phosphorus pentoxide-methanesulfonic acid (PPMA), triphenylphosphite (TPP) was selected as a dehydration agent. To avoid the formation of the amide structure by cross-linking, the reaction was first carried out at a lower temperature of 100 ºC for 3 h to form a single C−N bond between the carboxylic acid group and one amino group of 1,2-diaminobenzene, followed by heating at 150 ºC for longer time to form the C=N bond between the carboxylic carbon atom and the other amino group of 1,2-diaminobenzene. The PSf-BIm samples at various reaction times (10, 24, or 36 h) were obtained to study the conversion efficiency of the carboxylic acid groups into benzimidazole groups.

Fig. 6.2 shows the FT-IR spectra of CPSf, PSf-BIm-103, PSf-BIm-158, and PSf-BIm-190. The main absorption bands of PSf-BIm indicating the presence of benzimidazole are closely similar to those of PBI or poly(2,5-benzimidazole) (ABPBI) [160]. The bands around 3400 cm^{-1} in PSf-BIm are attributed to the isolated N-H stretching. The strong absorption at 1740 cm^{-1} due to the C=O asymmetric stretching in CPSf almost disappeared in PSf-BIm, indicating the conversion of the carboxylic acid groups into benzimidazole groups. The product after 3 h at 100 ºC was also collected and characterized by FT-IR. The observation of C=O asymmetric stretching and the isolated N-H stretching confirms the reaction of only one amino group of 1,2-diaminobenzene and the absence of the formation of the imidazole ring of benzimidazole at 100 ºC. More importantly, the C=N stretching at 1630 cm^{-1}, which distinguishes PSf-BIm from CPSf, increases as the DC in the starting CPSf increases.

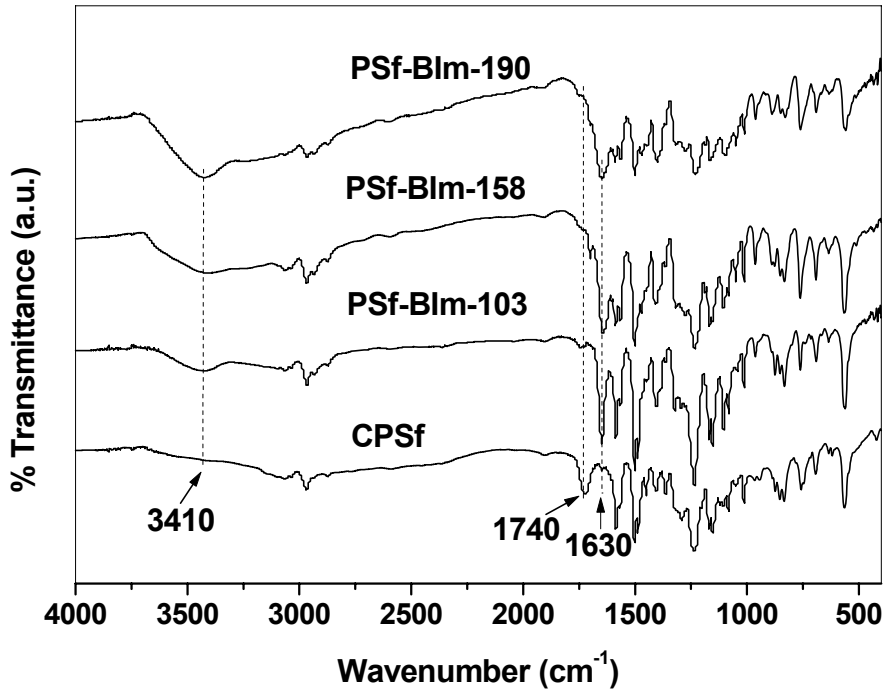

Figure 6.2. FT-IR spectra of CPSf and PSf-BIm with various degrees of substitution.

PSf-BIm-190 contains the highest degree of substitution (DS), and it could provide more sites for proton transfer. Therefore, only the synthesized PSf-BIm-190 was characterized by ^{1}H-NMR and evaluated in the blend membranes in fuel cells.

Fig. 6.3 shows the ^{1}H-NMR spectra of the PSf-BIm-190 sample synthesized with a reaction time of 10 h. This sample is not di-substituted, and therefore, the presence of different polymer repeat units results in a complex spectrum. However, useful information could be extracted from the integrated values of the 1D NMR spectra. The integration value of the polymer isopropylidene groups (CH_3-C-CH_3) at low frequencies (1.6 ppm) were set to 6 H. As a result of this, the ortho-sulfone proton signals at high

frequencies (7.8 - 8.4 ppm) resulted in an integrated value of 2 H as expected since the DS of PSf-COOH was close to 2 (1.9 to be exact). The rest of the aromatic proton signals should then integrate to:

(i) 12 H if no benzimidazole group is tethered (all COOH groups)

(ii) 16 H if one COOH is converted to benzimidazole group and 0.9 COOH still remains free

(iii) 20 H if all the COOH groups are converted to benzimidazole groups

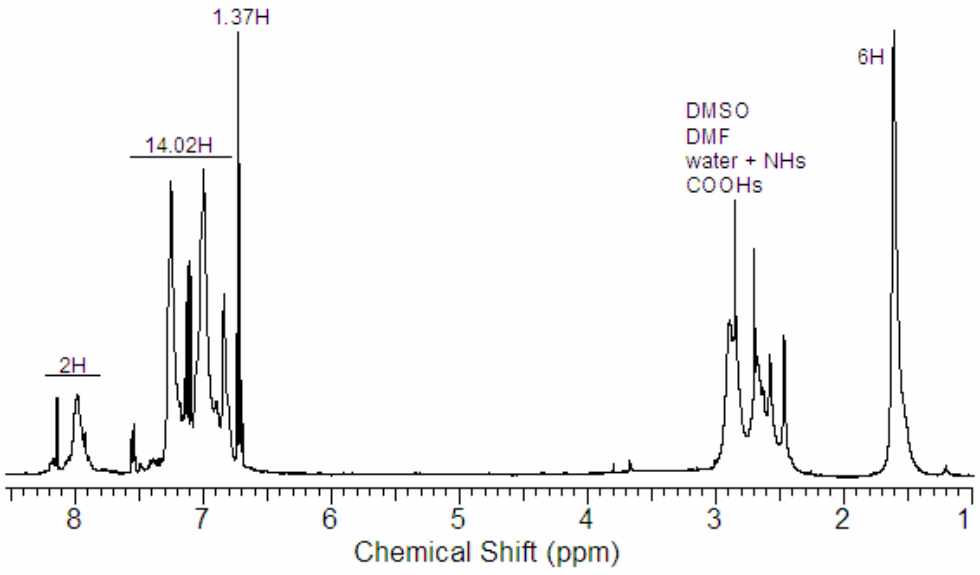

Figure 6.3. ^{1}H-NMR spectra of the PSf-BIm-190 sample synthesized with a reaction time of 10 h.

In Fig. 6.3, the rest of the aromatic signals integrated to 15.39 H, which would result in a tethering of benzimidazole groups of approximately 0.8 per repeat unit. The sharper

signals at 7.15 and 6.72 ppm would fit the expected two different aromatic benzimidazole protons because of their couplings and their integration values. The 6.72 ppm signal integrates to 1.37 H, which corresponds to a tethering of benzimidazole groups of 0.7 per repeat unit (0.685 to be exact). In this case, all of the integration values and extra signals suggest the presence of benzimidazole groups, but only to a maximum of 0.8 per repeat unit (48.4 % conversion). For the samples collected after a reaction time of 24 and 36 h, the rest of the aromatic proton signals integrate to 18.18 H (90.9 % conversion) and 18.98 H (94.9 % conversion), respectively, indicating longer reaction time results in a higher conversion efficiency of the carboxylic acid groups into benzimidazole groups.

6.3.2 Proton Conductivity of SPEEK/PSf-BIm Blend Membranes

Fig. 6.4 compares the proton conductivities of SPEEK and the SPEEK/PSf-BIm blend membranes (3:1 weight ratio) under anhydrous conditions. While the proton conductivity of SPEEK decreases with increasing temperature as the proton conduction becomes difficult at high temperatures in such acid-based polymers, the conductivity of the SPEEK/PSf-BIm blend membranes increases with increasing temperature due to the presence of benzimidazole tethered onto polysulfone. The pendant benzimidazole could act as a ‘bridge’ to promote proton conduction between sulfonic acid groups under low relative humidity conditions. Also, the proton conductivity increases as the DS of polysulfone to which benzimidazole is tethered increases, confirming the role played by benzimidazole on proton conduction.

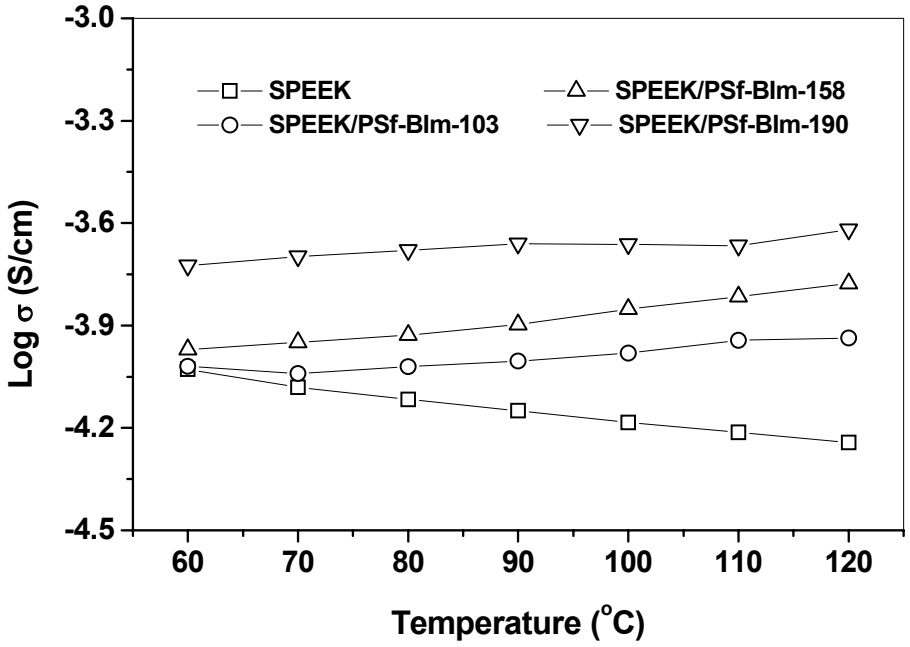

Figure 6.4. Variations of the proton conductivities of the SPEEK and SPEEK/PSf-BIm blend (3:1 weight ratio) membranes with temperature under anhydrous conditions.

The proton transfer mechanism in the SPEEK/PSf-BIm blend membrane is analogous to the Grotthuss-type mechanism proposed for the SPSf/DBImBenzene blend membrane as discussed in Chapter 5. The sulfonic acid group of SPEEK can protonate the imide site of benzimidazole, facilitating the hopping of the proton bound to the other nitrogen of the benzimidazole unit to another basic site of the benzimidazole unit or to the oxygen of another sulfonate anion group. Proton conduction in the blend membrane may occur by a mixed mechanism (a partial vehicle-type mechanism in the domain of sulfonic acid groups and a partial Grotthuss-type mechanism in the domain of benzimidazole groups). The presence of benzimidazole group thus promotes proton

conduction under anhydrous conditions at higher temperatures. Another advantage of pendant benzimidazole group is the ease of swaying, which could promote long-range proton motion in the polymer system.

6.3.3 Performance Evaluation of SPEEK/PSf-BIm Blend Membrane in High Temperature PEMFC

Fig. 6.5 compares the fuel cell performances of the SPEEK/PSf-BIm (3:1 weight ratio) blend membrane in single cell PEMFC at different temperatures with those of Nafion. In the case of the SPEEK/PSf-BIm blend membrane, the polarization loss decreases as the temperature increases from 80 to 90 ºC as one would expect due to the increasing proton conductivity as seen in Fig. 6.4, which is in contrast to the increase in polarization loss found with the Nafion membrane due to the decrease in water content.

Fig. 6.6 compares the performances of Nafion 115, SPEEK, and SPEEK/PSf-BIm membranes in single cell PEMFC at 90 and 100 ºC. The thicknesses of all the three membranes were kept the same and the electrodes were also fabricated in the same manner for all the three MEAs to have a good comparison of the intrinsic properties of the three membranes. Clearly, the SPEEK/PSf-BIm blend membrane exhibits better performance with lower polarization loss than both the Nafion and SPEEK membranes at 90 ºC or 100 ºC. The data demonstrate that the benzimidazole group present in PSf-BIm promotes proton conduction at higher temperatures. The decline in performance on going from 90 to 100 ºC is due to the use of Nafion in our electrodes (cathode and anode).

Additionally, the decline in performance on going from 90 to 100 ºC is drastic in the cases of SPEEK and Nafion membranes compared to that in the case of the SPEEK/PSf-BIm blend membrane. This is due to a significant decrease in the proton conductivity at 100 ºC with the SPEEK and Nafion membranes, arising from a loss of the proton conducting solvent, water.

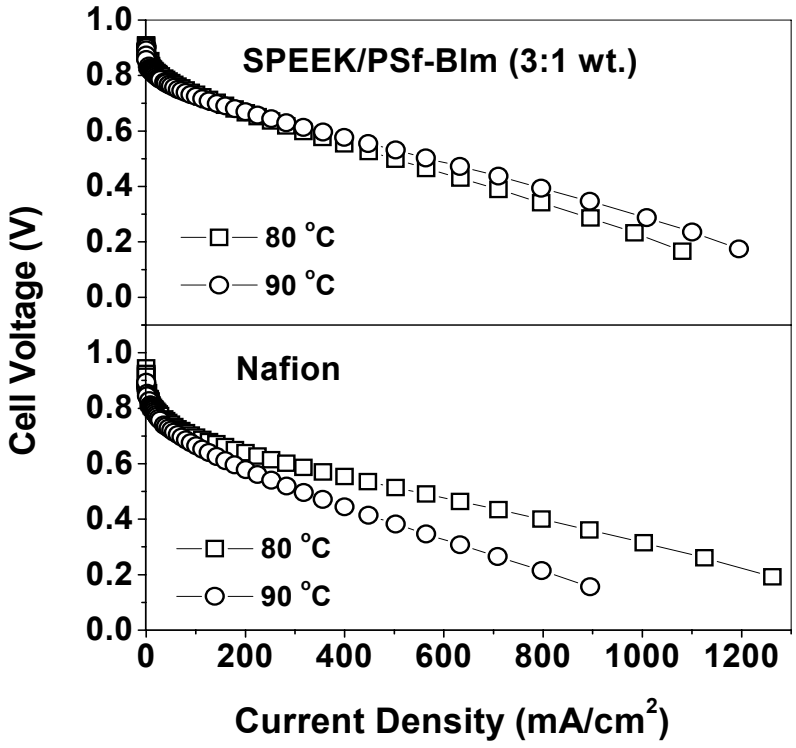

Figure 6.5. Comparison of the performances of the SPEEK/PSf-BIm (3:1 weight ratio) blend membranes at different temperatures in single cell PEMFC with those of Nafion and SPEEK membranes: $T_{H_2} = T_{O_2} = 80$ ºC and $T_{cell} = 80$ ºC or 90 ºC.

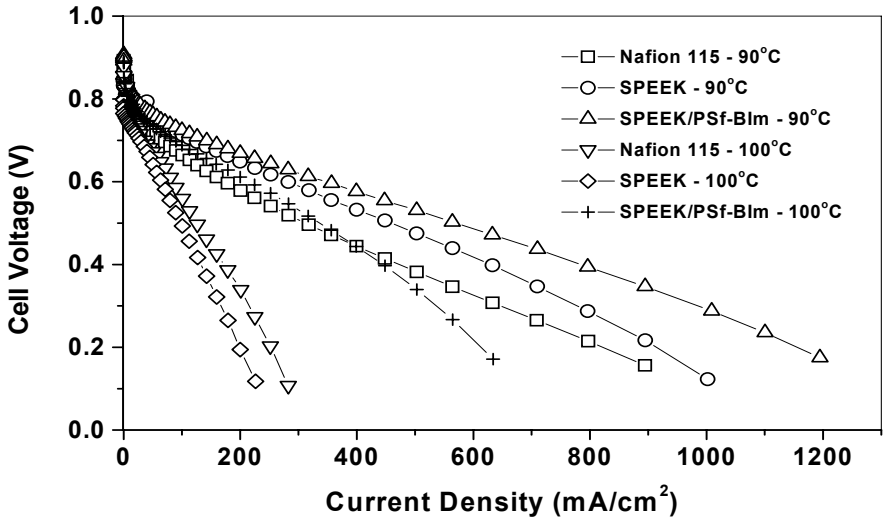

Fig. 6.6. Comparison of the performances of the Nafion 115, SPEEK, and SPEEK/PSf-BIm (3:1 weight ratio) blend membranes in single cell PEMFC: $T_{H_2} = T_{O_2}$ = 80 ºC and T_{cell} = 90 ºC or 100 ºC.

6.3.4 Determination of Ion Exchange Capacity (IEC), Proton Conductivity Under Humidified Conditions, and Liquid Uptake

Table 6.1 summarizes the [-SO_3H]/[BIm] mole ratio, ion exchange capacity (IEC), proton conductivity (σ) at 65 and 80 ºC and 100 % RH of the SPEEK/PSf-BIm blend membranes for various PSf-BIm contents. The IEC values of the blend membranes are lower than that of plain SPEEK, indicating the occurrence of acid-base interaction in the blend membranes, which reduces the amount of H^+ ions dissociating from sulfonic acid groups. As the PSf-BIm content increases, the IEC value decreases due to an increase in the degree of acid-base interaction.

Table 6.1. Comparison of the ion exchange capacity (IEC), proton conductivity (σ), and liquid uptake of the SPEEK/PSf-BIm blend membranes for various [-SO_3H]/[BIm] mole ratios with those of plain SPEEK membrane.

Wt.% PSf-BIm	Ratio of [-SO_3H]/ [BIm]	IEC (meq./g)	$\sigma \times 10^3$ (S/cm)		Methanol Concentration (M)	Liquid uptake (wt.%)	
			65 ºC	80 ºC		65 ºC	80 ºC
0	-	1.52	1.7	2.1	0	11.6	20.6
					1	15.7	22.4
					2	24.5	28.9
5	7.67	1.35	1.8	2.4	0	10.6	18.3
					1	15.2	19.2
					2	23.0	26.6
8	4.64	1.23	2.3	2.8	0	8.1	15.5
					1	13.1	16.2
					2	21.8	24.8
10	3.57	1.13	1.3	1.6	0	7.6	14.4
					1	12.4	15.1
					2	19.8	22.9

In Table 6.1, the conductivity of the SPEEK/PSf-BIm blend membranes increases with increasing temperature from 65 to 80 ºC similar to that found with the SPEEK membrane. At a given temperature, the conductivity increases as the PSf-BIm content increases from 0 to 8 wt.% due to the enhancement of proton conduction in the presence

of benzimidazole side groups tethered to polysulfone through acid-base interactions. However, as the PSf-BIm content increases to 10 wt.%, the proton conductivity decreases significantly and is lower than that of plain SPEEK, indicating an optimum PSf-BIm content of 8 wt.% maximizes the proton conductivity. This decrease in proton conductivity at higher BIm contents (or for $-SO_3H$/BIm molar ratio < 4.5 in Table 6.1) despite the availability of $-SO_3H$ groups still for further acid-base interactions suggests that the acid-base interaction between the sulfonic acid and the pendant benzimidazole units may be more complex than that in other acid-base systems [155,156].

It is believed that the morphology and the microscopic distribution of the sulfonic acid and pendant benzimidazole groups will be a critical factor in maximizing the acid-base interaction and enhancing the proton conductivity in this kind of blend membranes. Optimization of the microstructure and a uniform distribution of the sulfonic acid and pendant benzimidazole groups could increase the proton conductivity and lower the methanol crossover (see later) further.

Table 6.1 also compares the percent liquid uptake at different temperatures and methanol concentrations for various PSf-BIm contents. For a given PSf-BIm content, the liquid uptake increases as the temperature or the methanol concentration increases. At a given temperature or methanol concentration, the liquid uptake decreases with increasing PSf-BIm content. The membrane swelling, which is a critical issue for MEA stability in fuel cells, generally trends with liquid uptake. All the SPEEK/PSf-BIm blend membranes in Table 6.1 exhibit lower liquid uptake than plain SPEEK membrane, irrespective of water or methanol is being used, indicating a lower swelling and better stability. The

lower hydrophilicity of PSf-BIm compared to that of SPEEK and the acid-base interactions (similar to the ionic cross linking occuring in other acid-base systems like SPEEK/PBI) between the sulfonic acid and benzimidazole groups lead to lower liquid uptake. The lower liquid uptake could also help to lower the methanol crossover as the crossover is known to trend with the liquid uptake in the SPEEK membrane [104].

6.3.5 Evaluation of SPEEK/PSf-BIm Blend Membranes and Methanol Crossover in DMFC

Fig. 6.7 compares the electrochemical performance data of the SPEEK/PSf-BIm blend membranes with those of SPEEK and Nafion 112 membranes in DMFCs at 65 and 80 ºC with 1 M methanol solution. The SPEEK and SPEEK/PSf-BIm blend membranes exhibit higher polarization loss than Nafion 112 membrane due to the lower proton conductivities of the former and a possible better membrane-electrode interfacial contact in the latter. The incorporation of PSf-BIm into SPEEK decreases the polarization loss initially at 5 wt.% PSf-BIm and then increases it at a higher PSf-BIm content of 10 wt.%. The increased polarization loss at 10 wt.% PSf-BIm is due to the lower proton conductivity as seen in Table 6.1. The blend membranes with 5 and 8 wt.% PSf-BIm also show higher open circuit voltages (OCV) than plain SPEEK membrane. The better performance of the blend membrane with 8 wt.% PSf-BIm could be attributed to the higher proton conductivity and lower methanol crossover, as indicated by a lower methanol crossover limiting current density compared to that for the SPEEK membrane in Fig. 6.8.

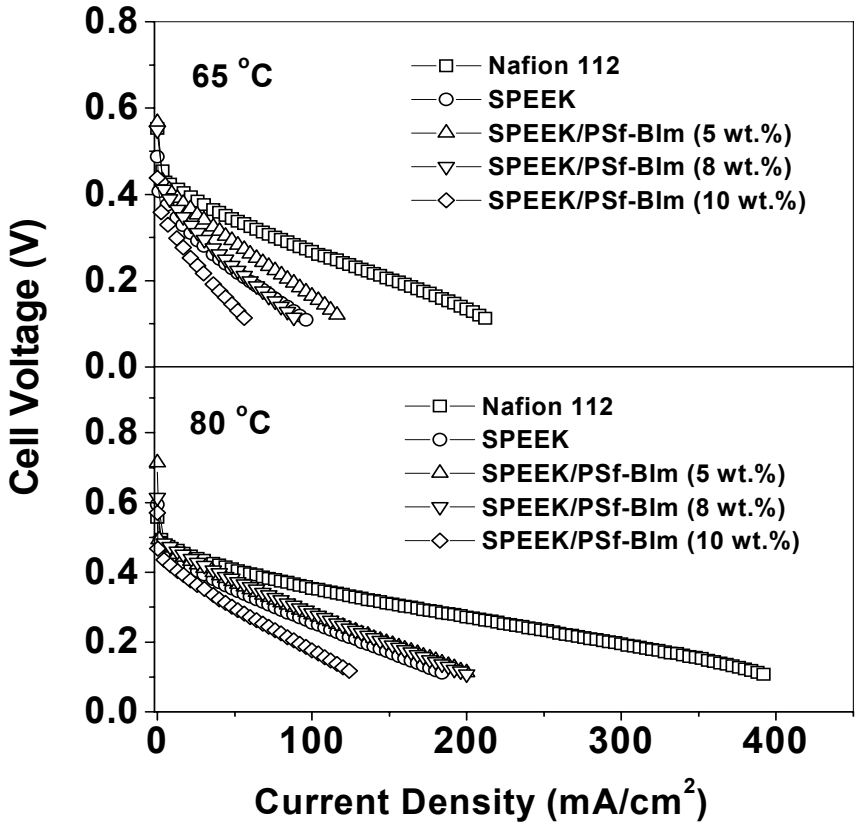

Figure 6.7. Comparison of the polarization curves of the Nafion 112 and SPEEK/PSf-BIm blend membranes with that of SPEEK in DMFC. Anode: 0.6 mg PtRu/cm^2, cathode: 1.0 mg Pt/cm^2, and methanol concentration: 1 M.

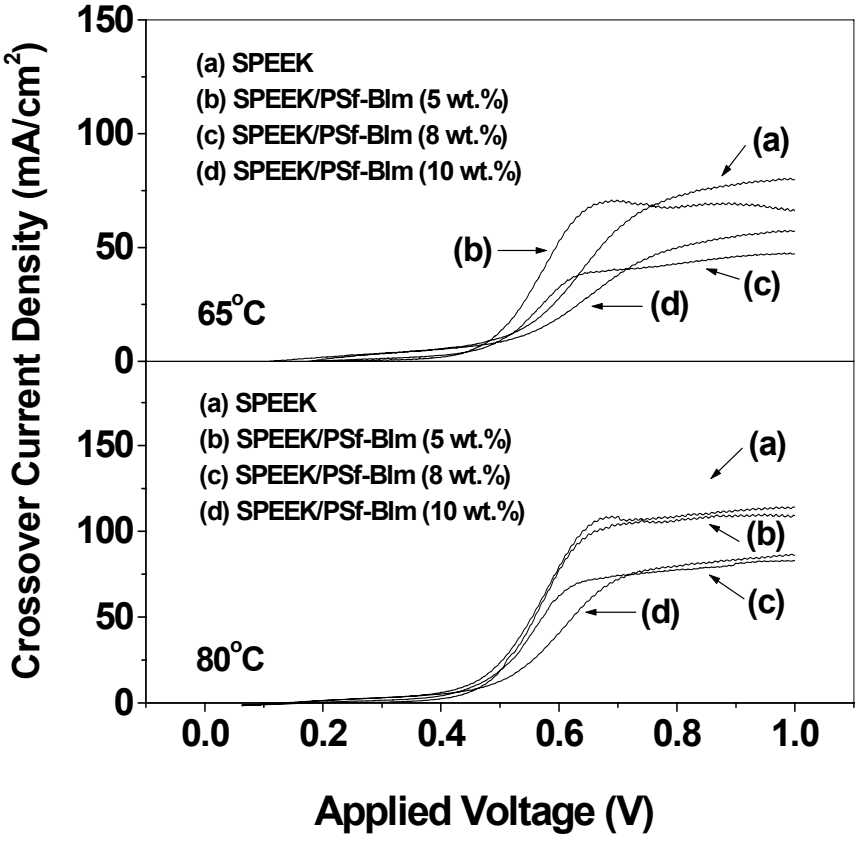

Figure 6.8. Comparison of the variations of the methanol crossover current density for the SPEEK/PSf-BIm and SPEEK membranes in DMFC at a methanol concentration of 1 M. Since the current exceeded the limit of our equipment, the data for Nafion 112 are not shown.

Although the thickness of the SPEEK/PSf-BIm blend membranes is same as that of SPEEK, the methanol crossover at 8 and 10 wt.% PSf-BIm is only 70 % of that found with plain SPEEK, indicating the effectiveness of the benzimidazole groups in

suppressing the methanol permeability. Furthermore, the SPEEK/PSf-BIm blend membranes exhibit a much reduced methanol crossover than Nafion 112 membrane, offering better long-term performance in the fuel cell. The methanol crossover current for Nafion 112 is not shown in Fig. 6.8 since its high value exceeded the limit of our equipment.

Fig. 6.9 compares the electrochemical performance data of the SPEEK/PSf-BIm blend membranes with those of SPEEK and Nafion 112 at a higher methanol concentration of 2 M. All the membranes in Fig. 6.9 show better performances than those found with 1 M methanol solution in Fig. 6.7 due to higher methanol flux. However, the blend membranes, for example, with 8 wt.% PSf-BIm exhibit better performance than the SPEEK as with 1 M methanol in Fig. 6.7 due to lower methanol crossover as seen in Fig. 6.10. In Fig. 6.10, the plots of methanol crossover currents of Nafion 112, SPEEK, and SPEEK/PSf-BIm with 5 wt.% PSf-BIm at 80 ºC are not shown because they exceeded the current limit of our equipment.

The electrochemical data indicate that the SPEEK/PSf-BIm blend membranes with an optimum PSf-BIm content exhibits better performance than SPEEK due to lower methanol crossover and higher proton conductivity. The lower methanol crossover could be attributed to the narrower pathways for methanol/water permeation in the former. It has been found that the separation between the hydrophobic and hydrophilic groups in SPEEK is already smaller compared to that in Nafion, resulting in a stronger confinement of water/methanol in the narrow channels and significantly lower water/methanol permeation [71,91,133]. PSf-BIm with an aromatic backbone similar to that in SPEEK

can be expected to have good compatibility with SPEEK at the molecular scale, and the insertion of the benzimidazole side groups into the hydrophilic groups of SPEEK can reduce methanol permeability further while enhancing proton conduction through acid-base interactions. Increase in the degree of sulfonation in SPEEK as well as optimization of the PSf-BIm content in SPEEK/PSf-BIm and the MEA fabrication process could improve the performance in DMFC further.

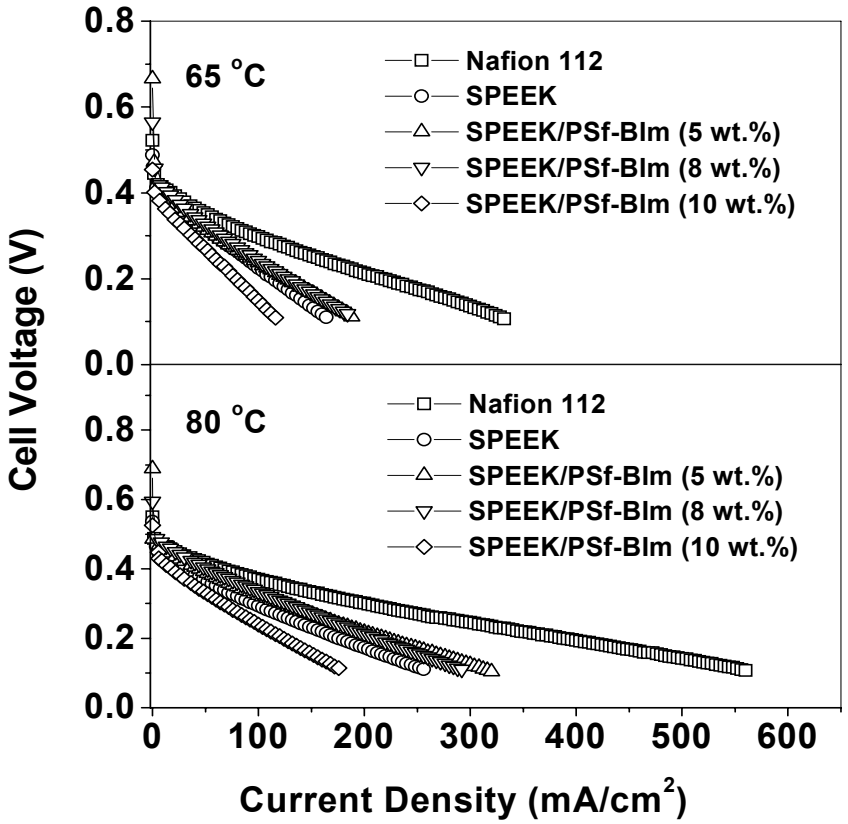

Figure 6.9. Comparison of the polarization curves of the Nafion 112 and SPEEK/PSf-BIm blend membrane with that of SPEEK in DMFC. The experimental conditions were same as those in Fig. 6.7 excepting the methanol concentration was 2 M.

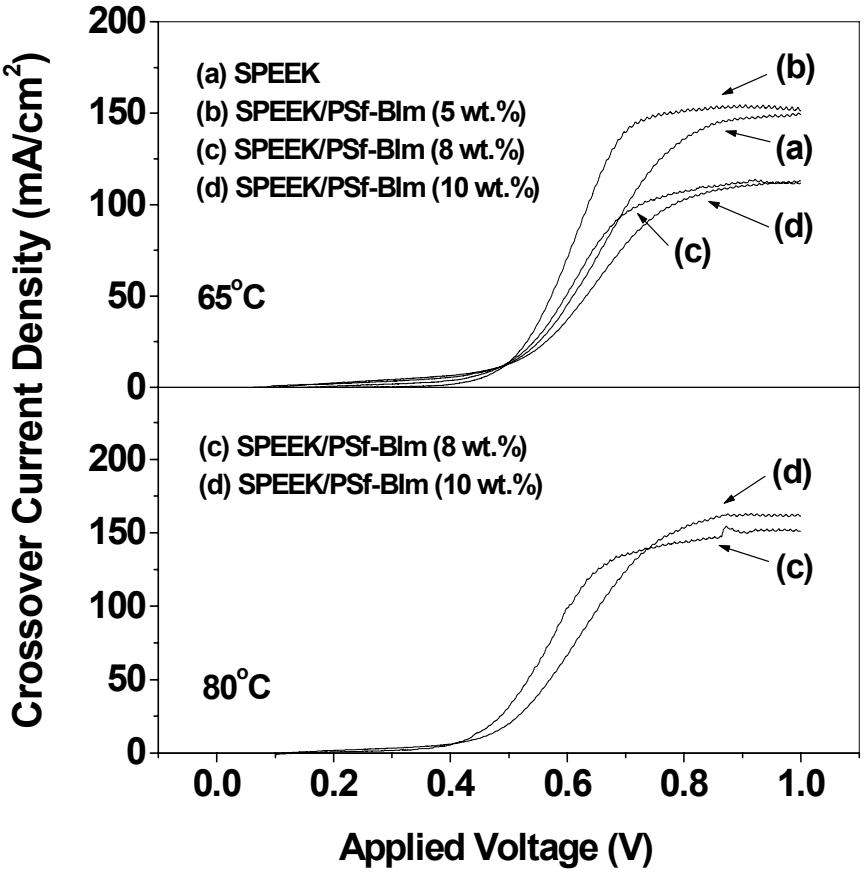

Figure 6.10. Comparison of the variations of the methanol crossover current density for the SPEEK/PSf-BIm and SPEEK membranes in DMFC at a methanol concentration of 2 M. The data for Nafion 112, SPEEK and SPEEK/PSf-BIm with 5 wt.% PSf-BIm at 80 ºC are not shown since the current exceeded the limit of our equipment.

6.4 CONCLUSIONS

In summary, a novel aromatic polymer (polysulfone) bearing a heterocycle (benzimidazole) side group has been synthesized. It is totally different from the well-known PBI polymer, and it has the benzimidazole units attached to the main chain. Blend membranes fabricated with sulfonated poly(ether ether ketone) and polysulfone bearing benzimidazole side group exhibit higher proton conductivity and better performance in PEMFC at 90 and 100 ºC compared to the SPEEK or Nafion membranes. The study demonstrates that polymers bearing benzimidazole side groups may become a viable strategy to develop new membranes that could enable the operation of PEMFC at higher temperatures and low relative humidity.

Additionally, the ion exchange capacity, proton conductivity, liquid uptake, electrochemical performance in DMFC, and methanol crossover of SPEEK/PSf-BIm blend membranes with different PSf-BIm contents (0 – 10 wt.%) have been compared with those of plain SPEEK membrane. The blend membranes with an optimum PSf-BIm content like 8 wt.% exhibit better performance in DMFC than plain SPEEK due to an enhancement in proton conductivity through acid-base interactions and a reduction in methanol crossover. Although the performance of the SPEEK/PSf-BIm blend membranes in DMFC are lower than that of Nafion 112 due to lower proton conductivity, the former exhibits much reduced methanol crossover, offering better long term stability and performance. The novel blend membrane strategy presented here could be explored further with various combinations of a variety of aromatic polymers, and it has the potential to overcome some of the critical barriers associated with the DMFC technology.

Chapter 7

Polymer Blends Containing N-heterocycles with More Than Two Nitrogen for DMFC

7.1 INTRODUCTION

It is an attractive strategy to achieve high proton conduction through acid-base interactions involving sulfonic acid groups in one polymer (acid polymer) and the N-heterocycle groups in another polymer (basic polymer) [70,155,161,162]. However, this strategy has been pursued with basic polymers having only one or two nitrogen atoms acting as proton donors or acceptors (e.g. pyridine, imidazole), limiting the extent of promotion of proton conduction and the fuel cell performance. Tethering of benzimidazoles to a polymer backbone followed by blending with a sulfonic acid polymer was demonstrated in Chapter 6. However, benzimidazole has only two proton donors or acceptors (only two N atoms).

In this Chapter, N-heterocycle units containing more than two N atoms (e.g. 2-amino-benzimidazole, 3-amino-1,2,4-1*H*-triazole), which could provide more proton transfer sites, are pursued. For example, the three nitrogen atoms of the 2-amino-benzimidazole unit and the four nitrogen atoms of the 3-amino-1,2,4-1*H*-triazole unit could possibly act equally as proton donors or acceptors as shown in Figs. 7.1 and 7.2, increasing the probability of proton transfer compared to one nitrogen atom of the pyridine- and two nitrogen atoms of the imidazole or benzimidazole systems and promoting proton conduction in the presence of a sulfonic acid polymer.

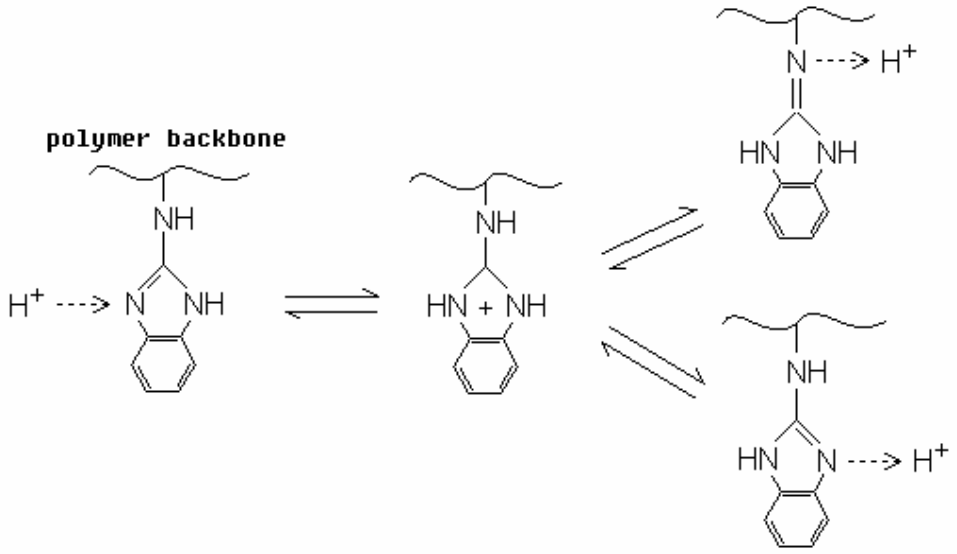

Figure 7.1. Mechanism of proton transfer with 2-amino-benzimidazole units.

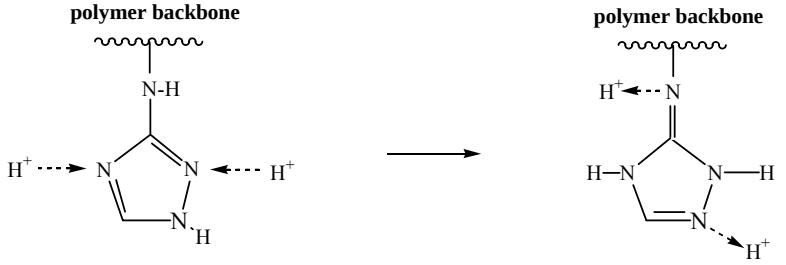

Figure 7.2. Mechanism of proton transfer with 3-amino-1,2,4-1*H*-triazole units.

To demonstrate the feasibility of these concepts, the synthesis of novel polymers such as (i) polysulfone-2-amide-benzimidazole (PSf-ABIm) using carboxylated polysulfone and 2-amino-benzimidazole and (ii) polysulfone-3-amide-1,2,4-1*H*-triazole (PSf-AHT) using carboxylated polysulfone and 3-amino-1,2,4-1*H*-triazole, as well as the electrochemical evaluation in DMFC of blend membranes consisting of PSf-ABIm or

PSf-AHT (basic polymers) and sulfonated poly(ether ether ketone) (SPEEK, an acid polymer) are presented here. These systems were selected based on the following: (i) polysulfone is a low-cost industrial polymer with good mechanical and chemical stabilities, (ii) carboxylated polysulfone precursor can be readily synthesized with a wide variation in the degree of carboxylation as discussed in Chapter 6, offering the flexibility to tune the content of N-heterocycle units in the polymer, (iii) polysulfone is an aromatic polymer and so the PSf-ABIm and PSf-AHT can be expected to have excellent compatibility with SPEEK, offering good long term stability, and (iv) the pendant 2-amino-benzimidazole or 3-amino-1,2,4-1*H*-triazole group could 'insert' into the sulfonic acid group domains of SPEEK, promoting proton conduction through acid-base interaction as well as blocking methanol crossover.

7.2 EXPERIMENTAL

The synthesis of PSf-ABIm was carried out by a condensation reaction between carboxylated polysulfone (CPSf) and 2-amino-benzimidazole (2-ABIm) using triphenylphosphite (TPP) as a dehydration agent at 100 ºC for 3 h to form the amide unit. Lithium chloride was used to enhance the dissolution of the reactants and product in *N,N*-dimethylformamide (DMF). The carboxylated polysulfones had degrees of carboxylation of of 1.03, 1.58, and 1.90.

The synthesis of PSf-AHT was carried out by a similar condensation reaction between CPSf and 3-amino-1,2,4-1*H*-triazole (3-AHT) using TPP as a dehydration agent at 100 ºC for 3 h to form the amide unit. Lithium chloride was used to enhance the

dissolution of the reactants and product in DMF. The carboxylated polysulfones had degrees of carboxylation of of 1.03, 1.58, and 1.90.

The synthesis of SPEEK was carried out by sulfonating PEEK in concentrated sulfuric acid at room temperature for 42 h and the details are available elsewhere [104].

The plain SPEEK and the blend membranes with various PSf-ABIm or PSf-AHT contents were prepared by casting onto a glass plate a *N*,*N*-dimethylacetamide solution of SPEEK or SPEEK + PSf-BIm or SPEEK + PSf-AHT polymers (~ 10 wt.% polymer) and drying at 95 ºC overnight, followed by boiling in de-ionized water for 2 h. Commercial Nafion 112 membrane with a thickness of 50 μm and Nafion 115 membrane with a thickness of 125 μm were selected for comparison, and they were pre-treated as described in Chapter 2.

The structures of the synthesized PSf-ABIm and PSf-AHT were characterized with FT-IR. Proton conductivity values of the membranes were obtained from the impedance data as described in Chapter 2. The percent liquid uptake was obtained from the weight change before and after equilibrating the dry membrane in de-ionized water or methanol solution at 65 and 80 ºC for 30 min.

The SPEEK/PSf-ABIm and SPEEK/PSf-AHT blend membranes were evaluated in DMFC using DMFC electrodes, which were prepared as described in Chapter 2. Methanol crossover was evaluated by a voltammetric method as described in Chapter 2.

7.3 RESULTS AND DISCUSSION

7.3.1 Synthesis and Characterization of Polysulfone-2-amide-benzimidazole (PSf-ABIm)

Fig. 7.3 gives the synthesis of PSf-ABIm by a reaction between CPSf and 2-ABIm using TPP as a dehydration agent. The condensation reaction between the carboxylic acid group and 2-ABIm was easier to occur compared to the formation of polysulfone-benzimidazole discussed in Chapter 6. PSf-ABIm samples with various degrees of substitutions (DS) were synthesized by this process.

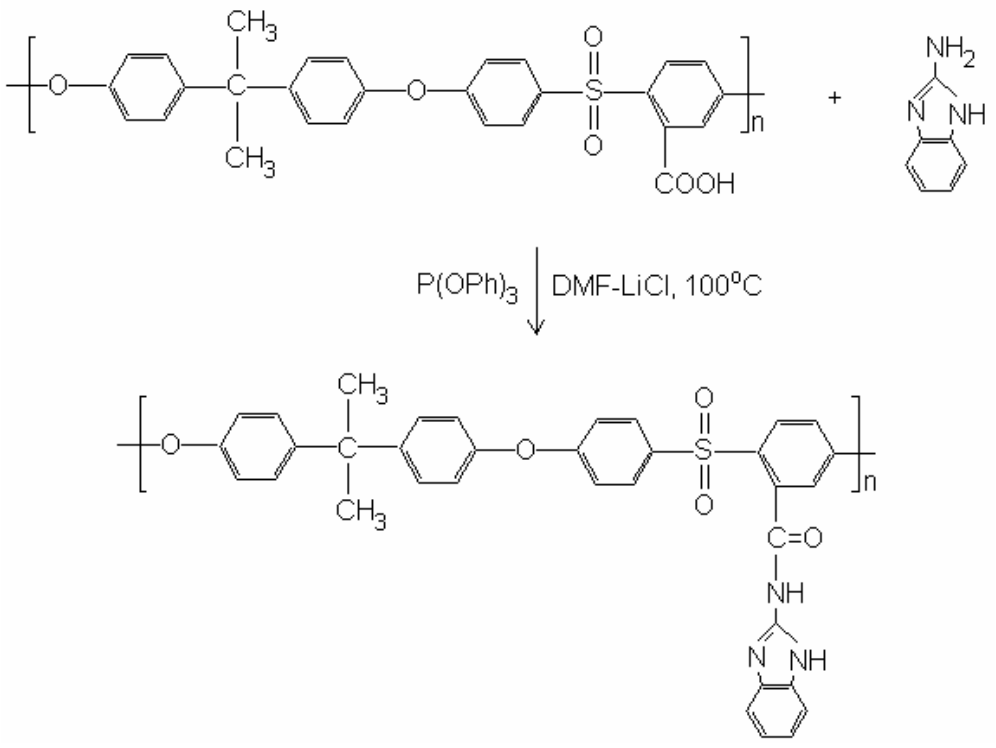

Figure 7.3. Synthesis of polysulfone-2-amide-benzimidazole.

Fig. 7.4 shows the FT-IR spectra of PSf-ABIm with various DS. The main absorption bands of PSf-ABIm indicating the presence of benzimidazole are closely similar to those of PSf-BIm. The bands around 3400 cm^{-1} in PSf-ABIm are attributed to the isolated N-H stretching. The strong absorption at 1740 cm^{-1} is due to the asymmetric C=O stretching in PSf-ABIm. More importantly, the C=N stretching at 1630 cm^{-1}, which indicates the tethering of benzimidazole, increase as the degree of carboxylation increases. These spectral data confirm the formation of 2-amide-benzimidazole side groups onto polysulfone.

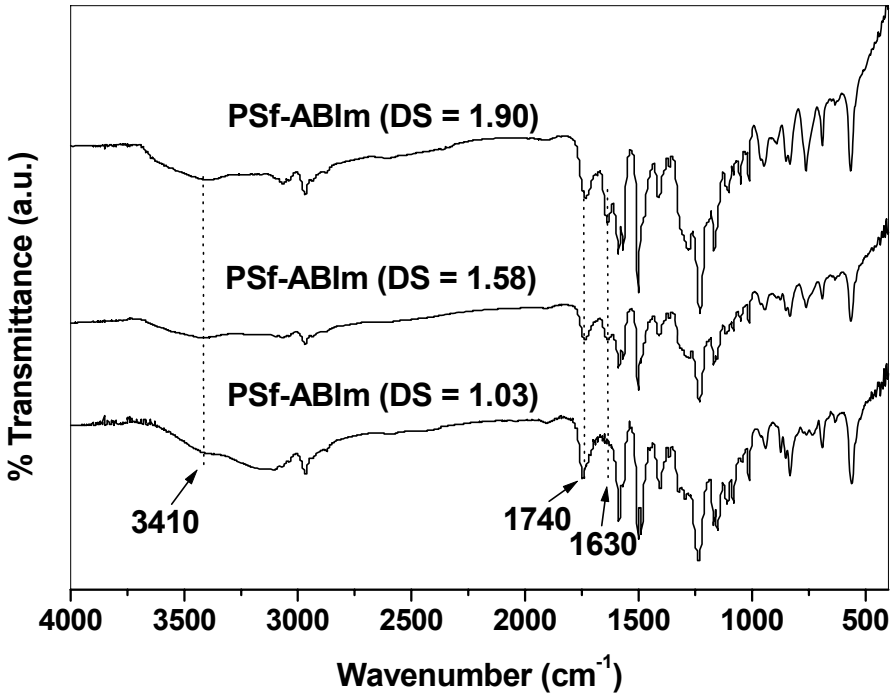

Figure 7.4. FT-IR spectra of polysulfone-2-amide-benzimidazole.

7.3.2 Proton Conductivity of SPEEK/PSf-ABIm Blend Membranes

PSf-ABIm with a DS of 1.90 was used in the following study due to the higher probability of proton transfer in it. Fig. 7.5 compares the proton conductivities of SPEEK and the blend membranes obtained with SPEEK and PSf-ABIm under anhydrous conditions.

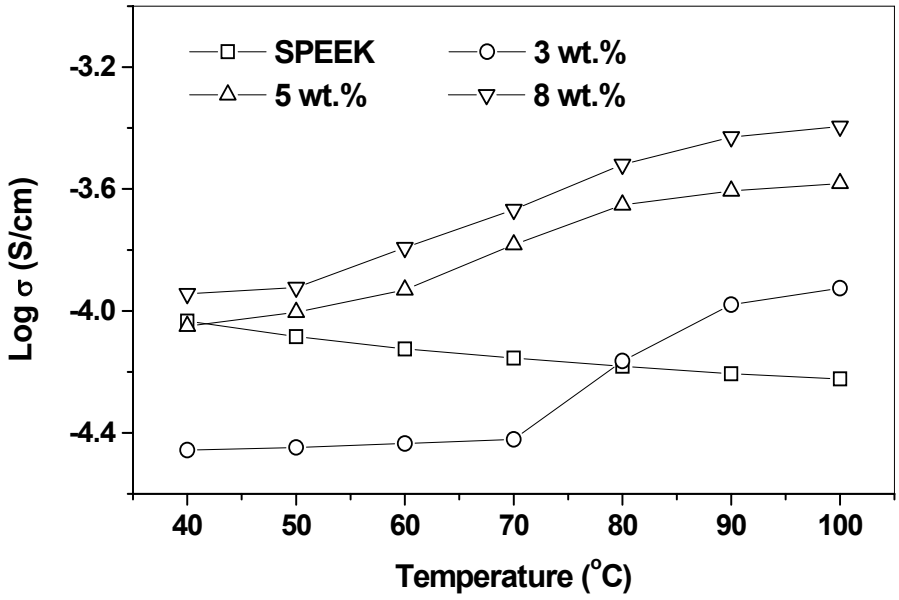

Figure 7.5. Variations of the proton conductivities of the SPEEK and SPEEK/PSf-ABIm blend membranes with temperature under anhydrous condition. The contents of PSf-ABIm in the SPEEK/PSf-ABIm blend membranes are 3, 5, and 8 wt.%.

While the proton conductivity of SPEEK decreases with increasing temperature as the proton conduction becomes difficult at high temperatures in such acid-based polymers,

the conductivity of the SPEEK/PSf-ABIm blend membranes increases with increasing temperature due to the presence of pendant 2-amino-benzimidazole tethered onto polysulfone. Compared to the pendant benzimidazole groups [162], the pendant 2-amino-benzimidazole groups could act as a better 'bridge' to promote proton conduction between sulfonic acid groups under low relative humidity conditions due to the higher numbers of N atoms. Also, the proton conductivity increases as the content of PSf-ABIm increases, confirming the role played by 2-amino-benzimidazole on proton conduction. It is believed that optimization of the microstructure and a uniform distribution of the sulfonic acid and pendant 2-amino-benzimidazole groups could increase the proton conductivity and lower the methanol crossover (see later) further.

7.3.3 Determination of Liquid Uptake in SPEEK/PSf-ABIm Blend Membranes

SPEEK with an ion exchange capacity (IEC) of 1.52 meq./g and a degree of sulfonation (DS) of 51 % was selected in this study, and it has good dimensional stability [104]. Table 7.1 summarizes the [-SO_3H]/[ABIm] mole ratio in the SPEEK/PSf-ABIm blend membranes, which was determined based on the weight fractions of PSf-ABIm and SPEEK, and also compares the percent liquid uptake at different temperatures and methanol concentrations for various PSf-ABIm contents of the SPEEK/PSf-ABIm blend membranes. The liquid uptake increases as the temperature or the methanol concentration increases at a given PSf-ABIm content, and decreases with increasing PSf-ABIm content at a given temperature or methanol concentration. Membrane swelling is a critical issue

for MEA stability in fuel cells, and it generally trends with liquid uptake. Irrespective of water or methanol is being used, the SPEEK/PSf-ABIm blend membranes exhibit lower liquid uptake than plain SPEEK and Nafion 115 membranes, indicating a lower swelling and better stability [102].

Table 7.1 Comparison of the liquid uptake of the SPEEK/PSf-ABIm blend membranes for various [-SO_3H]/[ABIm] mole ratios with those of plain SPEEK membrane.

Wt.% PSf-ABIm	Ratio of [-SO_3H]/[ABIm]	Methanol Concentration (M)	Liquid uptake (wt.%)	
			65 ºC	80 ºC
0	-	0	11.6	20.6
		1	15.7	22.4
		2	24.5	28.9
3	18.9	0	10.9	19.8
		1	15.3	21.4
		2	23.5	27.3
5	11.1	0	10.2	18.2
		1	15.0	20.4
		2	22.8	25.9
8	6.7	0	9.5	16.1
		1	14.1	17.5
		2	21.6	24.3

The lower liquid uptake is due to the lower hydrophilicity of PSf-ABIm compared to that of SPEEK and the acid-base interactions between the sulfonic acid and 2-ABIm groups. The lower liquid uptake could also help to lower the methanol crossover as the crossover is known to trend with the liquid uptake in the SPEEK membrane [104].

7.3.4 Evaluation of SPEEK/PSf-ABIm Blend Membranes and Methanol Crossover in DMFC

Fig. 7.6 compares the electrochemical performance data of the SPEEK/PSf-ABIm blend membranes with those of SPEEK and Nafion membranes in DMFC at 65 and 80 ºC, collected with 1 M methanol solution. The plain SPEEK membrane exhibits higher polarization loss and lower power density compared to both the Nafion 112 and Nafion 115 membranes due to low proton conductivity [104]. Nafion 112 shows better performance than Nafion 115 because it is thinner. The SPEEK/PSf-ABIm blend membrane with 5 wt.% of PSf-ABIm shows performance much better than those of Nafion 115 and plain SPEEK and similar to or slightly better than that of Nafion 112 at 65 and 80 ºC. Also, the blend membrane exhibits higher open circuit voltage (0.731 V and 0.733 V) than all the other three membranes (0.497 – 0.582 V), indicating lower methanol crossover. The better performance of the SPEEK/PSf-ABIm blend membrane compared to that of the plain SPEEK and Nafion membranes could be attributed, respectively, to the promotion of proton conduction through acid-base interaction and lower methanol crossover (see below). Furthermore, while it is difficult to get fuel cell performance data with membranes containing imidazole due to the poisoning of the Pt

catalyst by imidazole [50], the tethering of N-heterocycles like 2-amino-benzimidazole to a polymer backbone prevents or suppresses such poisoning.

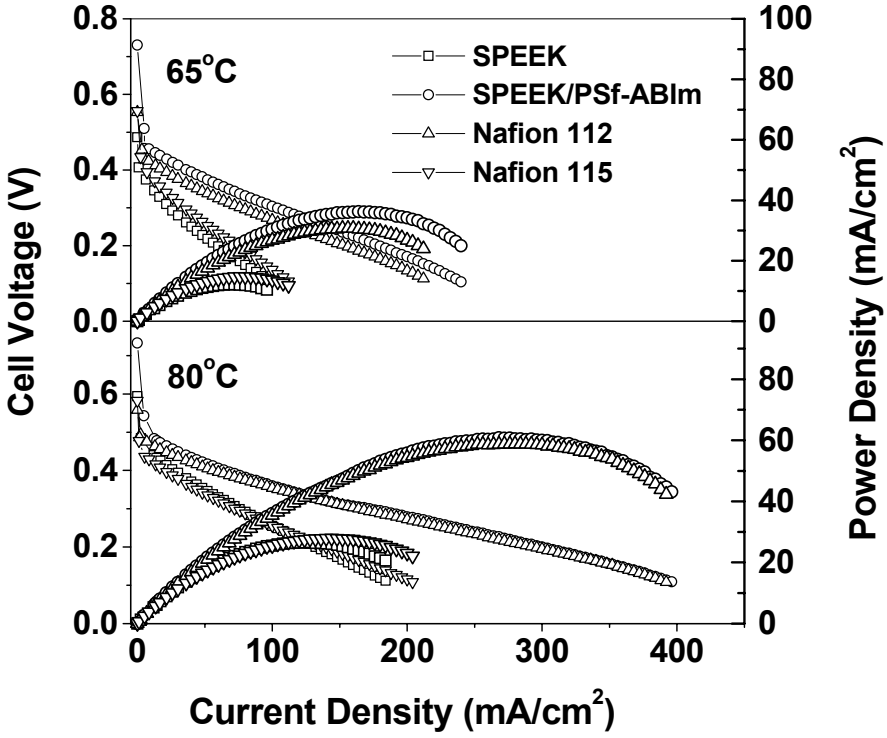

Figure 7.6. Comparison of the polarization curves of the SPEEK/PSf-ABIm (5 wt.% of PSf-ABIm) blend membrane with those of SPEEK, Nafion 112, and Nafion 115 membranes in DMFC at 65 ºC and 80 ºC. The methanol concentration was 1 M.

Fig. 7.7 compares the methanol crossover current density for the membranes. The crossover current density for the PSf-ABIm blend membrane is lower than that found with Nafion 115 at 65 and 80 ^{o}C and plain SPEEK membrane at 65 ^{o}C, but slightly higher

than that found with the plain SPEEK membrane at 80 ^{o}C. This is consistent with the literature data that SPEEK exhibits lower methanol permeability than Nafion 115 [104].

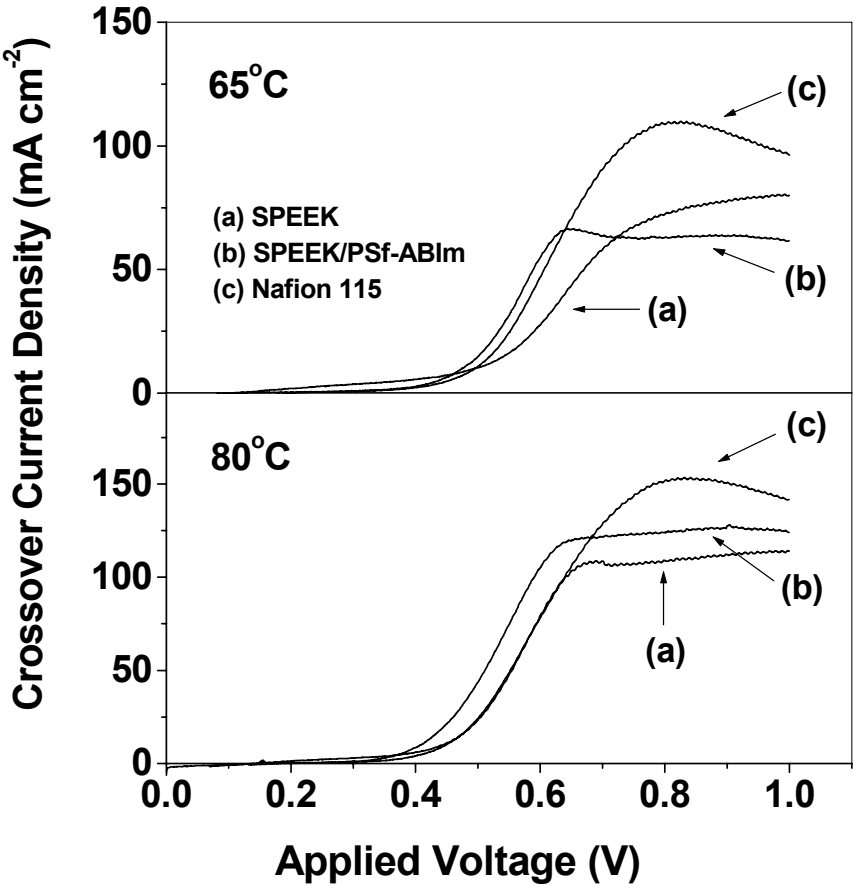

Figure 7.7. Comparison of the methanol crossover current densities of the SPEEK/PSf-ABIm (5 wt.% PSf-ABIm), SPEEK, and Nafion 115 membranes in DMFC at 65 ºC and 80 ºC. The methanol concentration was 1 M. Since the current exceeded the limit of our equipment, the data for Nafion 112 are not given.

The crossover current density for Nafion 112 is not shown in Fig. 7.7 as it was too high to measure due to its lower thickness and exceeded the current limit of our equipment (200 mA/cm^2). The lower methanol crossover observed with the SPEEK/PSf-ABIm blend membrane compared to that with the Nafion membrane could be attributed to the narrower pathways for methanol/water permeation in the former. It has been found that the separation between the hydrophobic and hydrophilic groups in SPEEK is smaller compared to that in Nafion, resulting in a stronger confinement of water/methanol in the narrow channels and significantly lower water/methanol permeation [71,91,133]. The 2-amino-benzimidazole side groups tethered to polysulfone and their interaction with the hydrophilic groups of SPEEK by Grotthuss-type mechanism helps to reduce the methanol crossover further.

Fig. 7.8a compares the electrochemical performance data of the SPEEK/PSf-ABIm blend membranes with various PSf-ABIm contents at 80 ºC that were collected with 2 M methanol solution. The fuel cell performance increases initially with increasing PSf-ABIm content up to 5 wt.% and then decreases on going to 8 or 10 wt.%. Fig. 7.8b compares the maximum power density P_{max} of the blend membranes for various ratios of sulfonic acid groups to 2-amino-benzimidazole units in the blend membranes. The blend membrane with 5 wt.% PSf-ABIm offers the highest P_{max}, suggesting that an optimum ratio between the sulfonic acid and 2-amino-benzimidazole groups may maximize the proton conductivity through acid-base interactions.

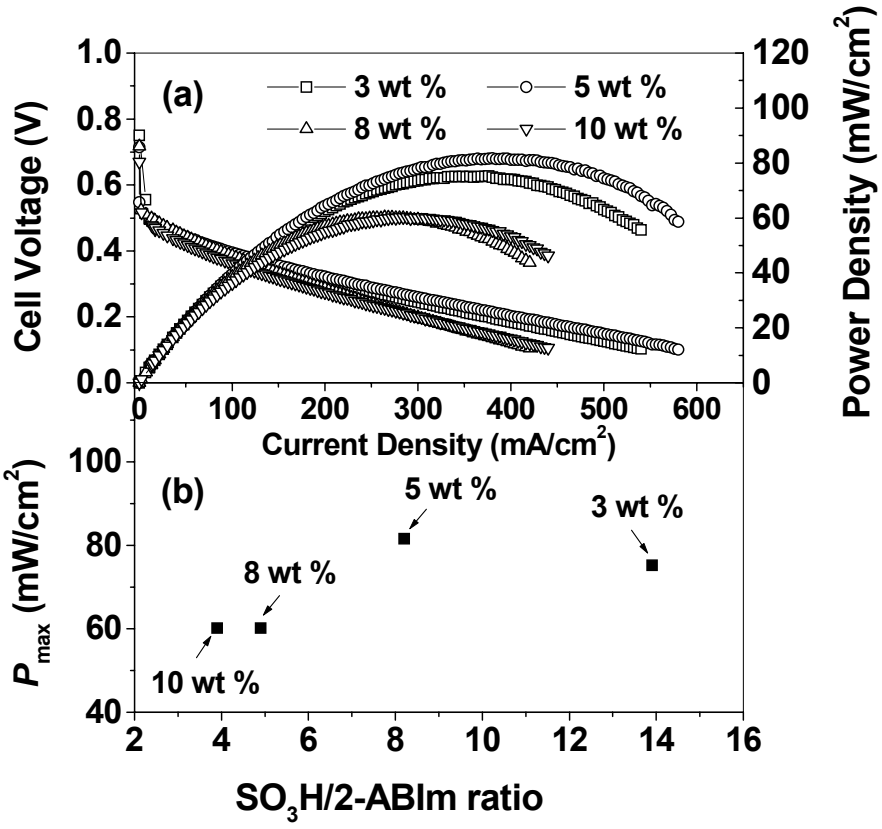

Figure 7.8. (a) Comparison of the polarization curves of the blend membranes with 3, 5, 8 and 10 wt.% of PSf-ABIm in the SPEEK/PSf-ABIm blend membranes in DMFC at 80 ºC with a methanol concentration of 2 M. (b) Variation of the maximum power density P_{max} of the blend membranes with the SO_3H/2-ABIm ratio in the blend membrane.

In order to assess the long-term performance, the SPEEK/PSf-ABIm blend membrane with 3 wt.% PSf-ABIm was evaluated continuously for 120 h. Little or no decline in performance was found after 120 h with the PSf-ABIm blend membrane due to suppressed methanol crossover, while the Nafion 112 membrane exhibited a decline in

performance due to a much higher amount of methanol crossover (Fig. 7.9). Thus, despite a similar initial performance in DMFC, the blend membrane exhibits much better long-term performance than Nafion 112. The superior performance of the blend membrane with lower methanol crossover compared to Nafion could also enable a lower Pt catalyst loading at the cathode, offering additional cost savings.

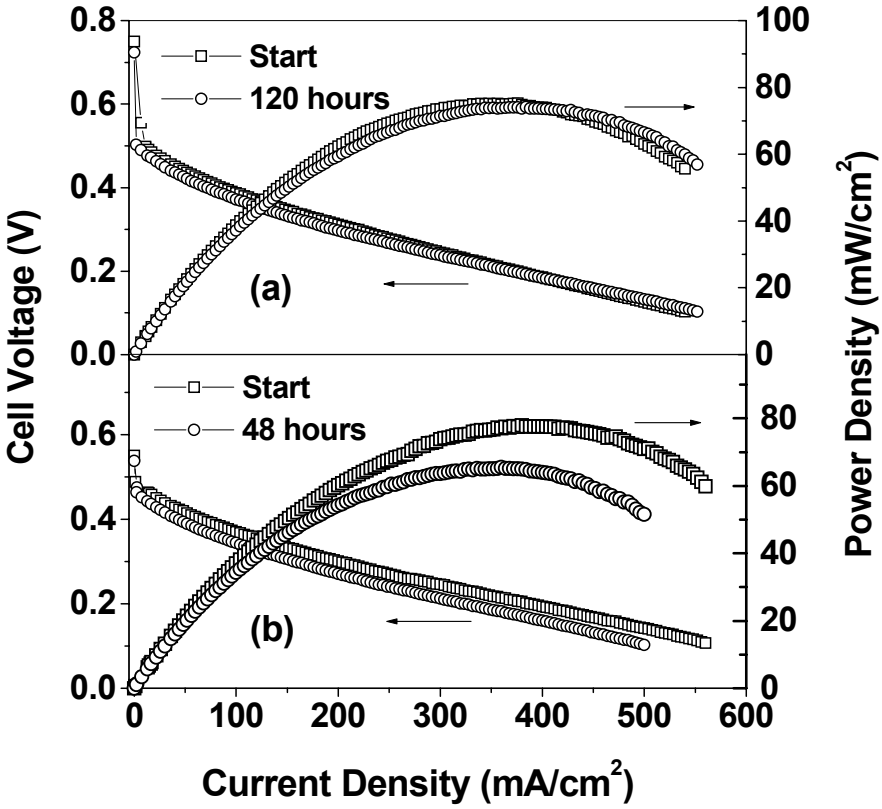

Figure 7.9. Long-term performance tests carried out with the (a) SPEEK/PSf-ABIm (3 wt.%) blend membrane and (b) Nafion 112 membrane at 80 ºC in DMFC. The methanol concentration was 2 M.

7.3.5 Synthesis and Characterization of Polysulfone-3-amide-1,2,4-1*H*-triazole (PSf-AHT)

Fig. 7.10 gives the synthesis of PSf-AHT by a reaction between CPSf and 3-amino-1,2,4-1*H*-triazole (3-AHT) using TPP as a dehydration agent. The condensation reaction between the carboxylic acid group and 3-AHT was similar to that of 2-amide-benzimidazole formation in PSf-ABIm. PSf-AHT samples with various DS were synthesized by this process.

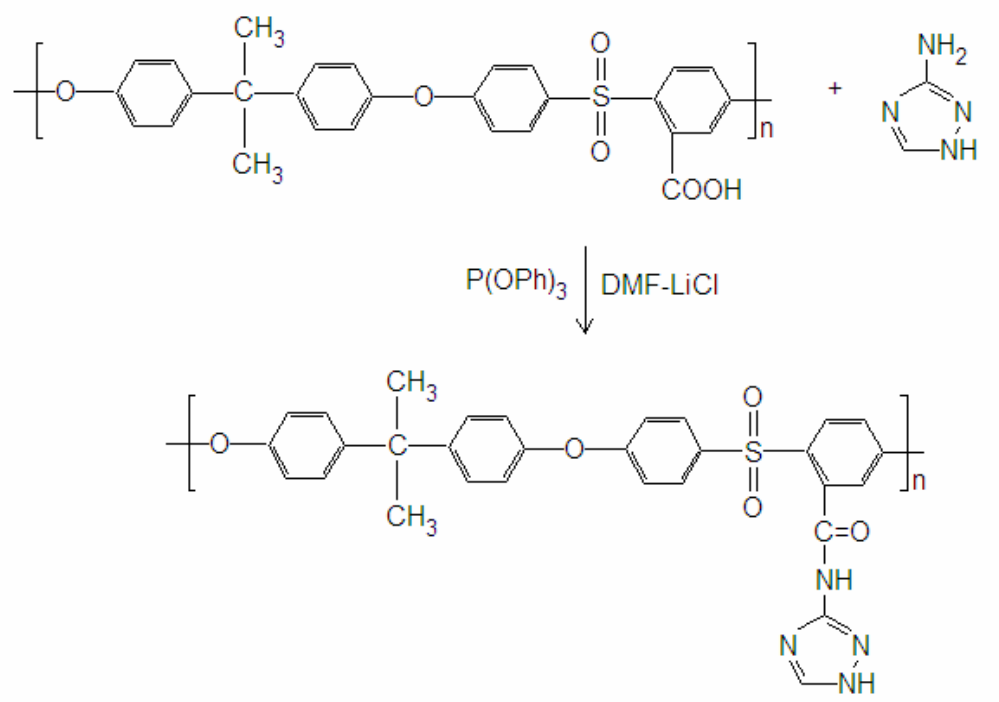

Figure 7.10. Synthesis route of polysulfone-3-amide-1*H*-1,2,4-triazole.

Fig. 7.11 shows the FT-IR spectra of PSf-AHT with various DS. The bands around 3400 cm^{-1} in PSf-AHT are attributed to the isolated N-H stretching. The strong

absorption at 1740 cm^{-1} is due to the asymmetric C=O stretching in PSf-AHT. The C=N stretching at 1630 cm^{-1} similar to that in PSf-ABIm indicates the tethering of triazole to polysulfone. These spectral data confirm the formation of 3-amide-1,2,4-1*H*-triazole side groups onto polysulfone.

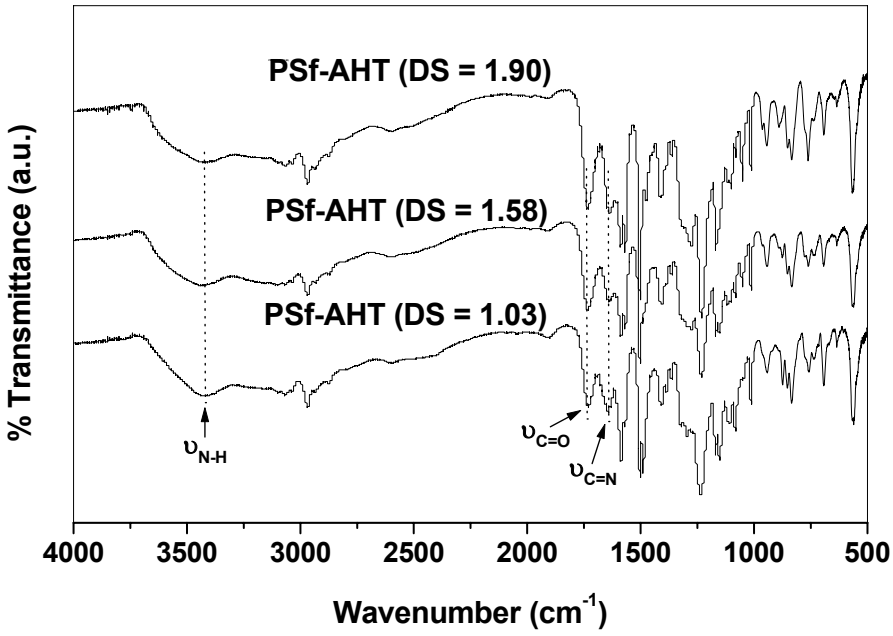

Figure 7.11. FT-IR spectra of carboxylated polysulfone and polysulfone-3-amide-1*H*-1,2,4-triazole.

7.3.6 Proton Conductivity of SPEEK/PSf-AHT Blend Membranes

PSf-AHT with a degree of substitution of 1.90 was used in the following study due to the higher probability for proton transfer. Fig. 7.12 compares the proton conductivities of SPEEK and the blend membranes obtained with SPEEK and PSf-AHT under

anhydrous condition. While the proton conductivity of SPEEK decreases with increasing temperature as the proton conduction becomes difficult at high temperatures in such acid-based polymers, the conductivity of the SPEEK/PSf-AHT blend membranes increase with increasing temperature due to the presence of pendant 3-amino-1,2,4-1*H*-triazole tethered onto polysulfone. The lower proton conductivities of SPEEK/PSf-AHT with 2 and 3 wt.% PSf-AHT compared to that of plain SPEEK at temperatures below 80 ^{o}C is due to the higher basicity of triazole containing three N atoms.

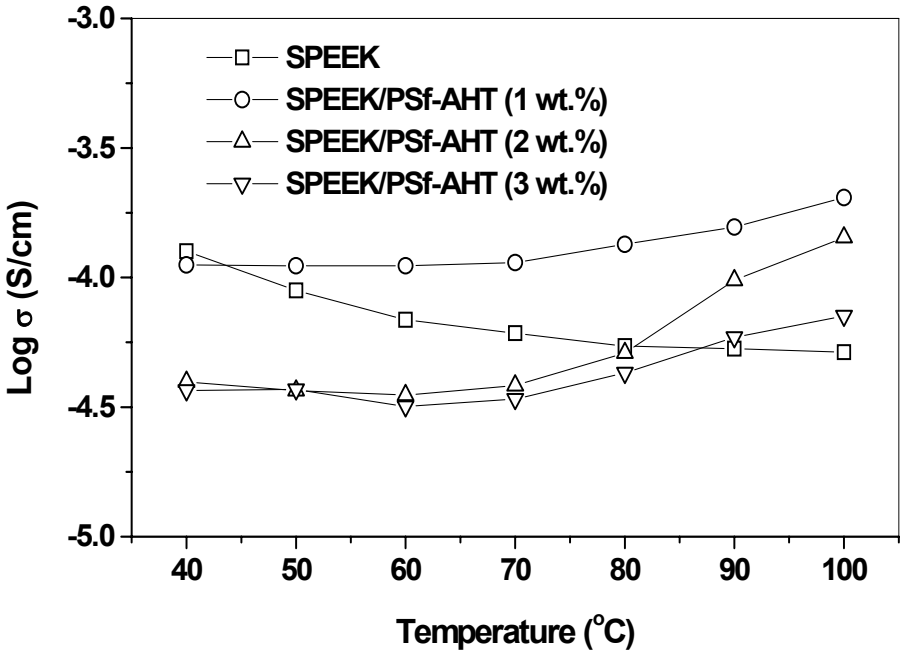

Figure 7.12. Variations of the proton conductivities of the SPEEK/PSf-AHT blend membranes with temperature under anhydrous conditions.

Compared to the pendant 2-amino-benzimidazole group, the pendant 3-amino-1,2,4-1*H*-triazole groups did not show better ability to promote proton conduction under anhydrous conditions. Also, the proton conductivity decreases as the content of PSf-AHT increases, indicating the effect of the higher basicity of 3-amino-1,2,4-1*H*-triazole on the proton conduction in the blend membranes. It is believed that optimization of the microstructure and a uniform distribution of the sulfonic acid and pendant 3-amino-1,2,4-1*H*-triazole groups could influence the acid-base interaction between them and proton conduction.

7.3.7 Evaluation of SPEEK/PSf-AHT Blend Membranes and Methanol Crossover in DMFC

Fig. 7.13 compares the electrochemical performance data of the SPEEK/PSf-AHT blend membranes with that of the plain SPEEK in DMFC at 65 ^{o}C, collected with 1 M methanol solution. The SPEEK/PSf-AHT blend membrane with 1 wt.% PSf-AHT shows performance better than that of the plain SPEEK. Also, it exhibits higher open circuit voltage than that of the plain SPEEK. The better performance of the SPEEK/PSf-AHT blend membrane compared to that of the plain SPEEK could be attributed to the promotion of proton conduction through acid-base interaction. However, the SPEEK/PSf-AHT blend membranes with 2 and 3 wt.% PSf-AHT show performance comparable or lower than that of the plain SPEEK, which is due to the higher basic property of 3-amino-1,2,4-1*H*-triazole as discussed above. Overall, the fuel cell performances of SPEEK/PSf-AHT blend membranes are consistent with the proton

conductivities measured under anhydrous condition. Compared to the SPEEK/PSf-ABIm blend membrane, the SPEEK/PSf-AHT blend membranes appear to be more complex due to the more numbers of N atoms present in the PSf-AHT.

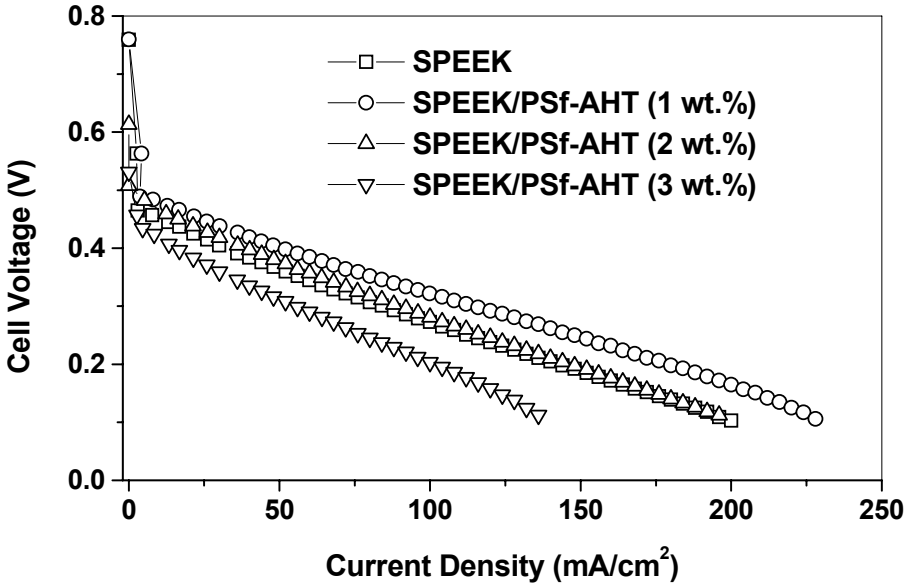

Figure 7.13. Comparison of the polarization curves of the SPEEK/PSf-AHT blend membranes with that of SPEEK in DMFC. The experimental conditions are same as those in Fig. 7.6. Cell temperature: 65 ^{o}C, methanol concentration: 1 M.

Fig. 7.14 compares the methanol crossover current density for the plain SPEEK and the SPEEK/PSf-AHT blend membranes. The SPEEK/PSf-AHT blend membrane with 3 wt.% PSf-AHT exhibits lower methanol crossover current density than the plain SPEEK. However, the other two blend membranes with 1 and 2 wt.% PSf-AHT show higher

methanol crossover current densities. It may be complex to predict the effect of PSf-AHT on methanol crossover in SPEEK/PSf-AHT due to the multiple N atoms present in AHT.

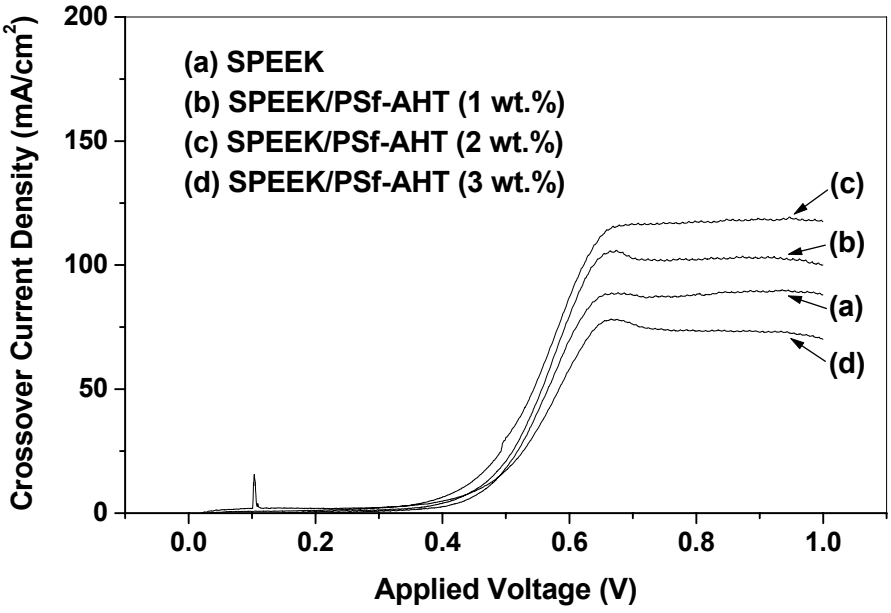

Figure 7.14. Comparison of the variations of the methanol crossover current density for the SPEEK/PSf-AHT and SPEEK membranes in DMFC. Cell temperature: 65 ^{o}C, methanol concentration: 1 M.

7.4 CONCLUSIONS

In summary, two novel polymeric membrane materials based on 2-amino-benzimidazole and 3-amino-1,2,4-1*H*-triazole units have been synthesized and characterized. Blend membranes consisting of polysulfone-2-amide-benzimidazole or polysulfone-3-amide-1,2,4-1*H*-triazole (basic polymers) and sulfonated poly(ether ether

ketone) (acid polymer) demonstrate a viable strategy to facilitate proton conduction through acid-base interactions and suppress methanol crossover sometimes, while preserving good mechanical and chemical stabilities. The SPEEK/PSf-ABIm blend membrane exhibits superior, long-term performance in DMFC with little or no decline with time due to a significant reduction in methanol permeability. These membranes based on acidic and basic polymer blends offer a promising strategy for DMFC. Although the concept is demonstrated here with polysulfone and SPEEK, the strategy could be applied with a wide variety and combination of other aromatic polymers. These membranes involving acid-base interactions also offer the possibility of exhibiting high proton conductivity and good performance in proton exchange membrane fuel cells (PEMFC) at higher temperatures (> 100 ^{o}C) and low relative humidity. However, the SPEEK/PSf-AHT blend membranes exhibit more complex effects on fuel cell performance and methanol crossover. Further work needs to be done to utilize the N-heterocycles containing multiple nitrogen atoms effectively.

Chapter 8

Summary

With an aim to develop high performance and low cost membrane materials for high temperature proton exchange membrane fuel cells (PEMFC) and direct methanol fuel cells (DMFC), sulfonated polysulfone (SPSf) membranes, Nafion-Imidazole composite membranes, blend membranes containing SPSf and 1,3-1*H*-dibenzimidazole-benzene, blend membranes containing sulfonated poly(ether ether ketone) (SPEEK) and polysulfone-benzimidazole, and blend membranes containing SPEEK and polymer-N-heterocycles with more than two nitrogen atoms have been developed and investigated.

The SPSf membranes with different degrees of sulfonation of 50 - 70 % were prepared and investigated in DMFC. They exhibit performances comparable to that of Nafion 115 due to lower methanol crossover, but the performances at high current densities with high concentrations of methanol (2 M) are lower than that of Nafion 115 due to the lower proton conductivity. The lower methanol crossover of SPSf membrane is attributed to the narrower hydrophilic channels, resulting in a stronger confinement of water/methanol in the narrow channels and significantly lower water/methanol permeation compared to that in Nafion 115 membrane. The lower proton conductivity is due to the weaker acidity of sulfonic acid in SPSf membrane compared to that in Nafion 115 membrane. In addition, detachment of the electrodes from the SPSf membranes were observed after 2 days of operation in DMFC due to the poor adhesion and bonding

properties. Modification of the electrodes and the electrode-membrane interface is needed to overcome this problem and improve the long-term stability. Nevertheless, the lower cost and methanol crossover compared to those in Nafion make the SPSf membranes promising alternatives for DMFC.

Replacement of water by imidazole in Nafion offers higher operating temperatures for PEMFC. The presence of imidazole in Nafion membrane facilitates proton conduction by Grotthuss-type mechanism, resulting in high proton conductivity at temperature higher than 100 ^{o}C. Unfortunately, imidazole poisons the Pt catalyst. Doping the Nafion-Imidazole composite membranes with H_3PO_4 partly suppresses the poisoning, but the doping of imidazole with phosphoric acid to form the imidazolium salt suppresses the poisoning further. As a result, the performance of the Nafion-Imidazole-H_3PO_4 membranes with the conventional Pt catalyst is better than that of Nafion-Imidazole with the Pt catalyst, but it is still lower than that of Nafion with Pt catalyst. To further improve the fuel cell performance at high temperatures, Pd-Co-Mo catalyst was employed with the Nafion-Imidazole-H_3PO_4 membranes. The Nafion-Imidazole-H_3PO_4 membranes with the Pd-Co-Mo catalyst offer electrochemical performance in PEMFC at 100 ^{o}C superior to that of Nafion membrane with the Pt or Pd-Co-Mo catalyst, demonstrating a tolerance of the Pd-Co-Mo catalyst to imidazole poisoning. The study demonstrates that water-free membranes based on Nafion and heterocycles that could successfully operate at elevated temperatures ($\geq$ 100 ^{o}C) could be developed with non-platinum catalysts such as Pd-Co-Mo. However, the long term stability of the heterocycle groups within the membrane needs to be fully assessed.

Compared to imidazole, benzimidazole has a lower pK_a value, which makes it potential for application in PEMFC and DMFC. 1,3-1*H*-dibenzimidazole-benzene containing two benzimidazole groups was selected and synthesized using phosphorus pentoxide-methanesulfonic acid (PPMA) as a solvent and dehydration agent. It was blended with SPSf and employed as a membrane for DMFC. The presence of benzimidazole in the blend membrane improves the proton conductivity by acid-base interactions between the sulfonic acid and benzimidazole groups as well as lowers methanol crossover. The SPSf/DBImBenzene blend membranes with various DBImBenzene contents (0 - 2 wt.%) were prepared and compared with those of plain SPSf membrane. The blend membranes with an optimum DBImBenzene content of 0.5 - 1.0 wt.% exhibit better performance in DMFC than plain SPSf membrane due to an enhancement in proton conductivity through acid-base interactions and a reduction in methanol crossover. The SPSf/DBImBenzene blend membranes also show performance comparable to that of Nafion 115 membrane, but the latter exhibits much higher methanol crossover. This type of blend membranes have the potential to overcome some of the issues associated with DMFC.

To overcome the possible long-term instability of small molecules in the blend membranes, a novel aromatic polymer (polysulfone) bearing benzimidazole side group was designed and synthesized. It is totally different from the well-known PBI polymer, and it has the benzimidazole units attached to the main chain. Blend membranes fabricated with sulfonated poly(ether ether ketone) (SPEEK) and polysulfone bearing benzimidazole side groups exhibit higher proton conductivity and better performance in

PEMFC at 90 and 100 ºC compared to the SPEEK or Nafion membranes. The study demonstrates that polymers bearing benzimidazole side groups may become a viable strategy to develop new membranes that could enable the operation of PEMFC at higher temperatures and low relative humidity. Additionally, the SPEEK/PSf-BIm blend membranes with different PSf-BIm contents (0 – 10 wt.%) have been prepared and compared with those of plain SPEEK membrane in DMFC. The blend membranes with an optimum PSf-BIm content of 8 wt.% exhibit better performance in DMFC than plain SPEEK due to an enhancement in proton conductivity through acid-base interactions and a reduction in methanol crossover. Although the performance of the SPEEK/PSf-BIm blend membranes in DMFC is lower than that of Nafion 112 due to lower proton conductivity, the former exhibits much reduced methanol crossover, offering better long term stability and performance. The lower methanol crossover could be attributed to the following reasons: (i) SPEEK has narrow pathways for methanol/water permeation and (ii) PSf-BIm with an aromatic backbone similar to that in SPEEK can be expected to have good compatibility with SPEEK at the molecular scale, and the insertion of the benzimidazole side groups into the hydrophilic groups of SPEEK can reduce methanol permeability further while enhancing proton conduction through acid-base interactions. Also, increase in the degree of sulfonation in SPEEK as well as an optimization of the PSf-BIm content in SPEEK/PSf-BIm and the MEA fabrication process could improve the performance in DMFC further.

Two other novel polymeric membrane materials based on 2-amino-benzimidazole and 3-amino-1,2,4-1*H*-triazole units have also been synthesized and characterized. They

provide more than two proton transfer sites compared to benzimidazole group. Blend membranes consisting of polysulfone-2-amide-benzimidazole (PSf-ABIm) or polysulfone-3-amide-1,2,4-1*H*-triazole (PSf-AHT) (basic polymers) and SPEEK (acid polymer) demonstrate a viable strategy to facilitate proton conduction through acid-base interactions and suppress methanol crossover sometimes, while preserving good mechanical and chemical stabilities. The SPEEK/PSf-ABIm blend membrane exhibits superior, long-term performance in DMFC with little or no decline with time due to a significant reduction in methanol permeability. These membranes based on acidic and basic polymer blends offer a promising strategy for DMFC. Although the concept is demonstrated with polysulfone and SPEEK, the strategy could be applied with a wide variety and combination of other aromatic polymers. These membranes involving acid-base interactions also offer the possibility of exhibiting high proton conductivity and good performance in proton exchange membrane fuel cells (PEMFC) at higher temperatures (> 100 ^{o}C) and low relative humidity. However, the SPEEK/PSf-AHT blend membranes exhibit complex effects on the fuel cell performance and methanol crossover. Further work needs to be done to utilize the N-heterocycles containing multiple nitrogen atoms effectively.

In summary, this investigation demonstrates that significant improvements in the performance of PEMFC and DMFC and important cost savings can be achieved by developing new proton exchange membranes. Successful development of high temperature membranes that can operate at high temperatures (> 100 ^{o}C) can have a profound impact in the fuel cell technology. It can alleviate the CO poisoning problem

considerably and could possibly allow the exploration of non-platinum catalysts. This can lower the fuel cleanup and raw materials costs significantly, and make the fuel cell technology more cost competitive with the other existing technologies like internal combustion engines (ICE). Development of alternative membrane materials with much low methanol crossover can also have significant impact in the direct methanol fuel cell technology by allowing the use of high concentration methanol solution and low loading of Pt catalyst at the cathode, which is important in increasing the energy density and fabricating miniaturized DMFCs for portable electronic device applications.

Bibliography

[1] K. Kordesch, G. Simader, Fuel Cells and Their Applications, VCH, 1996.

[2] P. Costamagna, S. Srinivasan, J. Power Sources 102 (2001) 242.

[3] S. Srinivasan, R. Mosdale, P. Stevens, C. Yang, Annu. Rev. Energ. Env. 24 (1999) 281.

[4] B. D. McNicol, D. A. J. Rand, K. R. Williams, J. Power Sources 100 (2001) 47.

[5] B. Yang, Ph.D. dissertation, The University of Texas at Austin, August, 2004.

[6] M. S. Wilson, S. Gottesfeld, J. Appl. Electrochem. 22 (1992) 1.

[7] E. A. Ticianelli, C. R. Derouin, A. Redondo and S. Srinivason, J. Electrochem. Soc. 135 (1988) 2209.

[8] M. S. Wilson and S. Gottesfeld, J. Electrochem. Soc. 139 (1992) L28.

[9] M. S. Wilson, J. A. Valerio and S. Gottesfeld, Electrochim. Acta 40 (1995) 355.

[10] X. M. Ren, P. Zelenay, S. Thomas, J. Davey, S. Gottesfeld, J. Power Sources 86 (2000) 111.

[11] Y. H. L. Eisenberg A., Perfluorinated Ionomer Membranes, ACS Symposium Series 180, American Chemical Society, Washington, DC, 1982.

[12] S. R. Samms, S. Wasmus, R. F. Savinell, J. Electrochem. Soc. 143 (1996) 1498.

[13] A. Steck, O. Savadogo, P.R. Roberge, T.N. Veziroglu (Eds.), Proceedings of the First International Symposium on New Materials for Fuel Cell Systems, Montreal, Canada, July 9 -13, 1995, p. 74.

[14] E. J. Roche, M. Pineri, R. Duplessix, J. Polym. Sci. Polym, Phys. Ed. 20 (1982) 107.

[15] N. J. Bunce, S. J. Sondheimer, C. A. Fyfe, Macromolecules 19 (1986) 333.

[16] B. D. Cahan, J. S. Wainright, J. Electrochem. Soc. 140 (1993) L185.

[17] R. A. Komoroski and K. A. Mauritz, J. Am. Chem. Soc. 100 (1978) 7487.

[18] W. Y. Hsu and T. D. Girerke, J. Membr. Sci. 13 (1983) 307.

[19] T. D. Gierke, G. E. Munn, F. C. Wilson, J. Polym. Sci. Polym. Phys. Ed. 19 (1981) 1687.

[20] W. C. Heitner, Polymer 20 (1979) 371.

[21] J. Ceynowa, Polymer 19 (1978) 73.

[22] Y.-Z. Fu, M. S. dissertation, Dalian Institute of Chemical Physics, Chinese Academy of Science, June, 2003.

[23] F. Barbir, T. Gomez, Int. J. Hydrogen. Energy 21 (1996) 891.

[24] C. Gavach, G. Pamboutzouglou, M. Nedyalkov, and G. Pourcelly, J. Membr. Sci. 45 (1989) 37.

[25] Q. F. Li, R. H. He, J. A. Gao, J. O. Jensen, N. J. Bjerrum, J. Electrochem. Soc. 150 (2003) A1599.

[26] M. W. Verbrugge, J. Electrochem. Soc. 136 (1989) 417.

[27] J. T. Wang, S. Wasmus, R. F. Savinell, J. Electrochem. Soc. 143, (1996) 1233.

[28] P. Colomban (Ed.), Proton Conductors: Solids, Membranes and Gels-Materials and Devices (Chemistry of Solid State Materials, No 2), Cambridge University Press, 1992.

[29] K. D. Kreuer, Solid State Ionics 136 (2000) 149.

[30] K. T. Adjemian, S. Srinivasan, J. Benziger, A. B. Bocarsly, J. Power Sources 109

(2002) 356.

[31] N. Miyake, J. S. Wainright, R. F. Savinell, J. Electrochem. Soc. 148 (2001) A898.

[32] P. L. Antonucci, A. S. Arico, P. Creti, E. Ramunni, V. Antonucci, Solid State Ionics 125 (1999) 431.

[33] A. S. Arico, P. Creti, P. L. Antonucci, V. Antonucci, Electrochem. Solid-State Lett. 1 (1998) 66.

[34] B. Baradie, J. P. Dodelet, D. Guay, J. Electroanal. Chem. 489 (2000) 101.

[35] M. Watanabe, H. Uchida, M. Emori, J. Phys. Chem. B 102 (1998) 3129.

[36] C. Trakanprapai, V. Esposito, S. L. Coccia, E. Traversa, V. Baglio, A. D. Blasi, A. S. Arico, V. Antonucci, P. L. Antonucci, Abstract No. 1080, The 204th Meeting of The Electrochemical Society, Orlando, FL, Oct. 12 -17, 2003.

[37] B. Yang and A. Manthiram, J. Electrochem. Soc. 151 (2004) A2120.

[38] G. Alberti, M. Casciola, Solid State Ionics 97 (1997) 177.

[39] P. Costamagna, C. Yang, A. B. Bocarsly, S. Srinivasan, Electrochim. Acta 47 (2002) 1023.

[40] G. Alberti, M. Casciola, Annu. Rev. Mater. Res. 33 (2003) 129.

[41] J. Roziere, D. J. Jones, Annu. Rev. Mater. Res. 33 (2003) 503.

[42] M. Rikukawa, K. Sanui, Prog. Polym. Sci. 25 (2000) 1463.

[43] D. A. Boysen, T. Uda, C. R. I. Chisholm, S. M. Haile, Science 303 (2004) 68.

[44] S. M. Haile, D. A. Boysen, C. R. I. Chisholm, R. B. Merle, Nature 410 (2001) 910.

[45] M. E. Schuster, W. H. Meyer, Annu. Rev. Mater. Res. 33 (2003) 233.

[46] R. A. Zoppi, I. V. P. Yoshida, S. P. Nunes, Polymer 39 (1998) 1309.

[47] G. Alberti, M. Casciola, R. Palombari, J. Membr. Sci. 172 (2000) 233.

[48] K. A. Mauritz, I. D. Stefanithis, S. V. Davis, R. W. Scheetz, R. K. Pope, G. L. Wilkes, H. H. Huang, J. Appl. Polym. Sci. 55 (1995) 181.

[49] P. L. Shao, K. A. Mauritz, R. B. Moore, Chem. Mater. 7 (1995) 192.

[50] C. Yang, P. Costamagna, S. Srinivasan, J. Benziger, A.B. Bocarsly, J. Power Sources 103 (2001) 1.

[51] C. Yang, S. Srinivasan, A.S. Arico, P. Creti, V. Baglio, V. Antonucci, Electrochem. Solid-State Lett. 4 (2001) A31.

[52] R. Savinell, E. Yeager, D. Tryk, U. Landau, J. Wainright, D. Weng, K. Lux, M. Litt, C. Rogers, J. Electrochem. Soc. 141 (1994) L46.

[53] P. Donoso, W. Gorecki, C. Berthier, F. Defendini, C. Poinsignon, M. B. Armand, Solid State Ionics 28 (1988) 969.

[54] J. Przyluski, A. Zalewska, J. Maron, W. Wieczorek, Polish J. Chem. 71 (1997) 968.

[55] M. F. Daniel, B. Desbat, F. Cruege, O. Trinquet, J. C. Lassegues, Solid State Ionics 28 (1988) 637.

[56] R. Tanaka, H. Yamamoto, A. Shono, K. Kubo, M. Sakurai, Electrochim. Acta 45 (2000) 1385.

[57] D. Rodriguez, C. Jegat, O. Trinquet, J. Grondin, J.C. Lassegues, Solid State Ionics 61 (1993) 195.

[58] P. Musto, F. E. Karasz, and W. J. MacKnight, Polymer 34 (1993) 2934.

[59] J. S. Wainright, J. T. Wang, D. Weng, R. F. Savinell, M. Litt, J. Electrochem. Soc. 142 (1995) L121.

[60] S. Wasmus, B. A. Dauch, and H. Moadel, Proceedings of the 187th Electrochemical Society Meeting, Reno, Abstract 466, 1995.

[61] Q. Li, R. He, J. O. Jensen, N. J. Bjerrum, Fuel Cells 4 (2004) 147.

[62] R. Bouchet, S. Miller, M. Duclot, and J. L. Souquet, Solid State Ionics 145 (2001) 69.

[63] R. Bouchet and E. Siebert, Solid State Ionics 118 (1999) 287.

[64] Y. L. Ma, J. S. Wainright, M. H. Litt, R. F. Savinell, J. Electrochem. Soc. 151 (2004) A8.

[65] X. Glipa, B. Bonnet, B. Mula, D.J. Jones, J. Roziere, J. Mater. Chem. 9 (1999) 3045.

[66] R. H. He, Q. F. Li, G. Xiao, N. J. Bjerrum, J. Membr. Sci. 226 (2003) 169.

[67] K. D. Kreuer, Chem. Mater. 8 (1996) 610.

[68] K. D. Kreuer, A. Fuchs, M. Ise, M. Spaeth, and J. Maier, Electrochim. Acta 43 (1998) 1281.

[69] J. Sun, L. R. Jordan, M. Forsyth, D. R. MacFarlane, Electrochim. Acta, 46 (2001) 1703.

[70] P. Jannasch, Curr. Opin. in Colloid and Inter. Sci. 8 (2003) 96.

[71] K. D. Kreuer, Solid State Ionics 97 (1997) 1.

[72] H. G. Herz, K. D. Kreuer, J. Maier, G. Scharfenberger, M. F. H. Schuster, W. H. Meyer, Electrochim. Acta 48 (2003) 2165.

[73] W. Münch, K. D. Kreuer, W. Silvestri, J. Maier, G. Seifert, Solid State Ionics 145 (2001) 437.

[74] M. Schuster, W. H. Meyer, G. Wegner, H. G. Herz, M. Ise, K. D. Kreuer, J. Maier, Solid State Ionics 145 (2001) 85.

[75] M. F. H. Schuster, W. H. Meyer, M. Schuster, K. D. Kreuer, Chem. Mater. 16 (2004) 329.

[76] H. Pu, L. Qiao, Macromol. Chem. Phys. 206 (2005) 263.

[77] S. M. Haile, P. M. Calkins, and D. Boysen, Solid State Ionics 97 (1997) 145.

[78] C. R. I. Chisholm and S. M. Haile, Solid State Ionics 136-137 (2000) 229.

[79] B. Yang, A. M. Kannan, A. Manthiram, Mater. Res. Bull. 38 (2003) 691.

[80] E. B. Easton, B. L. Langsdorf, J. A. Hughes, J. Sultan, Z. G. Qi, A. Kaufman, P. G. Pickup, J. Electrochem. Soc. 150 (2003) C735.

[81] A. Sungpet, J. Membr. Sci. 226 (2003) 131.

[82] M. A. Smit, A. L. Ocampo, M. A. Espinosa-Medina, P. J. Sebastian, J. Power Sources 124 (2003) 59.

[83] T. Shimizu, T. Naruhashi, T. Momma, T. Osaka, Electrochemistry 70 (2002) 991.

[84] N. Y. Jia, M. C. Lefebvre, J. Halfyard, Z. G. Qi, P. G. Pickup, Electrochem. Solid-State Lett. 3 (2000) 529.

[85] B. Bae, B. H. Chun, H. Y. Ha, I. H. Oh, D. Kim, J. Membr. Sci. 202 (2002) 245.

[86] F. Finsterwalder, G. Hambitzer, J. Membr. Sci. 185 (2001) 105.

[87] W. C. Choi, J. D. Kim, S. I. Woo, J. Power Sources 96 (2001) 411.

[88] L. J. Hobson, H. Ozu, M. Yamaguchi, S. Hayase, J. Electrochem. Soc. 148 (2001) A1185.

[89] L. J. Hobson, H. Oozu, M. Yamaguchi, S. Hayase, J. New Mat. Electrochem. Syst.

5 (2002) 113.

[90] J. A. Kerres, J. Membr. Sci. 185 (2001) 3.

[91] K. D. Kreuer, J. Membr. Sci. 185 (2001) 29.

[92] D. J. Jones, J. Roziere, J. Membr. Sci. 185 (2001) 41.

[93] J. M. Bae, I. Honma, M. Murata, T. Yamamoto, M. Rikukawa, N. Ogata, Solid State Ionics 147 (2002) 189.

[94] L. Li, L. Xu, Y. X. Wang, Acta Polymerica Sinica (2003) 452.

[95] J. H. Fang, X. X. Guo, S. Harada, T. Watari, K. Tanaka, H. Kita, K. Okamoto, Macromolecules 35 (2002) 9022.

[96] C. Genies, R. Mercier, B. Sillion, R. Petiaud, N. Cornet, G. Gebel, M. Pineri, Polymer 42 (2001) 5097.

[97] K. Ramya, K. S. Dhathathreyan, J. Appl. Polym. Sci. 88 (2003) 307.

[98] K. Ramya, B. Vishnupriya, K. S. Dhathathreyan, J. New Mat. Electrochem. Syst. 4 (2001) 115.

[99] B. Vishnupriya, K. Ramya, K. S. Dhathathreyan, J. Appl. Polym. Sci. 83 (2002) 1792.

[100] F. Lufrano, G. Squadrito, A. Patti, E. Passalacqua, J. Appl. Polym. Sci. 77 (2000) 1250.

[101] F. Lufrano, I. Gatto, P. Staiti, V. Antonucci, E. Passalacqua, Solid State Ionics 145 (2001) 47.

[102] Y.-Z. Fu and A. Manthiram, J. Power Sources 157 (2006) 222.

[103] L. Jorissen, V. Gogel, J. Kerres, J. Garche, J. Power Sources 105 (2002) 267.

[104] B. Yang, A. Manthiram, Electrochem. Solid-State Lett. 6 (2003) A229.

[105] L. Li, J. Zhang, Y.X. Wang, J. Membr. Sci. 226 (2003) 159.

[106] X. G. Jin, M. T. Bishop, T. S. Ellis, F. E. Karasz, Bri. Polym. J. 17 (1985) 4.

[107] J. Lee, C. S. Marvel, J. Polym. Sci., Polym. Chem. Ed. 22 (1984) 295.

[108] R. Y. M. Huang, P. H. Shao, C. M. Burns, X. Feng, J. Appl. Polym. Sci. 82 (2001) 2651.

[109] D. Daoust, J. Devaux, P. Godard, Polym. Int. 50 (2001) 917.

[110] D. Daoust, J. Devaux, P. Godard, Polym. Int. 50 (2001) 925.

[111] D. Daoust, J. Devaux, P. Godard, Polym. Int. 50 (2001) 932.

[112] G. Hubner, E. Roduner, J. Mater. Chem. 9 (1999) 409.

[113] J. A. Kerres, W. Cui, S. Reichle, J. Polym. Sci., Polym. Chem. Ed. 34 (1996) 2421.

[114] S. P. Nunes, B. Ruffmann, E. Rikowski, S. Vetter, K. Richau, J. Membr. Sci. 203 (2002) 215.

[115] B. Ruffmann, H. Silva, B. Schulte, S. P. Nunes, Solid State Ionics 162 (2003) 269.

[116] L. Li, L. Xu, Y.X. Wang, Mater. Lett. 57 (2003) 1406.

[117] M. Takami, Y. Yamazaki, H. Hamada, Electrochemistry 69 (2001) 98.

[118] D. H. Jung, Y. B. Myoung, S. Y. Cho, D. R. Shin, D. H. Peck, Int. J. Hydrogen Energy 26 (2001) 1263.

[119] F. G. Wilhelm, I. G. M. Punt, N. F. A. van der Vegt, H. Strathmann, M. Wessling, J. Membr. Sci. 199 (2002) 167.

[120] J. A. Kerres, W. Zhang, L. Jorissen, V. Gogel, J. New Mat. Electrochem. Syst. 5 (2002) 97.

[121] J. A. Kerres, W. Zhang, A. Ullrich, C. M. Tang, M. Hein, V. Gogel, T. Frey, L. Jorissen, Desalination 147 (2002) 173.

[122] X. Ren, T. E. Springer, S. Gottesfeld, J. Electrochem. Soc. 147 (2000) 92.

[123] J. T. Wang, J. S. Wainright, R. F. Savinell, and M. Litt, J. Appl. Electrochem. 26 (2001) 175.

[124] A. Schechter and R. F. Savinell, Solid State Ionics 147 (2002) 181.

[125] N. Asano, K. Miyatake, M. Watanabe, Chem. Mater. 16 (2004) 2841.

[126] O. Yamada, Y. Yin, K. Tanaka, H. Kita and K. Okamoto, Electrochim. Acta 50 (2005) 2655.

[127] C. Genies, R. Mercier, B. Sillion, N. Cornet, G. Gebel, and M. Pineri, Polymer 42 (2001) 359.

[128] R. Nolte, K. Ledjeff, M. Bauer and R. Mulhaupt, J. Membr. Sci. 83 (1993) 211.

[129] K. D. Kreuer, M. Ise, A. Fuchs, J. Maier, J. Phys. IV 10 (2000) 279.

[130] T. Kobayash, M. Rikukawa, K. Sanui, N. Ogata, Solid State Ionics 106 (1998) 219.

[131] F. Trotta, E. Drioli, G. Moraglio, E. Baima Poma, J. Appl. Polym. Sci 70 (1998) 477.

[132] M. T. Bishop, F. E. Karasz, P. S. Russo, K. H. Lanley, Macromolecules 18 (1985) 86.

[133] B. Yang, A. Manthiram, J. Power Sources 153 (2006) 29.

[134] B. Bauer, D. J. Jones, J. Roziere, L. Tchicaya, G. Alberti, M. Casciola, L. Massinelli, A. Peraio, S. Besse, and E. Ramunni, J. New Mater. Electrochem. Syst. 3 (2000) 93.

[135] I. J. Choi, C. J. Ahn, T. H. Yoon, J. Appl. Polym. Sci. 93 (2004) 1211.

[136] M. Yamada, I. Honma, Electrochim. Acta 48 (2003) 2411.

[137] M. Yamada and I. Honma, J. Phys. Chem. B. 108 (2004) 5522.

[138] K. D. Kreuer, S. J. Paddison, E. Spohr, and M. Schuster, Chem. Rev. 104 (2004) 4637.

[139] M. Yamada, I. Honma, Polymer, 46 (2005) 2986.

[140] J. L. Fernández, V. Raghuveer, A. Manthiram, and A. J. Bard, J. Am. Chem. Soc. 127 (2005) 13100.

[141] V. Raghuveer, A. Manthiram, J. Phys. Chem. B. 109 (2005) 22909.

[142] P. C. Lee and D. Meisel, J. Am. Chem. Soc. 102 (1980) 5477.

[143] Q. Deng, C. A. Wilkie, R. B. Moore, and K. A. Mauritz, Polymer 39 (1998) 5961.

[144] Z. Zhou, S. Li, Y. Zhang, M. Liu, and W. Li, J. Am. Chem. Soc. 127 (2005) 10824.

[145] T. R. Hoye, Z. Ye, J. Am. Chem. Soc. 118 (1996) 1801.

[146] D. Davidson, M. Weiss, M. Jelling, J. Org. Chem. 2 (1937) 319.

[147] H. F. Ridley, R. G. W. Spicket, G. M. Timmis, J. Het. Chem. 2 (1965) 453.

[148] A. Meric, Z. Incesu, I. Isikdag, Il Farmaco 57 (2002) 543.

[149] J. A. Asensio, S. Borrós, P. Gómez-Romero, J. Polym. Sci.: A Polym. Chem. 40 (2002) 3703.

[150] M. Ueda, M. Sato, and A. Mochizuki, Macromolecules 18 (1985) 2723.

[151] J. A. Asensio, S. Borrós, P. Gómez-Romero, Electrochem. Commun. 5 (2003) 967.

[152] P. E. Eaton, G. R. Carlson, and J. T. Lee, J. Org. Chem. 38 (1973) 4071.

[153] M. D. Guiver, S. Croteau, J. D. Hazlett & O. Kutowy, Br. Polymer J. 23 (1990) 29.

[154] B. Yang and A. Manthiram, Electrochem. Commun. 6 (2004) 231.

[155] J. A. Kerres, J. Membr. Sci. 185 (2001) 3.

[156] M. Walker, K. M. Baumgärtner, M. Kaiser, J. Kerres, A. Ullrich, E. Räuchle, J. Appl. Polym. Sci. 74 (1999) 67.

[157] B. Kosmala, J. Schauer, J. Appl. Polym. Sci. 85 (2002) 1118.

[158] K. Bouzek, S. Moravcová, Z. Samec, J. Schauer, J. Electrochem. Soc. 150 (2003) E329.

[159] R. Wycisk, J. K. Lee, P. N. Pintauro, J. Electrochem. Soc. 152 (2005) A892.

[160] J. A. Asensio, S. Borrós, and P. Gómez-Romero, J. Electrochem. Soc. 151 (2004) A304.

[161] J. A. Kerres, Fuel Cells 5 (2005) 230.

[162] Y.-Z. Fu, A. Manthiram, M. D. Guiver, Electrochem. Commun. 8 (2006) 1386.

Vita

Yongzhu Fu was born in Hongxinglong, China on September 08, 1977, the son of Wenguang Fu and Shoucai Li. After completing his study at Hongxinglong High School of Heilongjiang province, China, in 1996, he entered Tsinghua University, Beijing, China. He received the degree of Bachelor of Science from Tsinghua University in July 2000. He received the Master's Degree in Chemical Engineering from Dalian Institute of Chemical Physics, Chinese Academy of Science in July 2003. In August 2003, he entered the Graduate School of the University of Texas at Austin.

Permanent address: No. 196, Fuyedui, Hongxinglong, Youyi County, Heilongjiang Province, 155801, P. R. China

This dissertation was typed by the author.